

IN SILICO CONFORMATIONAL ANALYSIS OF VANCOMYCIN AND ITS  
COMPLEXES



by  
Gülçin Cem Özeral

Submitted to Graduate School of Natural and Applied Sciences  
in Partial Fulfillment of the Requirements  
for the Degree of Doctor of Philosophy in  
Chemical Engineering

Yeditepe University  
2017

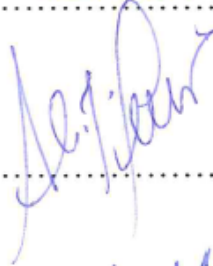
IN SILICO CONFORMATIONAL ANALYSIS OF VANCOMYCIN AND ITS  
COMPLEXES

APPROVED BY:

Prof. Dr. Seyda Malta  
(Thesis Supervisor)



Assoc. Prof. Dr. Ali Demir Sezer



Assoc. Prof. Dr. Kazım Yalçın Arga



Assoc. Prof. Dr. Nihan Çelebi Ölçüm



Assoc. Prof. Dr. Tuğba Davran Candan



DATE OF APPROVAL: 17.1.2017

## ACKNOWLEDGEMENTS

First and foremost, I owe my deepest gratitude to my Professor Seyda Malta, that without her support and “literally” hardwork this thesis would be a long-lasting dream. Thank you Professor! Professor Ebru Toksoy-Öner and Assistant Professor Kazım Yalçın Arga have been the milestones of this study. Their effort and belief made me work harder at hopeless times. I also would like to thank Rahmi Özışık, Nihat Baysal and Deniz Rende for their contribution to this thesis.

I would like to thank Melek Çetin, Binnaz Kavuşturan, Barış Emek and all my friends who share same fate through the hardest times of Doctoral path.

I would like to thank my family for their endless love and support, which makes everything more beautiful.

Finally, I would like to thank my biggest support Orçun Özeral for his understanding through my life and last 7 years of my education. Also I would like to thank our little man Aras Batu, his presence is more than enough to encourage me to achieve anything on earth.

## **ABSTRACT**

### **IN SILICO CONFORMATIONAL ANALYSIS OF VANCOMYCIN AND ITS COMPLEXES**

Vancomycin is a glycopeptide antibiotic used in treatment of infections caused by Gram-positive bacteria. Vancomycin and other related glycopeptide antibiotics are clinically very important because they are the last line of defence against bacteria that have developed resistance to antibiotics. Early use of vancomycin was associated with a number of adverse effects, including infusion-related toxicities, nephrotoxicity, and possible ototoxicity. Due to these adverse effects new ways of introducing vancomycin to body has been an interest of researchers. In this study, it is aimed to perform the conformational analysis of vancomycin drug in different conditions. Effect of temperature, surrounding media, ionic state and number of molecule are studied in terms of radius of gyration. The statistical significance of differences between compared states are investigated with t-test. Formation of hydrogen bonds with water molecules and arrangement of water molecules around amino and carboxy terminus of vancomycin are observed with pairwise radial distribution function analysis. As a novel method introducing vancomycin to body within levan biopolymer as a drug carrier is studied with molecular dynamics simulations. Vacuum conditions are used to simulate the encapsulation process. To observe the release mechanism encapsulated structures are simulated in aqueous media and MD is shown to be an appropriate method for these kinds of investigations.

## ÖZET

### VANKOMİSİN VE TÜREVLERİNİN SİLİKO ORTAMDA KONFORMASYONEL ANALİZİ

Vankomisin Gram-pozitif bakterilerin sebep olduğu enfeksiyonların tedavisinde kullanılan glikopeptid yapıda bir antibiyotiktir. Vankomisin ve diğer ilgili glikopeptid antibiyotikler, antibiyotiklere karşı direnç geliştiren bakterilere karşı savunmanın son adımını oluşturdukları için kliniksel olarak çok önemlilerdir. Vankomisinin kullanımı damardan kullanıma ait toksisite, nefrotoksisite, ve muhtemel ototoksisite gibi bir dizi yan etkiyi de beraberinde getirmekteydi. Bu sebeple vankomisini vücuda tanıtmanın yeni yollarını bulmak araştırmacıların ilgilerinden biri haline geldi. Bu çalışmada değişik şartlarda vankomisin ilacının konformasyonel analizinin yapılması hedeflenmiştir. Sıcaklık, çevreleyici ortam, iyonik durum ve molekül sayısı etkisi dönme yarı çapı bakımından incelendi. Değişiklikler arasındaki farkların istatistiksel önemi t-test ile incelendi. Hidrojen bağlarının oluşumu ve su moleküllerinin vankomisinin amino ve karboksil terminalleri etrafındaki dizilimi ikili çapsal dağılım fonksiyonu ile incelendi. Yeni bir metot olarak vankomisinin vücuda ilaç taşıyıcı olarak levan biyopolimeri içerisinde verilmesi moleküler dinamik simülasyonları ile çalışıldı. Bu çalışmalarda vakum ortamı enkapsülasyon işlemini simule etmek için kullanıldı. Salınım mekanizmasını gözlemlemek için enkapsüle olmuş yapılar su ortamında simule edildi ve moleküler dinamiğin bu tip incelemeler için uygun bir metot olduğu gösterildi.

## TABLE OF CONTENTS

ACKNOWLEDGEMENTS.....	iii
ABSTRACT.....	iv
ÖZET .....	v
TABLE OF CONTENTS.....	vi
LIST OF FIGURES .....	viii
LIST OF TABLES .....	xv
LIST OF SYMBOLS/ABREVIATONS.....	xvii
1. INTRODUCTION .....	1
2. LITERATURE SURVEY .....	2
2.1. GRAM POSITIVE AND GRAM NEGATIVE BACTERIA.....	5
2.2. VANCOMYCIN.....	7
2.3. USES OF VANCOMYCIN .....	9
2.4. VANCOMYCIN MECHANISM OF ACTION .....	12
2.5. DRUG DELIVERY .....	14
2.5.1. Nanoparticles as Drug Delivery Vehicles .....	15
2.5.2. Liposomes as Drug Delivery Vehicles.....	16
2.5.3. Polymers as Drug Delivery Vehicles .....	18
2.5.4. Vancomycin Delivery to Body.....	21
2.6. LEVAN.....	22
3. METHODOLOGY.....	24
3.1. MOLECULAR DYNAMICS .....	24
3.2. FORCE FIELDS .....	27
3.3. ENSEMBLES .....	31
3.4. NUMERICAL INTEGRATION.....	33
3.4.1. Initial Conditions.....	35

3.4.2. Boundary Conditions.....	35
3.5. ANALYSIS OF MD SIMULATION DATA .....	37
3.5.1. Radius of Gyration .....	37
3.5.2. Radial Distribution Function.....	38
3.6. TREATMENT OF SOLVENT IN MD SIMULATIONS .....	39
3.6.1. Explicit Treatment of Solvent .....	39
3.6.2. Implicit Treatment of Solvent .....	40
3.7. SIGNIFICANCE TEST IN MD SIMULATIONS .....	41
4. RESULTS .....	44
4.1. SIMULATIONS IN VACUUM WITH VANCOMYCIN .....	44
4.1.1. Visual Inspection.....	45
4.1.2. Radius of Gyration of Systems with Vancomycin in Vacuum .....	46
4.1.2.1.Effect of Ionic State on Radius of Gyration in Vacuum .....	47
4.1.2.2.Effect of Temperature on Radius of Gyration in Vacuum.....	53
4.1.2.3.Effect of Number of Vancomycin on Radius of Gyration in Vacuum....	59
4.2. TREATMENT OF SOLVENT: COMPARISON OF EXPLICIT AND IMPLICIT METHODS .....	62
4.3. SIMULATIONS IN AQUEOUS MEDIUM WITH VANCOMYCIN .....	68
4.3.1. Effect of Temperature on Radius of Gyration for Simulations in Aqueous Medium .....	68
4.3.2. Radial Distribution Function (RDF).....	73
4.4. SIMULATIONS IN VACUUM WITH VANCOMYCIN AND LEVAN .....	89
4.5. ENCAPSULATION AND RELEASE OF VANCOMYCIN .....	94
4.6. ENCAPSULATION OF VANCOMYCIN WITH POLYSTYRENE.....	103
5. CONCLUSION AND FUTURE WORK .....	105
REFERENCES .....	108

## LIST OF FIGURES

Figure 2.1. Crude infectious disease mortality rate in United States in 20th century .....	2
Figure 2.2. Gram-positive and Gram-negative Bacteria After Gram Staining Procedure.....	5
Figure 2.3. Gram-positive and Gram-negative Bacteria.....	6
Figure 2.4. Structure of Vancomycin.....	8
Figure 2.5. Possible sites for linkage to vancomycin free base .....	10
Figure 2.6. Structure of V-HCl .....	11
Figure 2.7. V-HCl in zwitter ionic form .....	11
Figure 2.8. Action of vancomycin .....	13
Figure 2.9. Mechanism of vancomycin action and resistance in sensitive and resistant bacteria.....	14
Figure 2.10. Different types of nanocarriers in drug delivery .....	16
Figure 2.11. Liposomes used as drug delivery vehicles .....	17
Figure 2.12. Drug release mechanisms of polymeric drug delivery vehicles.....	20
Figure 2.13. Levan molecular structure .....	22
Figure 3.1. Flow Chart of Molecular Dynamics .....	26
Figure 3.2. Energy vs Conformation through Molecular Dynamics Simulation Stages .....	27



Figure 3.3. Periodic Boundary Conditions .....	36
Figure 3.4. Radius of gyration of a molecule .....	37
Figure 3.5. Atomic model of a solute surrounded by explicit solvent molecules in a solvent environment modeled implicitly .....	39
Figure 3.6. Normal Distribution .....	41
Figure 4.1. Cl <sup>-</sup> ion position for 1 V-HCl at 310 K vacuum, t= 0 and t= 5 ns .....	45
Figure 4.2. Different number of V-HCl and ionic V-HCl molecules at t= 0 and t= 5 ns ....	46
Figure 4.3. Rg of 1 V-HCl and 1 ionic V-HCl at 298 K and 310 K.....	47
Figure 4.4. Rg of 2 V-HCl and 2 ionic V-HCl at 298 K and 310 K.....	48
Figure 4.5. Rg of 4 V-HCl and 4 ionic V-HCl at 298 K and 310 K.....	48
Figure 4.6. Rg of 9 V-HCl and 9 ionic V-HCl at 298 K and 310 K.....	49
Figure 4.7. Rg of 16 V-HCl and 16 ionic V-HCl at 298 K and 310 K.....	49
Figure 4.8. Cluster Rg of 2 V-HCl and 2 ionic V-HCl at 298 K and 310 K .....	50
Figure 4.9. Cluster Rg of 4 V-HCl and 4 ionic V-HCl at 298 K and 310 K .....	50
Figure 4.10. Cluster Rg of 9 V-HCl and 9 ionic V-HCl at 298 K and 310 K .....	51
Figure 4.11. Cluster Rg of 16 V-HCl and 16 ionic V-HCl at 298 K and 310 K .....	51
Figure 4.12. Temperature dependence of Rg of 1 V-HCl and 1 ionic V-HCl.....	54

Figure 4.13. Temperature dependence of Rg of 2 V-HCl and 2 ionic V-HCl.....	54
Figure 4.14. Temperature dependence of Rg of 4 V-HCl and 4 ionic V-HCl.....	55
Figure 4.15. Temperature dependence of Rg of 9 V-HCl and 9 ionic V-HCl.....	55
Figure 4.16. Temperature dependence of Rg of 16 V-HCl and 16 ionic V-HCl.....	56
Figure 4.17. Temperature dependence of Cluster Rg of 2 V-HCl and 2 ionic V-HCl .....	56
Figure 4.18. Temperature dependence of Cluster Rg of 4 V-HCl and 4 ionic V-HCl .....	57
Figure 4.19. Temperature dependence of Cluster Rg of 9 V-HCl and 9 ionic V-HCl .....	57
Figure 4.20. Temperature dependence of Cluster Rg of 16 V-HCl and 16 ionic V-HCl....	58
Figure 4.21. Effect of number of vancomycin molecules on Rg after 5 ns .....	60
Figure 4.22. Effect of number of vancomycin molecules on Rg after 10 ns .....	60
Figure 4.23. Effect of number of vancomycin molecules on Rg after 20 ns .....	60
Figure 4.24. Effect of number of the vancomycin molecules on cluster Rg after 5 ns .....	61
Figure 4.25. Effect of number of the vancomycin molecules on cluster Rg after 10 ns .....	61
Figure 4.26. Effect of number of the vancomycin molecules on cluster Rg after 20 ns .....	61
Figure 4.27. Rg of 1 ionic V-HCl at 298 K, water solvent treated explicitly and implicitly.....	63
Figure 4.28. Rg of 2 ionic V-HCl at 298 K, water solvent treated explicitly and implicitly.....	64

Figure 4.29. Rg of 4 ionic V-HCl at 298 K, water solvent treated explicitly and implicitly.....	64
Figure 4.30. Rg of 9 ionic V-HCl at 298 K, water solvent treated explicitly and implicitly.....	64
Figure 4.31. Rg of 1 ionic V-HCl at 298 K, water solvent treated explicitly and implicitly.....	65
Figure 4.32. Cluster Rg of 2 ionic V-HCl at 298 K, water solvent treated explicitly and implicitly.....	66
Figure 4.33. Cluster Rg of 4 ionic V-HCl at 298 K, water solvent treated explicitly and implicitly.....	66
Figure 4.34. Cluster Rg of 9 ionic V-HCl at 298 K, water solvent treated explicitly and implicitly.....	67
Figure 4.35. Cluster Rg of 16 ionic V-HCl at 298 K, water solvent treated explicitly and implicitly.....	67
Figure 4.36. Rg of 1 ionic V-HCl explicitly solvated at 298 K and 310 K.....	69
Figure 4.37. Rg of 2 ionic V-HCl explicitly solvated at 298 K and 310 K.....	69
Figure 4.38. Rg of 4 ionic V-HCl explicitly solvated at 298 K and 310 K.....	69
Figure 4.39. Rg of 9 ionic V-HCl explicitly solvated at 298 K and 310 K.....	70
Figure 4.40. Rg of 16 ionic V-HCl explicitly solvated at 298 K and 310 K.....	70
Figure 4.41. Effect of number of the vancomycin molecules on Rg of systems explicitly solvated at 298 K and 310 K after 20 ns.....	70

Figure 4.42. Cluster Rg of 2 ionic V-HCl explicitly solvated at 298 K and 310 K.....	71
Figure 4.43. Cluster Rg of 4 ionic V-HCl explicitly solvated at 298 K and 310 K.....	72
Figure 4.44. Cluster Rg of 9 ionic V-HCl explicitly solvated at 298 K and 310 K.....	72
Figure 4.45. Cluster Rg of 16 ionic V-HCl explicitly solvated at 298 K and 310 K.....	72
Figure 4.46. Hydration Shell and Bulk Solvent around a molecule .....	74
Figure 4.47. Interaction of water molecules to amino and carboxy terminus of vancomycin molecule.....	75
Figure 4.48. Pairwise Radial Distribution Function of nitrogen ion (n+) of 1 ionic V-HCl and hydrogen (hw) of water between 0-1 ns.....	76
Figure 4.49. Pairwise Radial Distribution Function of oxygen ion (o-) of 1 ionic V-HCl and hydrogen (hw) of water between 0-1 ns .....	76
Figure 4.50. Pairwise Radial Distribution Function of nitrogen ion (n+) of 1 ionic V-HCl and oxygen (o*) of water between 0-1 ns.....	77
Figure 4.51. Pairwise Radial Distribution Function of oxygen ion (o-) of 1 ionic V-HCl oxygen (o*) of water between 0-1 ns .....	77
Figure 4.52. Pairwise Radial Distribution Function of nitrogen ion (n+) of 1 ionic V-HCl and oxygen (o*) of water .....	79
Figure 4.53. Pairwise Radial Distribution Function of oxygen ion (o-) of 1 ionic V-HCl and oxygen (o*) of water.....	80
Figure 4.54. Pairwise Radial Distribution Function of nitrogen ion (n+) of 2 ionic V-HCl and oxygen (o*) of water .....	81

Figure 4.55. Pairwise Radial Distribution Function of oxygen ion (o-) of 2 ionic V-HCl and oxygen (o\*) of water ..... 82

Figure 4.56. Pairwise Radial Distribution Function of nitrogen ion (n+) of 4 ionic V-HCl and oxygen (o\*) of water ..... 83

Figure 4.57. Pairwise Radial Distribution Function of oxygen ion (o-) of 2 ionic V-HCl and oxygen (o\*) of water ..... 84

Figure 4.58. Pairwise Radial Distribution Function of nitrogen ion (n+) of 9 ionic V-HCl and oxygen (o\*) of water ..... 85

Figure 4.59. Pairwise Radial Distribution Function of oxygen ion (o-) of 9 ionic V-HCl and oxygen (o\*) of water ..... 86

Figure 4.60. Pairwise Radial Distribution Function of nitrogen ion (n+) of 16 ionic V-HCl and oxygen (o\*) of water ..... 87

Figure 4.61. Pairwise Radial Distribution Function of oxygen ion (o-) of 16 ionic V-HCl and oxygen (o\*) of water ..... 88

Figure 4.62. Cluster Rg of V-HCl and Levan systems at 298 K in vacuum..... 93

Figure 4.63. Representation of Simulated Systems with one vancomycin and varying number of levan molecules ..... 94

Figure 4.64. Encapsulation of 1 levan 1 vancomycin system..... 95

Figure 4.65. Encapsulation of 2 levan 1 vancomycin system..... 95

Figure 4.66. Encapsulation of 4 levan 1 vancomycin system..... 96

Figure 4.67. Cluster Rg of 1 Levan – 1 Vancomycin System .....	97
Figure 4.68. Cluster Rg of 2 Levan – 1 Vancomycin System .....	97
Figure 4.69. Cluster Rg of 4 Levan – 1 Vancomycin System .....	98
Figure 4.70. Cluster Rg of 1,2 and 4 Levan – 1 Vancomycin Systems at steady state .....	98
Figure 4.71. Sulfated levan structure .....	100
Figure 4.72. Encapsulation of Sulfated levan and vancomycin systems .....	100
Figure 4.73. Comparison of Cluster Rg of 1 sulfated Levan – 1 Vancomycin System with 1 Levan – 1 Vancomycin system.....	101
Figure 4.74. Comparison of Cluster Rg of 2 sulfated Levan – 1 Vancomycin System with 2 Levan – 1 Vancomycin system.....	101
Figure 4.75. Comparison of Cluster Rg of 4 sulfated Levan – 1 Vancomycin System with 4 Levan – 1 Vancomycin system.....	101
Figure 4.76. Cluster Rg comparison of systems with unmodified and sulfated levan at vacuum.....	102
Figure 4.77. Cluster Rg comparison of systems with unmodified and sulfated levan in aqueous medium .....	102
Figure 4.78. Structure of polystyrene .....	103
Figure 4.79. Cluster Rg of 4 Polystyrene – 1 Vancomycin System .....	103

## LIST OF TABLES

Table 2.1. Pathogenic bacteria for humans and related diseases .....	4
Table 2.2. Representative list of polymers used in drug delivery.....	19
Table 4.1. Simulations performed in vacuum (total duration= 22 ns).....	44
Table 4.2. Radius of gyration of all systems at 298 K and 310 K .....	52
Table 4.3. Significance Test for Rg Values of Ionic and Non-ionic States of Vancomycin	53
Table 4.4. Significance Test for Rg Values of Vancomycin at different temperatures .....	58
Table 4.5. Simulations treated explicitly and implicitly (total duration= 22 ns) .....	62
Table 4.6. Simulations performed in aqueous medium (total duration= 22 ns) .....	68
Table 4.7. Significance Test for Rg Values of Vancomycin at different temperatures .....	73
Table 4.8. Radial Distribution Function of amino and carboxy terminus of vancomycin for all systems.....	89
Table 4.9. Simulations performed in vacuum with 1 ionic V-HCl and 1 Levan (total duration= 22 ns).....	90
Table 4.10. Distance Data Obtained, Levan Position: above .....	90
Table 4.11. Distance Data Obtained, Levan Position: below .....	91
Table 4.12. Distance Data Obtained, Levan Position: behind .....	91

Table 4.13. Distance Data Obtained, Levan Position: in front.....	91
Table 4.14. Distance Data Obtained, Levan Position: left.....	92
Table 4.15. Distance Data Obtained, Levan Position: right .....	92
Table 4.16. Vancomycin/Levan simulations performed in vacuum at 298 K and solvated at 310 K (total duration= 44 ns).....	95





## LIST OF SYMBOLS/ABBREVIATIONS

$a$	Acceleration
$F$	Force
$g_{ij}(r)$	Density distribution
$k$	Boltzmann Constant
$k_b$	Spring Constant
$m$	Mass
$M$	Molecular Mass
$n_i$	Number of sample data from population $i$
$p$	Probability
$r$	Distance
$r_0$	Equilibrium bond length
$R_g$	Radius of Gyration
$s$	Standard Deviation
$s_{pool}$	Pooled Standard Deviation
$T$	Temperature
$U$	Force field
$t$	Time
$v$	Velocity
$\alpha$	Expansion Factor
$\Delta G$	Free Energy
$\epsilon$	Dielectric Constant
$\theta_0$	Equilibrium bond angle
$\sigma$	Diameter of particle
$\nu$	Degrees of freedom
$\phi$	Torsional angle
LAMMPS	Large-scale Atomic/Molecular Massively Parallel Simulator
LJ	Lennard Jones
MD	Molecular Dynamics

MVT	Grand Canonical Ensemble
NPT	Isobaric-Isothermal Ensemble
NVE	Micro Canonical Ensemble
NVT	Canonical Ensemble
PCFF	Polymer Consistent Force Field
RDF	Radial Distribution Function
V-HCl	Vancomycin HCl salt



## 1. INTRODUCTION

Vancomycin is a glycopeptide antibiotic that is active against staphylococci, streptococci, and other Gram-positive bacteria [1]. Vancomycin and other related glycopeptide antibiotics are very important because they act as the last line of defense against bacteria that become resistant to antibiotics with some modifications in their cell walls, which inhibits the drug to bind the cell wall to break the integrity of the wall. [2].

Molecular Dynamics (MD) simulations are recently used for biological systems in drug design and delivery. These simulations are complementary to experimental studies. However simulations require high computing power.

Pathogenic bacteria and the glycopeptides antibiotic vancomycin is introduced in the first part of the study. Then the mechanism of action of the drug is explained. Due to the adverse effects of vancomycin new ways to introduce the drug to body has been investigated by researchers. In the study it is suggested to use levan biopolymer, which is a soluble and biodegradable polymer, as drug carrier.

MD simulations are performed in order to investigate vancomycin in different media and investigate its interaction with levan biopolymer in vacuum and in aqueous medium at different temperatures. Different analysis methods has been performed as radius of gyration and pairwise radial distribution function. Encapsulation and release of vancomycin by and from levan and sulfated levan by MD simulations are performed to show that computational methods can be used for screening prior ro experiments as well as to support experimental data.

This thesis starts with theoretical background on vancomycin, drug delivery and levan biopolymer. In the next section, computational methods, approximations and parameters are given in detail, along with different analysis methods employed to evaluate the data. In the results and discussion section, MD results of all the simulations are given together with appropriated discussions of their analysis. The thesis is finalized with its conclusions and some suggestions for future work.

## 2. LITERATURE SURVEY

Infectious diseases are caused by germs, which can be divided into four main groups as bacteria, viruses, fungi and protozoa. Infection can spread by touching, breathing, eating or insect bites. Infectious diseases which include tuberculosis, rabies, AIDS, and strep throat, are considered to be the leading causes of death around the world. This is highly related with the emergence of new infectious diseases; re-emerge of old infectious diseases and persistence of intractable infectious diseases [1]. The deaths caused by infectious diseases in United States of America for a time period between 1900 and 1999, are investigated by Armstrong and coworkers. Although the study includes only United States, it can be accepted as a general trend through the world [2].

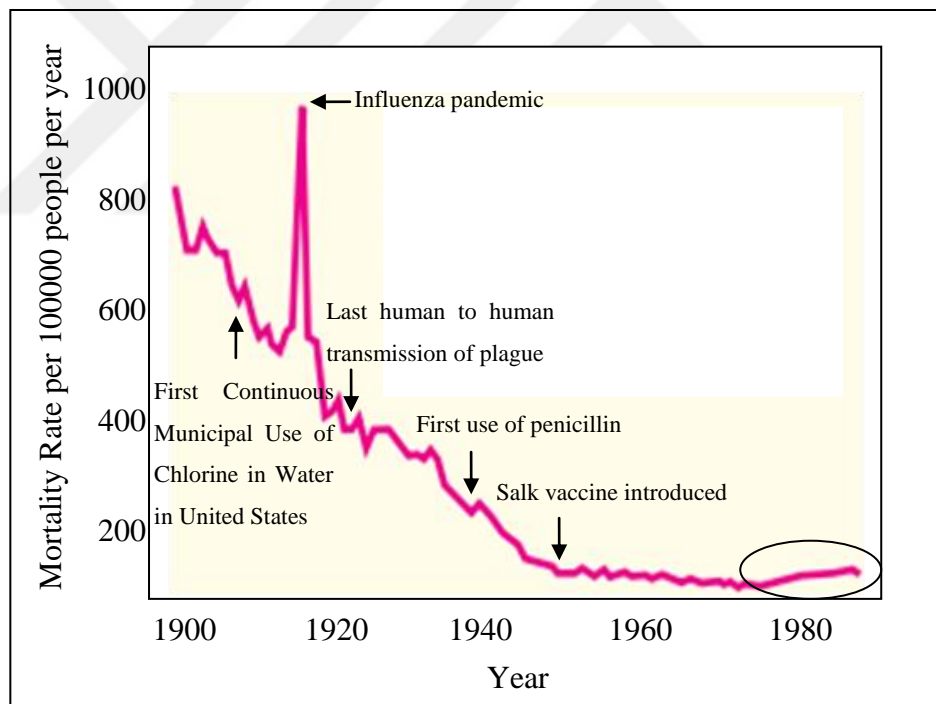


Figure 2.1. Crude infectious disease mortality rate in United States in 20<sup>th</sup> century [2]

In Fig. 2.1 the mortality rate caused by infectious diseases in United States of America for 20<sup>th</sup> century is represented with novel applications and breakthroughs. As seen in the chart after 1980s a slight increase in mortality rate is observed. The main reasons of this increase

can be related with aforementioned causes as re-emergence of diseases, resistant pathogens etc.

In history bacterial infections have been the major responsible for most deadly and widespread epidemics through civilization. Pneumonia, tuberculosis and diarrhea were the three leading causes of death in the early 20<sup>th</sup> century. The development of vaccines, antibiotics and also general hygiene precautions as water purification, inhibited the death rate from these kinds of diseases. However, in accordance with the Figure 1.1 it is reported that in the past 30 years new bacterial pathogens are recognized and many old ones re-emerged with resistance to antimicrobial drugs. [3]

Bacterial based infectious diseases, of which the most fatal one is respiratory infections, include tuberculosis, cholera, meningitis and urinary tract infections. For the treatment of this kind of diseases mostly antibiotics and vaccines are used. However more daily hygiene procedures such as hand washing should be considered. The main problem in medical treatment is, the bacteria may become resistant to antibiotics if imprudent usage of antibiotics is not precluded.

Bacteria can be classified by using many different criteria. These criteria are bacterial morphology, staining properties and growth requirements. Morphological features divide bacteria to these groups; Coccus (spherical), Bacillus (rod), Spirillum (spiral), Vibrio (curved rods). Growth requirements classify bacteria due to their need for oxygen to grow. The classes include anaerobic bacteria, which can grow in lack of oxygen and aerobic bacteria which requires oxygen to grow. The other criteria, staining properties (explained in detail in the following section) classify the bacteria into two groups as Gram-positive and Gram-negative. The classification can be enlarged with the criteria of dietary patterns as autotrophic, which can synthesize organic matter from inorganic, and heterotrophic, which can not synthesize organic matter and take aliment from outside.

Table 2.1 represents the types of bacteria, diseases caused by them and also transmission paths. The abbreviations for transmission paths are; C, *Contact*, E, *Endogenous*, F, *Food borne*, HA, *Hospital Acquired*, IA, *Infected Animal*, IV, *Insect Vector*, M, *Milk*, RC, *Respiratory Contact*, SC, *Sexual Contact*, S, *Soil*, W, *Water*.

Table 2.1. Pathogenic bacteria for humans and related diseases [3]

	<b>Bacteria</b>	<b>Disease(s)</b>	<b>Transmission</b>
<b>Gram-negative Bacteria</b>	<i>Escherichia coli</i>	Gastroenteritis, urinary tract infections, neonatal meningitis	F W E
	<i>E. coli</i> O157:H7	Diarrhea, hemolytic uremic syndrome (HUS)	F
	<i>Salmonella enterica</i>	Gastroenteritis	F W
	<i>Salmonella typhi</i>	Typhoid fever	F W
	<i>Shigella dysenteriae</i>	Bacillary dysentery	F W
	<i>Yersinia pestis</i>	Bubonic plague	IV
	<i>Pseudomonas aeruginosa</i>	Opportunistic infections, swimmer's ear, hot tub itch, cellulitis, pneumonia, more	S W C H A E
	<i>Vibrio cholerae</i>	Asiatic cholera	W
	<i>Bordetella pertussis</i>	Whooping cough	RC
	<i>Haemophilus influenzae</i>	Meningitis, pneumonia, sinusitis	RC
	<i>Helicobacter pylori</i>	Gastric and duodenal ulcers	F?
	<i>Campylobacter jejuni</i>	Gastroenteritis	F W
	<i>Neisseria gonorrhoeae</i>	Gonorrhea	S C
	<i>Neisseria meningitidis</i>	Meningococemia and meningitis	R C E
	<i>Brucella abortus</i>	Undulant fever	I A M
<i>Bacteroides fragilis</i>	Anaerobic infections	E	
<b>Gram-positive Bacteria</b>	<i>Staphylococcus aureus</i>	Food poisoning, wound infections, toxic shock	F C E H A I A
	<i>Streptococcus pyogenes</i>	Strep throat, scarlet fever, mastitis, necrotizing fasciitis	C
	<i>Streptococcus pneumoniae</i>	Pneumonia, otitis media, meningitis	R C E
	<i>Bacillus anthracis</i>	Anthrax	S I A
	<i>Bacillus cereus</i>	Food poisoning	F
	<i>Clostridium tetani</i>	Tetanus	S
	<i>Clostridium perfringens</i>	Food poisoning, gas gangrene, uterine infections	F S E
	<i>Clostridium botulinum</i>	Botulism, infant botulism	F
	<i>Clostridium difficile</i>	Antibiotic-associated diarrhea, pseudomembranous colitis	C H A E
	<i>Corynebacterium diphtheriae</i>	Diphtheria	RC
	<i>Listeria monocytogenes</i>	Listeriosis	F
<b>Not classified by Gram staining</b>	<i>Mycobacterium tuberculosis</i>	TB (tuberculosis)	R C M
	<i>Mycobacterium leprae</i>	Leprosy	C
	<i>Chlamydia trachomatis</i>	Chlamydia, lymphogranuloma venereum, trachoma	S C C
	<i>Chlamydia pneumoniae</i>	Pneumonia	RC
	<i>Mycoplasma pneumoniae</i>	Atypical pneumonia	RC
	Rickettsias	Rickettsiosis: typhus, RMSF	IV
	<i>Treponema pallidum</i>	Syphilis	SC
	<i>Borrelia burgdorferi</i>	Lyme disease	IV

## 2.1. GRAM-POSITIVE AND GRAM-NEGATIVE BACTERIA

Bacteria can be stained by crystal violet dye and methylene blue dye which have positive charges as the bacterial cytoplasm has an overall negative charge. The Gram staining technique has multi steps and as a result divides bacteria into two groups: Gram-positive and Gram-negative [4]. The method, discovered by H.C. Gram in 1884, has been useful and important technique to classify the bacteria to this day.

First bacteria are stained with crystal violet dye and rinsed then a special Gram dye containing iodine is added. With this step all bacteria are colored purple in light microscope. The differentiation is done by a decolorizer. When decolorizer is added to medium the bacteria which lose their color and become transparent are called Gram-negative bacteria. Others that retain violet color are called Gram-positive bacteria. Then a red dye to counterstain the Gram-negatives is added. So at the end of Gram's test while Gram-positives remain purple, Gram-negatives are observed as orange color as shown on the right side of Fig. 2.2 [5].

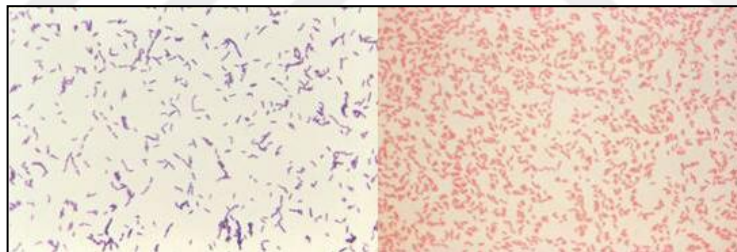


Figure 2.2. Gram-positive and Gram-negative Bacteria After Gram Staining Procedure [5]

Peptidoglycan is a construction element in bacterial cell wall acting as an exoskeleton. It consists of cross linked polysaccharides by peptide chains. According to type of bacteria the amount of peptidoglycan varies 5 to 90 percent of the cell wall mass. Gram-positive bacteria contain higher amounts of peptidoglycan than Gram-negative bacteria [6].

As seen in Fig. 2.3. Gram-positive bacteria have a thicker peptidoglycan layer while Gram-negative bacteria have an extra outer membrane. This peptidoglycan layer has also heavily crosslinked polymers of teichoic and lipoteichoic acid, which Gram-negative bacteria do

not produce. However, the outer membrane of Gram-negative bacteria has a complex of lipids and lipopolysaccharides.

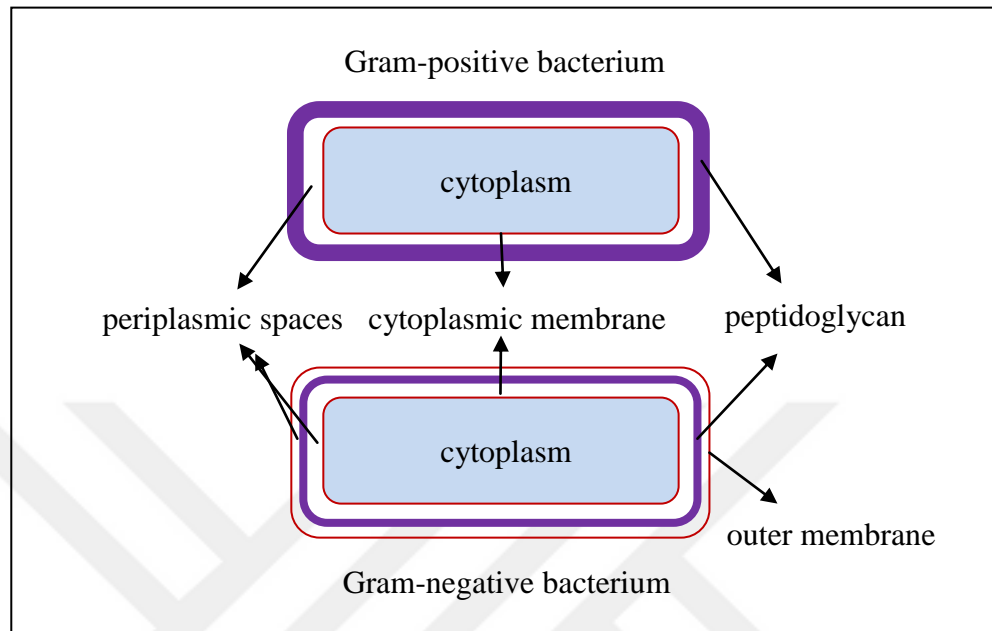


Figure 2.3. Gram-positive and Gram-negative Bacteria

In Gram-positive bacteria rigid peptidoglycan layer provides physical integrity to organism. However, this layer does not prevent the diffusion of small molecular weight species, such as antibiotics and dyes through. Antibiotics such as penicillin and vancomycin do not interact with cytoplasm. They corrupt the integrity of cell wall leading osmotic lysis of the bacterium. In Gram-negative bacteria species such as antibiotics must first cross the outer membrane to reach the peptidoglycan layer [7].

As a defense mechanism there are small cationic antimicrobial peptides in mammals that forms naturally. Studies on human immune system reveal that at normal conditions low levels of antimicrobial peptides are formed by skin and mucosal cells. However, in the presence of an injury or infectious bacteria, the production of these peptides increases dramatically. The spectrum that antimicrobial peptides are effective, include Gram-positive and Gram-negative species, some certain protozoan parasites and some viruses. With modifications and mechanisms antimicrobial peptide resistance emerged in some types of bacteria. Cell surface modification is one of the ways that bacteria gain resistance to antimicrobial peptides which occur naturally or synthetically. Modifications of teichoic



acid with amino sugars or the amino acid D-Alanine, in Gram-positive bacteria such as *Staphylococcus aureus*, enhances resistance. In Gram-negative bacteria modifications on the lipid, which is a part of outer membrane, play an important role in resistance. In both mechanisms the main aim is to reduce the negative charges of the anionic bacterial cell wall in order to repel the cationic antimicrobial peptides before attacking the cell wall. [7]

Other adaptations include neutralization of antimicrobial peptides by bacterial proteins. Jin and coworkers studied the neutralization of host peptides and showed the *Staphylococcus aureus* which produces staphylokinase, found to be resistant to  $\alpha$ -defensins, a type of antimicrobial peptides [8]. Also enzymes produced by bacteria inactivate the components of immune system. Although mammalian antimicrobial peptides are relatively resistant to degradation, certain bacteria which are pathogenic to humans have enzymes to cleave cationic antimicrobial peptides. Schmidtchen and coworkers studied the degradation of antibacterial peptide by proteinases of pathogens. First researchers investigated the activity of antimicrobial peptide LL 37 on various bacteria as, *Pseudomonas aeruginosa*, *E. faecalis*, *P. mirabilis*, and *S. pyogenes* and observed that the peptide killed bacteria effectively. Then *P. aeruginosa* elastase effects on LL 37 were investigated and studies show that antimicrobial peptide degraded immediately without intermediate peptides. [9]

Penicillin type of drugs interacts with the enzyme transpeptidase which catalyzes the formation of cross links in peptidoglycans. However, penicillin resistant bacteria emerged due to mutations in the cell wall. Mutations occur due to production of penicillinase enzyme, which deactivates the antimicrobial properties of the drug and also a mutant transpeptidase which lowers the binding affinity of drug to enzyme. According to these changes in the bacterial cell, only a few antibiotics remain effective at interfering with peptidoglycan layer and vancomycin is one of those antibiotics [10].

## **2.2. VANCOMYCIN**

Vancomycin was first discovered by an organic chemist, Dr. E. Kornfeld, on a program to discover new antimicrobial agents with activity against gram-positive bacteria. It was isolated from a soil sample collected from Borneo. This sample contained an organism that yielded a compound in fermentation. The new compound was found to be capable of

killing bacteria especially staphylococci, which is a gram-positive bacteria. The compound was later named “vancomycin” derived from the term “vanquish” [11].

Vancomycin is a large glycopeptide compound with a molecular formula of  $C_{66}H_{75}Cl_2N_9O_{24}$  (represented in Fig.2.4.) and a molecular weight of  $\sim 1450 \text{ g}\cdot\text{mol}^{-1}$ . Vancomycin is a concentration-independent antibiotic and also is referred to as a time dependent antibiotic. Increase in the concentration of the vancomycin beyond the minimum amount to produce the desired response, do not provide faster killing or has no effect on the amount of bacteria that are killed. Vancomycin efficacy is related with the length of time that its concentration is above minimum inhibitory concentration, which is the minimum concentration of a drug to inhibit the growth of bacteria. Factors that affect the overall activity of vancomycin include its distribution in tissue, inoculum size, and protein-binding effects [12].

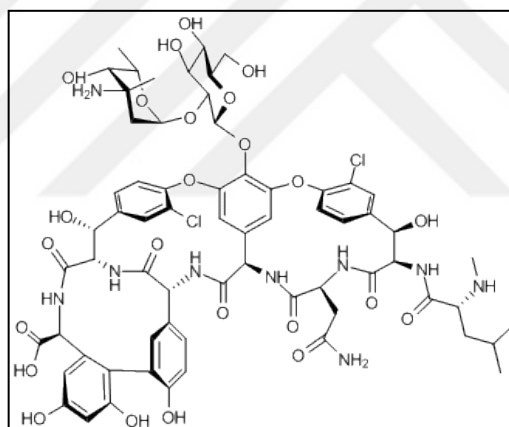


Figure 2.4. Structure of Vancomycin [13]

The first complete structure of vancomycin was proposed by Sheldrick et. al. in 1978 [14]. The structure formed was constituted of the following studies; Vancosamine sugar and amino acids found from the degradation studies, NMR studies which gave information on linkages and stereochemical relationships and X-ray diffraction studies of degradation products of vancomycin. Williamson and Williams in 1981 have revised the structure due to further NMR studies. [15]

The molecule consists of a seven membered peptide chain that is formed by parts of three phenylglycine systems, two chlorinated tyrosine units, aspartic acid, and N-methylleucine. Two ether bonds and a carbon-carbon bond join the various substituents on the peptide

chain into three large rings. A disaccharide, composed of glucose and vancosamine, is also present but is not part of the cyclic structure [16].

Penicillins and other antibiotics were modified to change the antibacterial features. However, fewer modifications were applied to vancomycin. It was found that removal of the disaccharide from the vancomycin structure causes a decrease in antibacterial activity. However, if the amide group in aspartic acid fragment is exchanged with a carboxyl group vancomycin loses its total antibacterial activity. [16]

### **2.3. USES OF VANCOMYCIN**

Vancomycin and other related glycopeptide antibiotics are clinically very important because they often represent the last line of defense against bacteria that have developed resistance to antibiotics [14].

Vancomycin did not play first role in the treatment of infections when it was first discovered. One of the reasons was that methicillin and penicillin were used primarily. And also clinical ototoxic (damages inner ear) and nephrotoxic (damages kidney) results were the other reasons. After purification studies in late 1970s, ototoxicity which restricted marketing of vancomycin in 1960s and 1970s, was no longer an issue. As new kinds of bacteria resistant to methicillin emerged, need to vancomycin was reemerged in 1980s [11].

In the study of Kosmidis and Chandrasekar, it is stated that vancomycin is used extensively in patients with cancer, suffering infectious diseases caused by gram-positive bacteria, due to its low cost and experience with its use. However for these patients nephrotoxicity is a major concern as other additional medications are used for cancer treatment. [17]

Vancomycin is very active against many Gram-positive bacteria including methicillin-resistant and penicillin-resistant bacteria. Also patients, allergic to penicillin utilize vancomycin [7]. However vancomycin resistance is a problem of concern for several years. It was thought that infections due to Gram-positive bacteria could be treated smoothly. As antibiotics are used extensively, new types of bacteria emerged with resistance to all available antibiotics [18]. Nowadays new complexes of vancomycin are being tried for competing vancomycin-resistant bacteria.

Napolitano reviewed the literature on diagnosis and management of infections caused by methicillin resistant *Staphylococcus aureus*, vancomycin-resistant *Enterococcus spp.* It was found that incidence of methicillin resistant *Staphylococcus aureus* was increased to 59.5%, where the 28.5% of *Enterococcus spp.* was found to be vancomycin resistant. As mentioned before vancomycin has been the only effective treatment for methicillin resistant bacteria. However with the emergence of vancomycin resistant bacteria novel treatments are being searched. [19]

Vancomycin is being modified for different uses. Mostly Vancomycin-HCl salt (V-HCl) is used due to solubility issues in blood. Other complexes are being studied for targeted delivery. Kahne and coworkers reported Vancomycin analogs containing modified carbohydrates to be very active against resistant microorganisms. It is proposed that carbohydrate-modified vancomycin compounds are effective against resistant bacteria because they interact directly with bacterial proteins involved in the transglycosylation step of cell wall biosynthesis [20].

The derivations of and bindage to vancomycin molecule is favored by three sites in the molecule as shown in Fig. 2.5. (1) is carboxyl terminus, (2) is amino terminus and (3) is amine of the vancosamine sugar. If one of the sites is already occupied then one of the remaining positions can be used for the attachment of different groups for chemical modification [21].

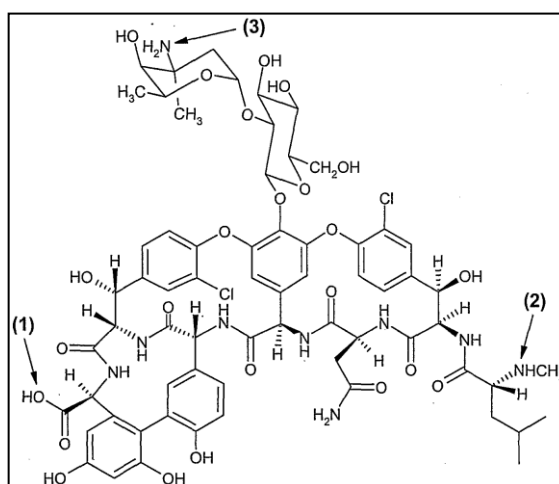


Figure 2.5. Possible sites for linkage to vancomycin free base [21]

When vancomycin free base in aqueous medium is treated with sufficient amount of hydrochloric acid to convert free base to hydrochloride salt, vancomycin hydrochloride solutions are formed. After freeze-drying process solid commercial form of V-HCl is obtained as shown in Fig. 2.6 [22].

The shelf life of vancomycin is highly affected by the deamidation of asparagines residue, which is the amino terminus and followed by zwitter-ion formation in the structure. Zwitterionic structure of V-HCl formed on the carboxyl and amino terminus of the molecule is shown in Fig. 2.7. It was shown previously by Antipas and coworkers [23] that the rate of deamidation is affected by the ionic state. In the study it was proposed that the ionic state of vancomycin results in conformational modifications.

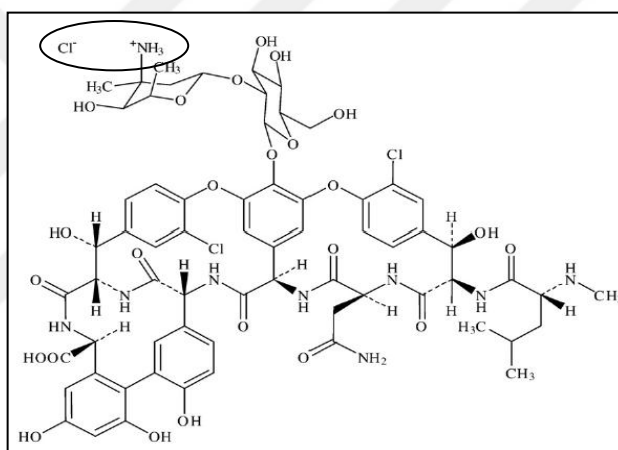


Figure 2.6. Structure of V-HCl [24]

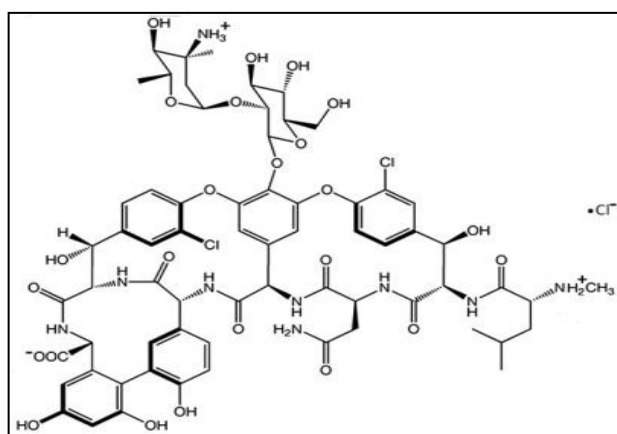


Figure 2.7. V-HCl in zwitter ionic form [25]

## 2.4. VANCOMYCIN MECHANISM OF ACTION

Both noncharged and charged (zwitterionic) forms of antibiotics play an important role on antibacterial activity. Noncharged forms are related with oral bioavailability. Vancomycin naturally can coexist in both states. However the yield of zwitterionic form is much more higher than the noncharged form. The charged forms have the polarity to diffuse through the outer cell membrane that the Gram-negatives have. However the diffusion of the Gram-negative bacteria porins are limited around 600 Da. Polar form of vancomycin can not diffuse through these porins as it is a large molecule of approximately 1500 Da. This form of vancomycin acts important role by interacting the ligand of cell membrane of Gram-positive bacteria. [26]

Vancomycin acts by binding the carboxy-terminal d-Ala-d-Ala peptides of the polymeric lipid-PP-disaccharide-pentapeptides, which interferes with the cross-linking of these chains in the growing peptidoglycan cell wall [25].

The synthesis of peptidoglycan in the production of bacterial cell walls requires several steps. Peptidoglycan layer of the cell wall is rigid due to its highly cross-linked structure. During the synthesis of the peptidoglycan layer of bacteria, in the cytoplasm, a racemase converts l-alanine to d-alanine (d-Ala), and then two molecules of d-Ala are joined by a ligase, creating the dipeptide d-Ala-d-Ala. The dipeptide then binds to N-acetylmuramic acid and N-acetylglucosamine. These new building blocks get inserted into the membrane. The enzyme transpeptidase forms peptide cross links by transpeptidation. Vancomycin binds with high affinity to the d-Ala-d-Ala C-terminus of the pentapeptide and prevents the transpeptidase from acting on these new formed blocks and thus prevents cross-linking of the peptidoglycan layer. As a result, the peptidoglycan layer gets less rigid and more permeable. This leads to the death of the bacteria [27].

There are several ways for bacteria to be resistant to vancomycin. One of them is replacement of the C-terminal d-Ala residue by d-lactate (d-Lac) or d-serine (d-Ser). When the terminal Ala is transformed to Lac, the amide group of the Ala is replaced by oxygen modifying the vancomycin-binding site. With this transformation the hydrogen bond of the Ala terminal is lost decreasing the binding affinity of vancomycin 1000 folds. [28]

In Fig. 2.8. the scheme on the left represents Vancomycin binding to the cell wall peptidoglycan, N-acyl-d-Ala-d-Ala, to inhibit the cell wall synthesis. The right scheme represents the modified cell wall peptidoglycan, N-acyl-d-Ala-d-Lac, removes one hydrogen bond between vancomycin. The dashed lines represent the hydrogen bonds between vancomycin and the ligand of bacterial cell wall. The solid arrow shows a charge-charge interaction between the N-terminus of vancomycin and C-terminus of the ligand [28].

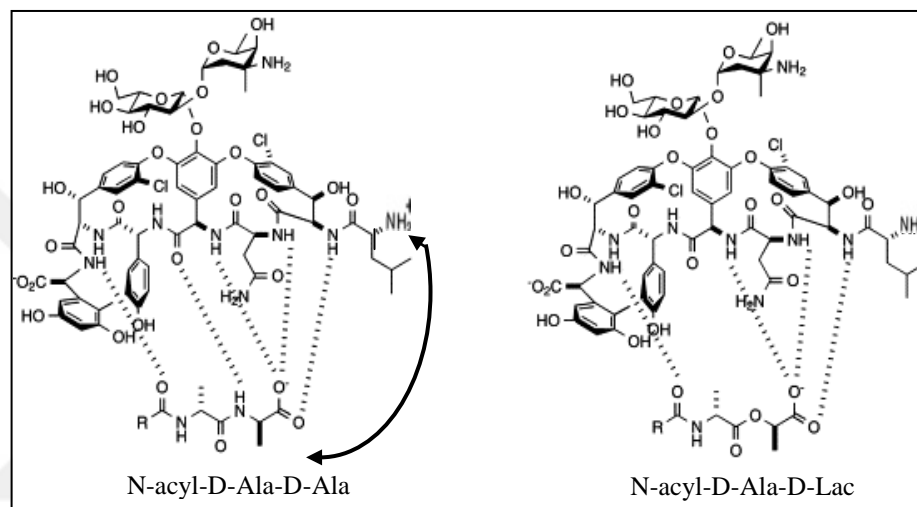


Figure 2.8. Action of Vancomycin [7], [21]

Fig. 2.9. shows vancomycin inhibiting of cell wall crosslinking (a) and a vancomycin resistant bacteria (b). At first step vancomycin is added to the bacterial environment during the synthesis of new cell wall. The cell wall strands are not crosslinked yet. At the second step vancomycin binds to the two d-Ala residues on the end of the peptide chains. In resistant bacteria, the last d-Ala residue has been replaced by a d-lactate, which prevents vancomycin to bind building blocks. At the third step in sensitive bacteria the vancomycin bound to the peptide chains prevents interaction with the cell wall crosslinking enzyme. In resistant bacteria, stable crosslinks are successfully formed. At the fourth step in sensitive bacteria the cell wall falls apart since crosslinks cannot be formed.

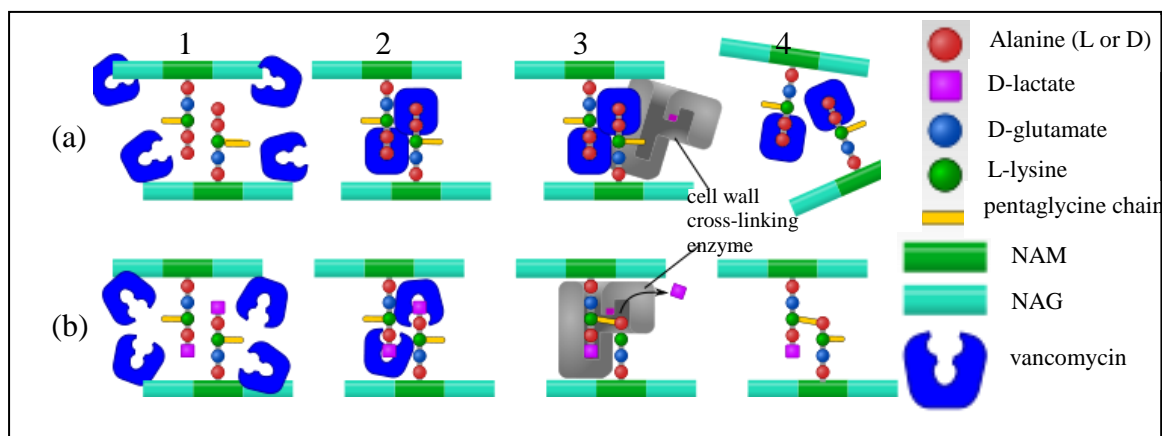


Figure 2.9. Mechanism of vancomycin action and resistance in sensitive (a) and resistant (b) bacteria.

## 2.5. DRUG DELIVERY

Drug delivery systems are improved and become varied in order to introduce therapeutic agents to the body. In earlier ages the examples of drug delivery are chewing leaves and inhaling smokes of the burned herbs. However the need for dosaging the drugs lead the development of syrups, tablets, and capsules etc, which mainly carries the actives of plant extracts. Modern medicine started to develop with the discovery of vaccines and penicillin. Conventional drug delivery methods include oral, topical, inhalation or injection [29].

The biological effects of the therapeutic agents are the result of the interaction of the drug with specific receptors. The aim of each delivery system is to increase the action of the therapeutic agents, with correct amount of drug at correct rate and timing.

Aforementioned conventional methods have various disadvantages. Topical treatment has an effect which is limited to dermatology rather than systemic effects. Injection methods are highly invasive. Also application of injection methods requires the help of health officers. Among these oral delivery is very prevalent. However, the physical constraints of the active material as poor solubility and absorption characteristics, tendency to degrade in alimentary canal, limit the usage area. [29]

To overcome the limitations of conventional delivery systems, novel ones, including carriers, are being developed. For novel drug delivery systems carriers as liposomes,



nanoparticles, nanotubes, polymers are utilized. Fig. 2.10 shows different types of nanocarriers that can be produced due to specific requirements for targeted drug delivery.

### **2.5.1. Nanoparticles as Drug Delivery Vehicles**

Nanomaterials have a size range between 1 and 100 nm with various shapes and forms. When a material is produced in nanoscale, surface area of the material increases. This surface area increase gives nanoparticles the ability to bind, adsorb and carry with drugs. [30]. Nanoparticles have high water solubility. This property is an advantage while carrying insoluble drugs to body as usage of toxic solvents is eliminated. With nanocarriers the release kinetics of the drugs can be adjusted due to the media conditions as pH and also external effects as ultrasound or heat. This tailor made drug release property precludes the drug accumulation and toxicity in blood [31].

Dendrimers are highly branched polymeric macromolecules, which can be both produced synthetically and naturally. Due to their well-defined shape, high density of functional groups, internal cavities and monodisperse size, dendrimers are used for treatment of viral diseases and cancer therapy. Dhanikula and coworkers studied the polyether-copolyester dendrimers for drug delivery to brain. As blood brain barrier is the main issue for drug delivery to brain, the aforementioned properties of dendrimers are utilized. The functional surface groups can conjugate ligands for transport through blood-brain barrier, and internal cavities give ability to carry drugs. The studied dendrimers were found to be nontoxic at high concentrations and increase in polyethylene glycol surface modifications increases the permeability across blood brain barrier [32].

Nanotubes and fullerenes emerge as a new delivery mechanism for drugs. Fullerenes can be defined as nanoscaled carbon cages. It was reported by Montellano and coworkers that water soluble fullerene derivative C<sub>60</sub> was used for the delivery of drugs such as paclitaxel and dexamethasone for cancer therapy, and delivery of some hormones [33]. As a member of nanotube class, carbon nanotubes gain attention for delivery of drugs. Unmodified carbon nanotubes are insoluble in water so surface modification and functionalization processes should be performed in order to increase the biocompatibility of carbon nanotubes. There is a wide application area for carbon nanotubes in drug delivery as patches for transdermal drug delivery, in cancer treatment and tissue regeneration. [34]

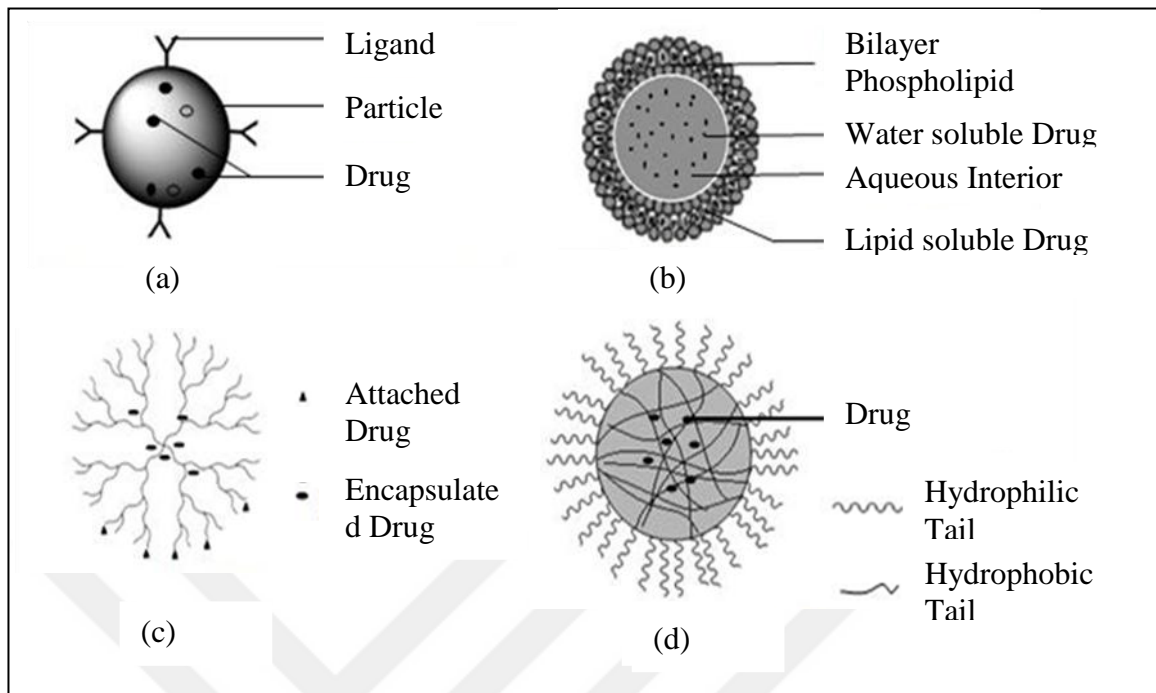


Figure 2.10. Different types of nanocarriers in drug delivery (a) Polymeric nanoparticles with targeting ligands, (b) Nanoliposome, (c) Dendrimer, (d) Micelle coated with polyethylene glycol [30]

Liposomes and polymeric carriers are covered in the following sections.

### 2.5.2. Liposomes as Drug Delivery Vehicles

Liposomes are particles with a lipid bilayer surrounding an aqueous core. The lipid bilayer acts as a membrane and gives ability to encapsulate aqueous solutions within the core, and hold lipophilic molecules on the bilayer. Thus, liposomes incorporate water-soluble and lipid-soluble molecules in aqueous and lipid phases, respectively giving ability to carry both hydrophilic and hydrophobic drugs as shown in Fig. 2.11 [35,36,37]. Prolonging the biological half-life of drugs in the body, reducing toxicity and modifying drug adsorption are achieved with drug delivery systems involving liposomes, leading to the reduction of negative effects of drug while the therapeutic efficacy is maintained [38].

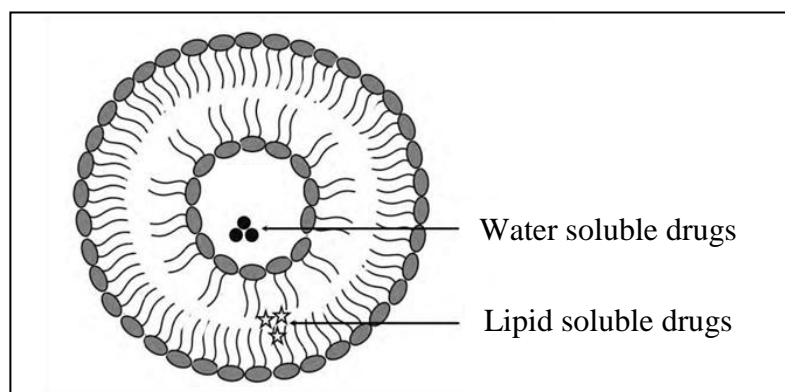


Figure 2.11. Liposomes used as drug delivery vehicles [39]

The hydrophilic drugs are dissolved in aqueous phase during liposome preparation and as a result the drug is captured during the formation of liposomes. Encapsulation efficiency of hydrophilic particles is usually very low and depends on the preparation methods of liposomes [39]. And through years different preparation methods have been proposed to increase the encapsulation efficiency of hydrophilic drugs in liposomes. Conventional methods of preparing liposomes include hydration of dry lipid film, adsorption of dissolved lipids at liquid interfaces and precipitation of lipids.

In the study of Xu and coworkers a mathematical model was proposed to predict the encapsulation of hydrophilic drugs in liposomes assuming all the carriers are spherical, there are no drug-lipid interactions, the drug is fully water soluble and spread equally on lipid layer. The final correlation that was built depends on the carrier particle size, measured experimentally with a particle sizer, lipid molecular surface area, characterized by a specific instrument, lipid concentration and lipid bilayer thickness. Among these parameters lipid surface area is known to be highly affected by the media conditions. As most lipids have ionic character in nature, the ionic strength of the media, affects the lipid surface area. The comparison of the developed model with earlier experimental studies shows significant resemblance, indicating that the method can be used during the early stages of formulation to predict drug encapsulation efficiency for hydrophilic molecules in unilamellar liposomes. [40]

The advantages of liposomal drug delivery can be listed as following. Controlled pharmacokinetics and pharmacodynamics of liposomes increase the circulation time of a drug in body keeping drug levels constant for longer time with respect to conventional

drugs. Modifications performed on liposome membrane enable target selective drug delivery. These modifications may include changing the charge of the membrane or adding different molecules in order to increase the affinity, producing liposomes sensitive to pH and temperature changes etc. [39] In the study of Salem, it was proven that anti-tuberculosis drugs encapsulated with liposomes showed increased efficacy with respect to free form of the drug [41]. Also in the study of Papagiannaros and coworkers it was shown that the toxicity levels of free drugs are reduced with liposomal carriers, even though no enhanced efficacy against pathogen is observed. [42]

The basic disadvantage of liposomal drug delivery is the high cost required for production. The sterilization of liposomes is an issue. However some methods were proposed by Sharma and New which include filtration of liposomes through a membrane filter. This method seems practical but ineffective for small pathogens such as viruses. The short shelf life and stability are major two disadvantages of the liposomal drug delivery, for which some methods such as freeze drying are proposed to increase the shelf life of the drugs encapsulated with liposomes. [39]

### **2.5.3. Polymers as Drug Delivery Vehicles**

In drug delivery applications polymers are being favored due to their surface properties as; hydrophilicity, lubricity, surface energy and bulk properties as molecular weight, solubility, release mechanism, adhesion. However the selection or design of polymer for a drug delivery application needs an understanding of the specified target by means of desired chemical, interfacial, mechanical and biological functions. [43] Table 2.2 shows the various types of polymers used in drug delivery applications.

The drug may be encapsulated by a polymer or may be entrapped in a polymer matrix. Polymeric drug delivery vehicles especially coated with hydrophilic polymers have better circulation times with respect to conventional systems. Thus this kind of systems is used for the drugs with short half lives in order to enhance their efficacy. [30]

In drug delivery applications the most important properties for a carriage system are biodegradability and biocompatibility. The carrier materials must be biocompatible, meaning non-toxic in order to prevent tissue damage. [44] The release mechanism of the

drug depends on the degradability of the carrier. The mechanisms can be drug diffusion-controlled, water diffusion-controlled (swelling controlled, and erosion. Fig. 2.12 represents the drug release mechanism of polymeric drug delivery vehicles.

Table 2.2. Representative list of polymers used in drug delivery [43]

Classification	Polymer
<b>Natural Polymers</b>	
Protein based polymers	Collagen, albumin, gelatin
Polysaccharides	Agarose, alginate, carrageenan, hyaluronic acid, dextran, chitosan, cyclodextrins
<b>Synthetic Polymers</b>	
Biodegradable	
Polyesters	Poly(lactic acid), poly(glycolic acid), poly(hydroxy butyrate), poly( $\epsilon$ -caprolactone), poly( $\beta$ -malic acid), poly(dioxanones)
Polyanhydrides	Poly(sebacic acid), poly(adipic acid), poly(terphthalic acid) and various copolymers
Polyamides	Poly(imino carbonates), polyamino acids
Phosphorus based polymers	Polyphosphates, polyphosphonates, polyphosphazenes
Others	Poly(cyano acrylates), polyurethanes, polyortho esters, polydihydropyrans, polyacetals
Non-Biodegradable	
Cellulose derivatives	Carboxymethyl cellulose, ethyl cellulose, cellulose acetate, cellulose acetate propionate, hydroxypropyl methyl cellulose
Silicones	Polydimethylsiloxane, colloidal silica
Acrylic polymers	Polymethacrylates, poly(methyl methacrylate), poly hydro(ethyl-methacrylate)
Others	Polyvinyl pyrrolidone, ethyl vinyl acetate, poloxamers, poloxamines

If the polymer is not bio-degradable, the accumulation of the drug in the body must be avoided. This kind of polymers is generally favored in transdermal implants [45]. For non-biodegradable drug delivery systems release mechanism is mainly diffusion-controlled. In the mechanism drug diffuses through the pores of the carrier or through a polymeric membrane in order to enter the bloodstream.

The need for degradable drug delivery systems emerge when researchers found that the removal of non-degradable implants from body was difficult and leaving foreign materials

in body may cause toxicity. However there are some disadvantages of the degradable systems that a high initial drug release is observed due to a burst in most systems. [46]

If the polymer is biodegradable, water penetrates the polymeric matrix, the length of polymer chain shortens which causes a decrease in the molecular weight of the polymer. This process is bulk erosion of the polymer. Surface erosion mechanism would also take place, if the penetration rate of water into matrix is slower than the conversion rate of polymer to water soluble materials. Mostly bulk erosion process is favored in drug delivery systems with biodegradable polymer vehicles. [43] However, especially for hydrophilic matrices both mechanisms are observed. Polymers containing more reactive groups as polyanhydrides tend to degrade via surface erosion, while polymers containing less reactive groups as poly (lactic-co-glycolic acid) tend to degrade via bulk erosion. [47] The degradation time of the polymer varies from a few days to years. The degradation product depends on the nature of the polymer and may be non-toxic acids or alcohols. The elimination time of these products from body is affected by their chemical linkage, molecular weight and solubility. In the case of swelling controlled drug release mechanisms, initially carriage system is dry and when delivered to body adsorb water or other body fluids and swell. Swelling creates voids through interior polymer and enables the diffusion of the drug to body environment.

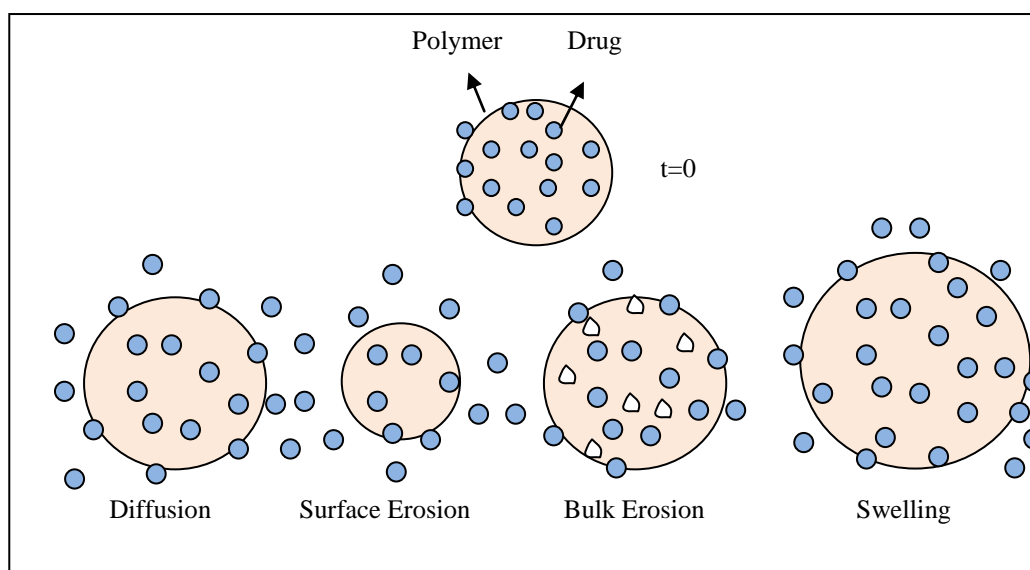


Figure 2.12. Drug release mechanisms of polymeric drug delivery vehicles

#### 2.5.4. Vancomycin Delivery to Body

Vancomycin is generally used in intravenous way to utilize veins during delivery of the drug in soft tissue. Also it is used for intestinal infections as it is not absorbed in blood when taken orally.

It was reported by Gbureck and coworkers that vancomycin is used in implants or bone cements, as modification of implants with antibiotics enables a direct and a well-defined application of drugs to infected hard tissue [48]. Also this method is suggested by Gautier and coworkers. The study includes loading vancomycin into a biomaterial, calcium-phosphate, which is reported to be resorbed and replaced by bone in a few weeks that no other surgical operations are needed to remove the carriage from body [49]. Ginebra and coworkers reviewed the cement systems composed of calcium phosphate used for antibiotic delivery. [50]

Some studies were performed for different ways to introduce vancomycin to body. As an example Khangragool and coworkers studied ocular delivery of vancomycin by using a polycationic biopolymer, chitosan as a carriage while the conventional methods include dispersion of vancomycin in artificial tears or saline solution [51]. For ocular delivery Gavini and coworkers studied poly(lactide-co-glycolide) microspheres, prepared by emulsification followed by spray drying method, for delivery of vancomycin.[52]

Yang and coworkers suggested a pH-sensitive carriage system, composed of carboxylic acid modified silica rods and poly- (dimethyldiallylammonium chloride) for delivery of vancomycin. Vancomycin is stored in the carriage and released when the pH of the medium changes [53].

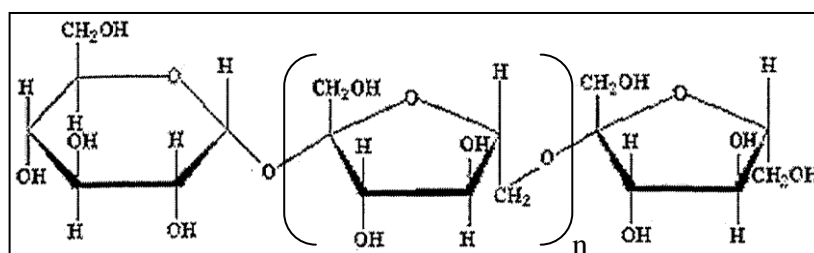
Other than the aforementioned ones, there are various types of carriage systems for vancomycin delivery reported such as hydrogels, collagens, layered polymeric nanogels, etc. [54, 55, 56].

Among the materials used for delivery of drugs naturally derived polymers as polysaccharides became on focus in recent years. The similarity of these polymers with the extracellular matrix in body is the main reason for using naturally derived materials. The examples consist of starch, chitosan, alginate and so on [44].

In this study, a naturally derived polymer levan, which is composed of fructose units, is selected as carrier for vancomycin delivery.

## 2.6. LEVAN

Levan is a linear biopolymer which is composed of fructose monomers. It is naturally produced by both plants and microorganisms. Microorganism based levan is more industrially applicable. However due to its high cost usage of levan is limited. There are different kinds of bacteria which are known to produce levan such as *Acetobacter*, *Aerobacter*, *Azotobacter*, *Bacillus*, *Corynebacterium*, *Erwinia*, *Gluconobacter*, *Mycobacterium*, *Pseudomonas*, *Streptococcus*, and *Zymomonas*. Levans produced by bacteria have molecular weight ranging from 0.5 million to 40 million, which highly depends on the branching of the biopolymer. However, levans produced by plants have smaller molecular weight, under 10,000 g/mol, with respect to microbial ones [57]. Uppuluri studied production of levan with *Acetobacter xylinum* NCIM 2526 [58]. Also Küçükaşık and coworkers studied the production of levan with *Halomonas* sp. which is a halophilic bacteria, in semi-chemical medium containing sucrose. [59] Fig. 2.13 shows the molecular representation of levan.



2.13. Levan molecular structure [60]

Levan is a biocompatible and water soluble polymer. However, it does not swell in water which makes it a useful material for tablets if dissolution is required in a short time after digestion. The structure of levan is densely packed spherical structure, which is enhanced by the flexibility of fructose rings. This dense packed structure provides low intrinsic viscosity even for high molecular weight [57]. Also branches of levan entangled from the surface of the spherical structure contribute its cohesion, which brings levan strong



adhesive properties. Other properties of levan include high solubility in oil, heat, acid and alkali stability. Also it has high chemical holding capacity which makes levan an attractive material for medicine. [59] Levan has good film forming properties. Also if the film forming is supported by plasticizing agents as glycerol, flexible films may be obtained. Sima and coworkers studied matrix-assisted pulsed laser evaporation for the controlled growth of biopolymer films in nano-scale [61].

Pharmacological and biological properties of biopolymers may be empowered by chemical modifications. Previous studies show the immunological properties to be affected by the C3-C4 and C6 regions of polysaccharides. Gonta studied oxidation with potassium periodate, reduction with sodium borohydride, and modification of oxidised levan with hydrazine, glycine, diglycine and triglycine [62]

Sezer and coworkers studied levan-based nanocarrier system for drug delivery. In the study bovine serum albumin-encapsulated levan nanoparticles were prepared and levan produced from *Halomonas sp.* was found to be a compatible carriage system for proteins and peptides [63]. Also they used these findings in another study showing levan nanoparticles may be used as carriages for vancomycin experimentally. [64]

In this study molecular dynamics simulations are carried out complementary to the study of Sezer and coworkers. Vancomycin drug is encapsulated with levan bio-polymer and release mechanism is mimicked by performing the simulations of encapsulated molecules in aqueous media. Also the effect of modification in biopolymer structure is investigated as levan chains are modified with sulfate groups.

### 3. METHODOLOGY

#### 3.1. MOLECULAR DYNAMICS

Molecular dynamics (MD) simulations are principal tools in the theoretical study of biological molecules and it is used to mimic the behavior of molecules and molecular systems [65]. In these simulations, molecules are computationally generated and then allowed to move within the system parameters for a certain amount of time giving information on conformational changes, molecular interactions and cluster behaviour of the molecules involved. MD simulations are being utilized complementary to experiments as simulations which are designed according to experimental conditions and parameters shows the molecular behavior of these systems at that specific condition [66]. Also a fully atomistic point of view, MD simulations provide detailed information on the fluctuations and conformational changes of molecules [67]. The information obtained from MD simulations shed light on changes that would otherwise be untraceable by experimental methods.

Molecular dynamics was first introduced as one of the simulations by the study of Alder and Wainwright on dynamics of liquids in 1957. Then in 1964 Rahman's study on MD of liquid argon was the next advance in the field. Regarding the advances in technology MD has been used since the early 1970's as a valuable tool in chemistry and physics to study more complex systems such as proteins, macromolecules, etc [68].

MD simulations require three different stages; energy minimization, equilibration, and dynamics. Before dynamic simulations, it is important to have a molecular system at the lowest potential energy state which is achieved by energy minimization step. Minimum energy arrangements of the atoms correspond to stable states of the system. In an MD simulation, more than one energy minimums, stable states can be achieved. These points can be classified as local and global energy minimums. Local energy minimum corresponds to a relative minimum energy, where global minimum represents the absolute minimum energy of the system. Energy minimization looks for the nearest local energy minimum to the starting conformation. It may require extended amount of computing

power and time to find the global minimum in a system. However, with energy minimized systems it is easier to find a global energy minimum through the simulation. There are several algorithms used for energy minimization. A minimization is considered converged if the root mean squared deviation of the gradient is approximately zero. In addition, the energy changes from one step to the next step should be very small when the minimization is close to convergence [69]. Energy minimization physically means a point where no atom in a static structure feels a net force which corresponds to a temperature of 0 K. To start the energy minimization step set of coordinates of atoms in the system and functions provided by assigned force field are required.

In order to start the MD simulations system must be elevated to a temperature of interest, as at minimization step the system is considered to be at 0 K. At equilibration or initialization stage by changing the velocities of each atom a new temperature is obtained. This kinetic energy change is distributed to the system and is converted to potential energy.

Dynamic or production stage determines thermodynamic averages and samples new structural characteristics and dynamics. Time dependent behavior of a molecular system is calculated with computational method and the atomic trajectories of a system of  $N$  particles are generated by numerical integration of Newton's equation of motion,  $F=ma$ , for a specific inter atomic potential, with certain initial condition (IC) and boundary condition (BC). As the force on each atom is calculated, it is possible to determine the acceleration of each atom in the system. Then equations of motion are integrated to give positions, velocities and accelerations of atoms with respect to time. The method is deterministic; once the positions and velocities of each atom are known, the state of the system can be predicted at any time in the future or the past [70]. The simple flow chart of molecular dynamics is represented in Fig. 3.1.

The different spatial arrangements that a molecule can adopt due to rotation about single bonds are called conformations and these conformations can be identified at minimum potential energy levels as mentioned previously. One molecule can have more than one local energy minima. However, to find the most stable conformation one should look for global energy minimum. Fig. 3.2 represents the energy state and conformation relation of a molecule through a MD simulation. Initial coordinates have bad contacts causing high energies and forces. As stated in energy minimization case, the aim is to reach the nearest

energy minimum. At equilibration stage with low energy barriers due to temperature change local minima is overpassed. In production stage with assigned forcefields atoms are allowed to move. If this stage is long enough different conformations can be observed, especially if the energy obtained by temperature is high.

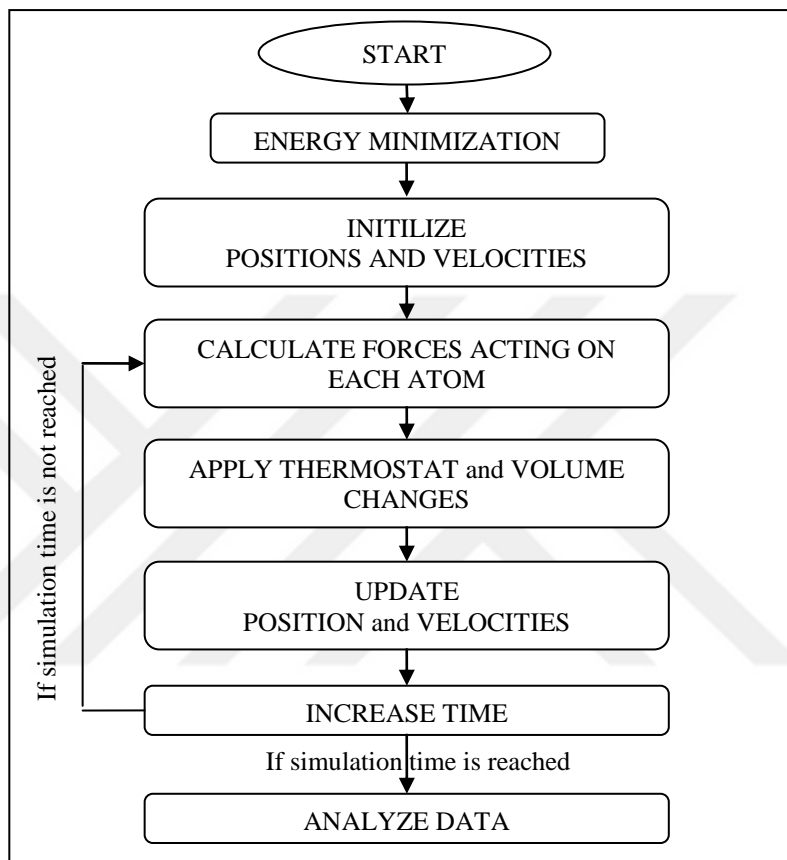


Figure 3.1. Flow Chart of Molecular Dynamics

Antipas and coworkers used molecular dynamics simulations to investigate the pH dependent conformations of vancomycin. The simulations were performed for two different pH values where the changes in pH were modeled by changing the ionization states of vancomycin. At pH 4 vancomycin is a monocation, whilst at pH 9 it is a monoanion. Conformation at pH 9 was found to be more expanded than the conformation at pH 4. The expanded structure results in an increase in the distance between reacting protonated amine and deprotonated carboxy group. [23]

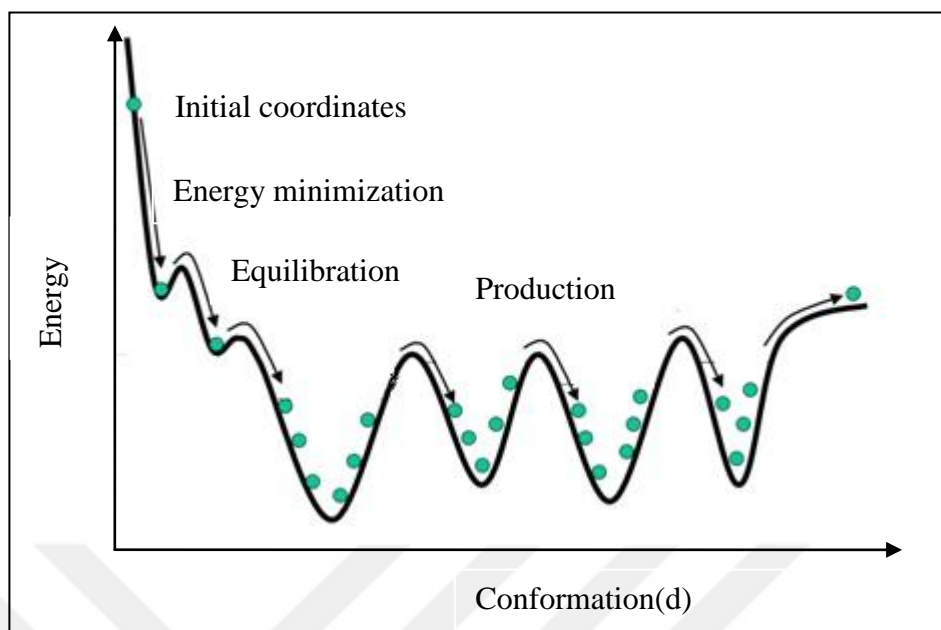


Figure 3.2. Energy vs Conformation through Molecular Dynamics Simulation Stages

In this study molecular dynamic simulations are used to investigate conformational changes of the vancomycin molecule in different conditions. After observing different stable conformations of the molecule, e.g. in conditions which mimic the body conditions, the resulting data would be used in drug delivery design. From experimental studies the compositions of media in which vancomycin is prepared, encapsulated and delivered is obtained and these conditions are recreated in silico.

### 3.2. FORCE FIELDS

In MD simulations accuracy of the results highly depends on forces acting on the atoms, which can be considered as one of the limitations for the method. Forces acting on each atom are calculated by force fields which are used with empirical parameters of electrostatic and van der Waals interactions, bond and angle vibrations, and internal torsion rotations to predict the molecular structures and potential energies [71],[72]. So to avoid errors and inaccurate results selection of force field is important [70].

A force field describes the dependence of the energy of a system on the coordinates of its particles by using mathematical expressions. It consists of an analytical form of the inter

atomic potential energy, and a set of parameters entering into this form. The parameters of a force field are typically obtained either from ab-initio or semi-empirical quantum mechanical calculations or by fitting to experimental data such as neutron, X-ray and electron diffraction, NMR, infrared, Raman and neutron spectroscopy, etc [73]. Also it is used to describe the time evolution of bond lengths, bond angles and torsions, also the non-bonding van der Waals and electrostatic interactions between atoms.

A typical expression for a force field is represented in Eq. 3.1. The first four terms, bond, angles, torsions and impropers are local contributors to total energy, which can also be mentioned as intramolecular contributions. The last two terms express the repulsive, Coulombic and Van der Waals interactions.

$$\begin{aligned}
 U = & \sum_{bonds} \frac{1}{2} k_b (r - r_0)^2 + \sum_{angles} \frac{1}{2} k_a (\theta - \theta_0)^2 \\
 & + \sum_{torsions} \frac{V_n}{2} k_b [1 + \cos(n\phi - \delta)] \\
 & + \sum_{improper} V_{imp} + \sum_{LJ} 4\epsilon_{ij} \left( \frac{\sigma_{ij}^{12}}{r_{ij}^{12}} - \frac{\sigma_{ij}^6}{r_{ij}^6} \right) + \sum_{elec} \frac{q_i q_j}{r_{ij}}
 \end{aligned} \tag{3.1}$$

Intramolecular forces hold the atoms of a molecule together and are stronger than intermolecular forces, which are present between molecules. Chemical bonds between atoms can be considered as springs, of which stretchings are represented with harmonic function controlling the bond length. In bond stretching term  $r$  is the distance between two bonds, and  $r_0$  is the equilibrium bond length, which can be obtained from X-ray diffraction experiments. The spring constant  $k_b$  can be estimated from Raman or infrared Spectroscopy. The limitation with MD studies using force field approach is that the harmonic function of bond stretching term describes the bonds as unbreakable. Thus, no chemical reaction can take place. Bond angle bending term, which is also defined as harmonic function, represents the oscillations of three atoms about an equilibrium bond angle  $\theta_0$ . If the molecule in concern has more than four atoms in a row, the torsion (dihedral) term should be added to system. Torsional motions in the system define the rigidity of the molecule and with the torsional rotations conformational changes occur. Torsional energy is usually represented by a cosine function, where  $\phi$  is the torsional angle,  $\delta$  is the phase,  $n$  defines the number of minima or maxima between 0 and  $2\pi$ , and  $V_n$  determines the height of the potential barrier. The torsional parameters are usually derived

from *ab initio* calculations and then refined using experimental data such as molecular geometries or vibrational spectra. For planarity of particular groups an additional improper term is required, as aforementioned normal torsion terms are not sufficient to represent planarity.[73]

Intermolecular forces which are also called as non-bonded interactions are represented with Van der Waals interactions and electrostatic interactions like Coulombic interactions. Van der Waals interactions between atoms emerge from the balance between repulsive and attraction forces other than those due to bond formation or electrostatic interactions. Usually 12-6 Lennard Jones (LJ) potentials are used to represent Van der Waals interactions as it combines the attractive and repulsive forces.  $\epsilon$  is the minimum potential energy, located at  $r = 2^{1/6}\sigma$  and  $\sigma$  is the diameter of the particle, since for  $r < \sigma$  the potential becomes repulsive. The attractive term has an inverse 6<sup>th</sup> power term, whilst the repulsive term has an inverse 12<sup>th</sup> power term. A higher order repulsive term often causes overestimation of pressure for dense systems. The power terms of the Lennard Jones interaction can be replaced by weaker or stronger terms. [74] Short range interactions as Van der Waals interactions take into account only neighbored particles up to a certain cutoff distance. If electrostatic charges are present Coulomb potentials are added. This term uses Coulomb's law to compute the contribution of assigned partial atomic charges to total energy. Commonly *ab-initio* calculations and quantum mechanics derivations are used to obtain partial charges for each nucleus. Coulomb potential is considered to be a long range interaction, where interactions between all particles in the system are taken into account.

The force fields using an energy expression similar to equation (3.1) are called class I force fields. Class I force fields include CHARMM, which is used to simulate a variety of systems, from small molecules to complex large biological macromolecules [75], AMBER, which is widely used for proteins [76], CVFF, which is a classic forcefield used to simulate peptide and proteins. First generation class I force fields are mainly applicable to biochemistry. Secondary generation, class II force fields include extra term for hydrogen bonding potential and are capable of predicting many properties. Hydrogen bonding can be included by an choice of van der Waals parameters and partial charges, but sometimes an extra term is utilized to improve the accuracy of the H-bonding energy. The larger quantity of force field parameters yields more complexity in this class. Among other Class II force

fields as Merck Molecular Force Field (MMFF94), Consistent Force Field (CFF) [73] family of forcefields are parameterized against a wide range of experimental observables for organic compounds containing H, C, N, O, S, P, halogen atoms and ions, alkali metal cations, and several biochemically important divalent metal cations. All the CFF forcefields (CFF91, CFF, PCFF, COMPASS) have the same functional form, differing mainly in the range of functional groups to which they were parameterized. According to studies the CFF force fields are found to be more effective on reproducing experimental results more accurately than classical forcefields [73]. Polymer consistent force field (PCFF) is a class II force field derived from CFF91 force field, where the nonbonded interactions are composed of a 9-6 Lennard Jones potential (van der Waals) and a Coulombic pairwise (electrostatic) interaction [69]. PCFF is used for polymers and organic materials. The functional form of PCFF can be shown in Eq. 3.2.

First three term of the equation belongs to bonded energy terms. (1) covalent bond stretching energy term (2) bond angle bending energy term (3) torsion angle rotation energy term. The improper term is represented as a harmonic function (4). Cross interactions terms, which are represented with five terms in the function, include dynamic variations among bond stretching, bending and torsion angle rotation (5-10). Van der Waals interactions and Coulombic interactions are represented with the last two terms of the function respectively (11-12).

In this study PCFF is selected for molecular dynamics simulations as this force field was developed for polymers and organic molecules. The systems simulated in this study consist of levan and vancomycin, which are a biopolymer and a drug respectively. PCFF can be applied for both molecules.



$$\begin{aligned}
U = & \sum_{bonds} [K_2(b - b_0)^2 + K_3(b - b_0)^3 + K_4(b - b_0)^4] \\
& + \sum_{angles} [H_2(\theta - \theta_0)^2 + H_3(\theta - \theta_0)^3 + H_4(\theta - \theta_0)^4] \\
& + \sum_{torsions} \{V_1[1 + \cos(\varphi - \varphi_1^0)] + V_2[1 + \cos(2\varphi - \varphi_2^0)] \\
& + V_3[1 + \cos(3\varphi - \varphi_3^0)]\} \\
& + \sum_{improper} K_x x^2 + \sum_b \sum_{b'} F_{bb'}(b - b_0)(b' - b'_0) \\
& + \sum_{\theta} \sum_{\theta'} F_{\theta\theta'}(\theta - \theta_0)(\theta' - \theta'_0) \\
& + \sum_b \sum_{\theta} F_{b\theta}(b - b_0)(\theta - \theta_0) \\
& + \sum_b \sum_{\varphi} (b - b_0)[V_1 \cos \varphi + V_2 \cos 2\varphi + V_3 \cos 3\varphi] \\
& + \sum_{b'} \sum_{\varphi} (b' - b'_0)[V_1 \cos \varphi + V_2 \cos 2\varphi + V_3 \cos 3\varphi] \\
& + \sum_{\varphi} \sum_{\theta} \sum_{\theta'} K_{\varphi\theta\theta'} \cos \varphi (\theta - \theta_0)(\theta' - \theta'_0) + \sum_{LJ} 4\epsilon_{ij} \left( \frac{\sigma_{ij}^9}{r_{ij}^9} \right. \\
& \left. - \frac{\sigma_{ij}^6}{r_{ij}^6} \right) + \sum_{elec} \frac{q_i q_j}{r_{ij}}
\end{aligned} \tag{3.2}$$

### 3.3. ENSEMBLES

Macroscopic properties of a large system are identical to microscopic configurations. Thus, it is possible to guess properties of a system without investigating detailed motion of every particle in the system [77] by taking averages of every possible system that have similar macroscopic but different microscopic properties [78]. These ensemble averages correspond the formulations of macroscopic observables. Statistical ensembles are usually characterized by fixed values of thermodynamic variables such as energy, E; temperature, T; pressure, P; volume, V; particle number, N; or chemical potential,  $\mu$

Thermostats due to used ensembles are applied to system. Using thermostats one can keep temperature, energy and pressure of the system constant. If temperature is kept constant, thermostats which require a heat bath can be chosen. If pressure is kept constant systems with a barostat, one that controls pressure with the change of the volume can be used.

- **Canonical (NVT) Ensemble:** NVT ensemble describes a system with constant number of moles, N, constant volume, V, and constant temperature (average kinetic

energy),  $T$ . There are various ways to keep temperature constant as velocity scaling, weak coupling of the system in a heat bath, etc. Berendsen thermostat uses an external heat bath with fixed temperature to maintain the temperature. This heat bath acts as a reservoir of thermal energy that provides or removes heat when necessary to keep the temperature constant. The velocities are scaled at each step, such that the rate of change of temperature is proportional to the difference in temperature of the system  $T(t)$  and temperature of the heat bath  $T_{bath}$  [79]. When limit of coupling parameter approaches infinity Berendsen scheme becomes inactive and system behaves as microcanonical ensemble. [Hünenberger]. To reach a target temperature the Berendsen thermostat is highly efficient. Using the Nosé-Hoover thermostat is another method. In this case the heat bath becomes an integral part of the system by adding an artificial variable with an associated effective mass [73]. For most MD simulations, systems are initially equilibrated using the Berendsen thermostat in order to reach target temperature, while properties are calculated using the widely known Nosé-Hoover thermostat, which correctly generates trajectories consistent with a canonical ensemble.

- **Microcanonical (NVE) Ensemble:** NVE ensemble describes a system with constant number of moles,  $N$ , constant volume,  $V$ , and constant (Hamiltonian) energy,  $E$ . As these fixed parameters define an isolated system, NVE is not preferred for real systems. Generally, if the simulation system is sufficiently large, the small part of it may be considered as a canonical system. For large NVE systems the fluctuations in temperature are small, and it may be considered approximately constant [80]. Constant-energy simulations are not recommended for equilibration because, without the energy flow facilitated by the temperature control methods, the desired temperature cannot be achieved [81].
- **Isobaric-Isothermal (NPT) Ensemble:** In NPT ensemble number of moles,  $N$ , pressure,  $P$ , and temperature,  $T$ , are kept constant. The pressure is adjusted by adjusting the volume. The system exchanges heat with the thermostat and it also exchanges volume (and work) with the barostat [82]. This is the ensemble of choice when the correct pressure, volume, and densities are important in the simulation [81].

- **Grand Canonical ( $\mu VT$ ) Ensemble:** In the grand canonical ensemble, the chemical potential,  $\mu$ , the volume,  $V$ , and the temperature,  $T$  are kept constant. The total particle number  $N$  is therefore allowed to fluctuate. It describes systems in contact with a thermostat and a particle reservoir. The system exchanges heat with the thermostat and it also exchanges particles with the reservoir [82].

MD simulations which are performed to investigate of the behavior of a system at specific temperature should use NVT ensemble. In this study number of particles is constant. Constant temperature is assigned for the system to define the conditions. Also volume of the simulation box is defined. Thus, NVT ensemble is chosen for the study and in order to keep temperature constant, Nose-Hoover thermostat is used which provides most accurate trajectories of the atoms in system.

### 3.4. NUMERICAL INTEGRATION

Numerical integration is mainly used to find the new position and velocities of the atoms by Newton's equation of motion in terms of already known positions at time  $t$ , for a specific interatomic potential, with certain initial condition (IC) and boundary condition (BC).

$$F_i(t) = m_i a_i(t) \quad (3.3)$$

where  $F_i$  is the force,  $m_i$  is the mass, and  $a_i$  is the acceleration of atom  $i$ . The force on atom  $i$  can be computed from the derivative of the potential energy  $V$  with respect to the coordinates  $r_i$ :

$$-\frac{\partial V}{\partial r_i} = m_i \frac{\partial^2 r_i}{\partial t_i^2} \quad (3.4)$$

Molecular dynamics is usually applied to a large model. Thus, energy evaluation is time consuming and the memory requirement is large. Energy conservation is also important to generate the correct statistical ensembles. A good integrator should be fast, ideally requiring only one energy evaluation per timestep and should require little computer memory [83].

A standard method of solving an ordinary differential equation such as Eq. 3.3 numerically is the finite-difference method. When the initial coordinates and velocities and other dynamic information at time  $t$  are given, the positions and velocities at time  $t + \Delta t$  are calculated. The timestep  $\Delta t$  depends on the integration method as well as the system itself.

Although the initial coordinates are determined in the input file or from a previous operation such as minimization, the initial velocities are randomly generated at the beginning of a dynamics run, according to the desired temperature.

The efficiency of the molecular dynamics can be enhanced by stable algorithms for numerical integration. Although several algorithms have been proposed, the most commonly used is Verlet velocity integrator, which is an explicit algorithm. However, as integration time step is increased in explicit integration methods, systems tend to quickly become unstable. Implicit methods as Runge-Kutta Method can be used for systems requiring larger time steps [84].

First the position is updated according to the usual equations of motion, then at the new position acceleration is calculated. The new velocity is computed from the average of the two accelerations as shown in equations 3.5 to 3.7 [85].

$$r(t+\Delta t)=r(t)+\Delta t v(t)+\frac{\Delta t^2 a(t)}{2} \quad (3.5)$$

$$a(t+\Delta t)=\frac{F(t+\Delta t)}{m} \quad (3.6)$$

$$v(t+\Delta t)=v(t)+\frac{1}{2}\Delta t(a(t)+a(t+\Delta t)) \quad (3.7)$$

In the study the velocity Verlet integration is used to integrate the Newton's equation of motion to calculate the trajectories of particles in MD simulations. Despite its simplicity the Velocity-Verlet algorithm is very stable. The advantages of Verlet integrators is that these methods require only one energy evaluation per step, and require less computer storage, and also allow a relatively large timestep to be used [86].

### 3.4.1. Initial Conditions

Initial conditions as initial positions and velocities of each atom in the system are required to start the numerical integration in MD simulations. The velocity of each atom is assigned randomly according to desired temperature and then adjusted in order to set the angular momentum and the center of mass velocity of the total system to zero. [73]

### 3.4.2. Boundary Conditions

In MD simulations boundary conditions are classified as fixed or periodic boundary conditions while the boundary refers to the faces of the simulation box.

With fixed boundary conditions particles do not interact across the boundary and do not move from one side of the box to the other. If an atom moves outside the simulation box it is deleted on the next timestep that reneighboring occurs.

Using periodic boundaries is equivalent to considering an infinite, space-filling array of identical copies of simulation region. Fig. 3.3. shows the representation of periodic boundary conditions. The volume of interest is in the middle of the figure and it is surrounded by identical copies. If an atom leaves the simulation region through a face of the simulation box, it immediately reenters the region through the opposite face as shown in Fig.3.3. Also in that condition atoms that are near to one face of the simulation box, they also interact with the atoms in an neighboring copy of the system at the opposite, which is called the wraparound effect. This effect should be taken in to consideration during the integration of Newton's equation that if an atom's new trajectory is calculated to be out of the simulation region, its coordinates must be adjusted to bring it back [87].

Boundary condition of a system affects the types of interactions between atoms. In periodic boundary condition interactions between each atom and nearest periodic image is used for short range interactions. The distance between the interacting atoms should be smaller than a cut off distance. If the distance between atoms is larger than this cut off distance, the atoms do not interact. Periodic boundary conditions are not suitable for properties influenced by long range correlations. [89]

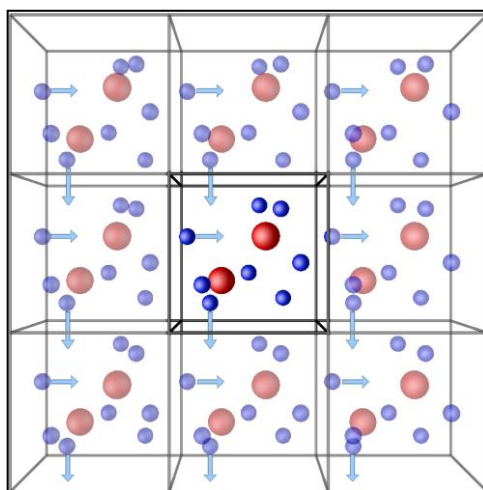


Figure 3.3. Periodic Boundary Conditions [88]

In this study periodic boundary conditions are chosen and the calculations are performed accordingly.

For creating the structures Xenoview [90] program is used due to its graphical user interface. However this graphical interface would be time consuming when dealing with large systems. Xenoview has various force fields and ensembles included. Simulation box size was set as 6.0x6.0x6.0 nm with periodic boundary conditions. The structures are then converted to LAMMPS [91] program. LAMMPS program run simulations without a graphical representation. It calculates and saves the new possible trajectories of the system. Also LAMMPS can divide the simulation into portions of the computer's processors with mpi mode, which shortens the simulation time. Polymer Consistent Force Field (PCFF) was applied to the simulations with 0.9 nm cut-off distance. NVT ensemble was applied with specified temperature and 1 atm pressure. After simulations are performed, graphical analysis of the system is done with VMD [92] program, which is a molecular graphics viewer, used for displaying static and dynamic structures, and for structure generation and dynamic analysis. Analysis of simulation data with obtained positions of each atom is performed with Python programming language.

### 3.5. ANALYSIS OF MD SIMULATION DATA

At the end of the MD simulations atomic positions and velocities are generated. These data are required to define structural, equilibrium and transport properties of a system. [89]

The structural properties include radius of gyration, end-to-end distance and radial distribution function. Equilibrium properties include temperature and energy of the system, where transport properties include thermal conductivity and viscosity.

Visual inspection with software such as VMD may be done to observe the movement of atoms in simulation. However this kind of information is subjective without any supporting data or calculation. Therefore, these structural properties are evaluated as described in the following sections.

#### 3.5.1. Radius of Gyration

The radius of gyration ( $R_g$ ), of a molecule, shown in Fig. 3.4, defines its dimensions. It is a measure of the size and compactness of a molecule and is calculated as the root mean square distance between its center of gravity and position of each atom as shown in Eq. 3.8. [93, 94, 95]

$$R_g^2 = \frac{\sum_{i=1}^N M_i (r_i - r_{mean})^2}{\sum_{i=1}^N M_i} \quad (3.8)$$

where  $M_i$  is the molecular weight of atom  $i$ ,  $r_{mean}$  is the center of mass of all atoms and  $|r_i - r_{mean}|$  is the distance of atom  $i$  to center of mass [95].

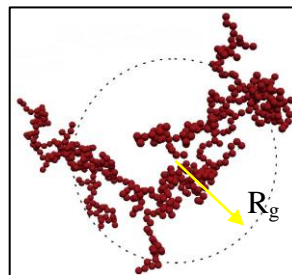


Figure 3.4. Radius of gyration of a molecule [96]

Radius of gyration of molecules in each system is calculated via the trajectory files created by LAMMPS. Trajectory files keep the position of each atom at each time step on the basis of three dimensional coordinates,  $x$ ,  $y$  and  $z$ . These data are used in a Python programming code in order to calculate average  $R_g$  [97]. The code calculates the  $R_g$  for each molecule in the system at each time step. Then these data are averaged to represent one average  $R_g$ .

To investigate the cluster behavior of each system,  $R_g$  analyses were performed for the cluster. Instead of treating each molecule separately, all atoms in the system are treated as one molecule. This would give an idea, how molecules as a group behave over a period of time. Increase in the cluster  $R_g$  through simulation time, would be an indication of dispersion of molecules in the medium. As the cluster  $R_g$  values of systems composed of one molecule are the same with the average  $R_g$  results of each molecule, these systems are not considered in cluster calculations.

### 3.5.2. Radial Distribution Function

The pairwise radial distribution function (RDF),  $g_{ij}(r)$  is used to express the density distribution of a species  $i$  as the function of distance from another species  $j$  [98]. This method is generally used to investigate the solvation dynamics, to determine the structure and dynamics of water around solute molecules [99]. Also hydrogen bonds are extracted from molecular dynamics simulations using RDF, which gives coordination of water molecules around the solute. However, it can not be assured that all neighbor water molecules are hydrogen bonded [100].

$$g_{ij}(r) = \frac{d\langle N_{ij}(r) \rangle}{4\pi\langle \rho_{ij} \rangle r^2 dr} \quad (3.9)$$

where  $N_{ij}(r)$  is the number of solvent molecules  $i$ , at a distance between  $r$  and  $r + \Delta r$  from solvent atom  $j$ , and  $\langle \rho_{ij} \rangle$  is the average solvent density within a spherical volume centered on solute atom  $i$  [99].

The integrated value of  $g_{ij}(r)$  ;

$$\langle N_{ij}(r) \rangle = \int g_{ij}(i) 4\pi i^2 di \quad (3.10)$$

gives the coordination number for the solvent around site  $j$  at a distance of  $r$  [99].



In this study RDF is used to investigate the behavior of water molecules around vancomycin molecule. For this purpose solvated systems which are treated explicitly are used. The number of water molecules interacting with specified atoms is calculated. Increase in the number may be associated with the solvation mechanism of the molecules.

### 3.6. TREATMENT OF SOLVENT IN MD SIMULATIONS

Computational approaches of solvents in molecular dynamics simulations can be classified as implicit and explicit treatment [101]. In MD simulations solvents play an important role to screen the electrostatic interactions. These interactions are can be modeled explicitly or implicitly. The schematic representation of both models is shown in Fig. 3.5.

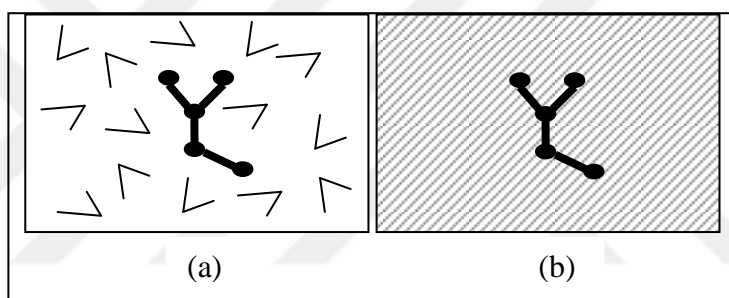


Figure 3.5. Atomic model of a solute (a) surrounded by explicit solvent molecules (b) in a solvent environment modeled implicitly

#### 3.6.1. Explicit Treatment of Solvent

In explicit method all solvent and the interactions in the simulation are described in a fully atomistic manner. The energy parameters of the system contain parameter characteristics of atoms included as mentioned in section 3.2. In both electrostatic and van der Waals equations summation extends over solute and solvent atom pairs that are not covalently bonded [101].

The calculated trajectory for explicitly treated systems provides detailed information on the time dependent atomic motions. In these kinds of systems large numbers of solvent molecules are required to mimic a real dense system, which requires a large fraction of computing power and time to simulate the detailed trajectory of the bulk solvent [102]. As

the solvent molecules are represented fully atomistic, the accuracy of the MD simulations increases, but at greatly increasing computational cost and time [103].

### 3.6.2. Implicit Treatment of Solvent

In implicit treatment method of solvent, rather than having each solvent atom, the effect of the solvent is mimicked with the use of dielectric constants. This approach considers the solvent to be a dielectric continuum. As the number of total atoms in the system decrease, the computational cost and time decreases [103]. However, this decrease in the system size may cause loss of detail and accuracy in simulations.

The dielectric constant of a material represents the collective response of its constituent molecules to electric fields. By definition, the dielectric constant of vacuum is 1 and it is the default value for a simulation if the dielectric constant is not assigned.

The values of the dielectric constant of water measured over the range 0.1° to 99° C fit the equation;

$$\epsilon=87.740-0.4008T+9.398 \times 10^{-4} T^2-1.410 \times 10^{-6} T^3 \quad (3.11)$$

where  $T$  is the temperature in degrees Celsius [104]. According to the equation above dielectric constant of water at 25° C was calculated as 78.304.

Other than these implicit and explicit methods, there emerged combined ones to have advantages of both systems. In one of these methods at least a part of the solvent receives explicit treatment while the remaining bulk solvent is treated implicitly as a continuum [101]. Another approach proposes that solvent molecules can be substituted by neutral spherical atoms, which reduces the total number of atoms, hence the computational effort significantly [103].

In this study before running simulations in aqueous medium, the implicit and explicit treatment methods of solvent are compared and based on the obtained results simulations are continued using explicit solvent despite the additional computational power and time.

### 3.7. SIGNIFICANCE TEST IN MD SIMULATIONS

After a data set is obtained from an experiment or from a simulation, significance test is used to investigate if the effect of a variable over a parameter of sample population is statistically significant. A test of significance compares observed data with a hypothesis. The estimation starts with the null hypothesis, which is a statement that there is no relation with the variable and parameter, where the alternative hypothesis states the existence of the relation between the variable and parameter. At the end conclusion is always given in terms of null hypothesis that it is either accepted or rejected. The result is concluded with a probability which is a measure of how much the data and hypotheses agree. Mostly in educational researches significance levels are 0.05 and 0.01. In general 0.05 and lower probability can be considered to be statistically significant.

In a system the data is divided into two groups as discrete and continuous data. If the data is discrete, it can only take particular values. It can be numeric that by rolling a dice one can only get numbers 1 to 6. Also discrete data can be categorical, as gender, color etc. If the data is continuous, it can be measured as weight, height, time, distance. Choice of the test method for the hypothesis firstly depends on the data gathered from an experiment. If the data collected is continuous and has a normal distribution then mean tests or standard deviation tests can be applied. If the data is discrete then proportion or count tests may be applied.

A normal distribution which describes the shape of the data plotted on a histogram or a frequency diagram in Fig. 3.6 is symmetric around its mean. It is often called “bell curve” distribution. The area under the distribution curve is 1.0, where 0.95 of the area is within two standard deviations of the mean. Many tests in statistics are based on the assumption of normality and normal distribution is the most favored distribution in statistics.

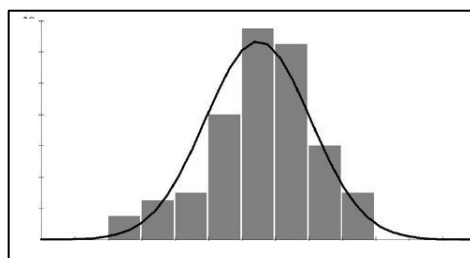


Figure 3.6. Normal Distribution

To test the significance of the difference between two means t-tests are mainly used. However, f-test is favored when the difference in standard deviations are tested. While comparing the means, three scenarios may take place. If one mean value is to be tested (1 sample t-test), then the hypothesis considers the equality of the mean with a specific target value. If means of two independent populations are compared (2 sample t-test), the hypothesis is built on the equality of the two means. The third option is to compare means of two dependent populations (paired t-test), where the difference of the two means is compared with a value or with zero.

In this study the means of radius of gyration are compared for different states and temperature. The data is normally distributed and continuous as it can be measured. In molecular dynamics simulations, the test is performed individually without pairing two data sets, that the simulation is repeated at different conditions. In this case, 2 sample t-test is used in order to test the null hypothesis.

The two sample t-test is performed to make inferences on the difference between two population means. First null hypothesis based on means is constructed. Then confidence intervals should be chosen. As mentioned before the confidence level is determined to be 0.05. If the calculations are performed manually critical t-value is found from the t-distribution table according to degrees of freedom. Degree of freedom for a 2 sample t-test is determined with the formula below;

$$v = [(n_1 - 1) + (n_2 - 1)] \quad (3.12)$$

Where  $v$  is degree of freedom,  $n_1$  and  $n_2$  corresponds to the number of sample data from first and second population respectively. As more than 1000 data points for each simulation exists, the degree of freedom is considered to be infinite and the critical t value is determined accordingly to be 1.960.

Means of the populations are calculated with equation 3.13 separately.  $x_{mean}$  is the mean of the data and  $n$  is the sample size.

$$x_{mean} = (\text{sum of data})/n \quad (3.13)$$

Then standard deviation for each population is calculated to give a pooled standard deviation, which defines the subgroup deviations as;

$$s = \sqrt{\frac{\sum(x_i - x_{mean})^2}{n - 1}} \quad (3.14)$$

$$s_{pool} = \sqrt{\frac{\sum(n_1 - 1)s_1^2 + (n_2 - 1)s_2^2}{n_1 + n_2 - 2}} \quad (3.15)$$

Where,  $s$  is the standard deviation of each population and  $s_{pool}$  is the pooled standard deviation. In pooled standard deviation method, the standard deviation of samples is assumed to be constant while the mean of the samples may vary relatively. The method is used to estimate the standard deviation of different samples with different conditions.

T value is calculated as follows;

$$t = \frac{[x_{mean,1} - x_{mean,2}]}{s_{pool} \times \left[ \sqrt{\frac{1}{n_1} + \frac{1}{n_2}} \right]} \quad (3.16)$$

The calculated t-value is compared with the critical t-value determined from the t-distribution table. If calculated t-value is bigger than the critical t-value, the null hypothesis is rejected and the difference between two means of two populations is statistically significant with the pre-determined confidence level. If calculated t-value is smaller than critical t-value, then the null hypothesis is accepted that statistically there is no difference between the means of the two populations.

The calculations in this study were performed with statistics software, Minitab version 17 [105], where only the data to be compared are tabulated in the software and relevant calculations are performed by the program according to the chosen test method.

## 4. RESULTS

### 4.1. SIMULATIONS IN VACUUM WITH VANCOMYCIN

In vacuum V-HCl and zwitter ionic V-HCl, which will be referred as ionic V-HCl for the rest of the study, were simulated in order to investigate the conformation of vancomycin and see the effect of the zwitter ionic state on the conformation of the molecule. The number of molecules in the simulation box was increased to understand the effect of neighboring molecules on the conformation of the molecules as well as the interactions in between. Simulations were performed at room temperature, 298 K, and body temperature, 310 K. Table 4.1. represents the simulations performed in vacuum with vancomycin molecule.

Table 4.1. Simulations performed in vacuum (total duration= 22 ns)

		# of V-HCl	T (K)
<b>1</b>	Ionic V-HCl	1	298
<b>2</b>	V-HCl	1	298
<b>3</b>	Ionic V-HCl	2	298
<b>4</b>	V-HCl	2	298
<b>5</b>	Ionic V-HCl	4	298
<b>6</b>	V-HCl	4	298
<b>7</b>	Ionic V-HCl	9	298
<b>8</b>	V-HCl	9	298
<b>9</b>	Ionic V-HCl	16	298
<b>10</b>	V-HCl	16	298
<b>11</b>	Ionic V-HCl	1	310
<b>12</b>	V-HCl	1	310
<b>13</b>	Ionic V-HCl	2	310
<b>14</b>	V-HCl	2	310
<b>15</b>	Ionic V-HCl	4	310
<b>16</b>	V-HCl	4	310
<b>17</b>	Ionic V-HCl	9	310
<b>18</b>	V-HCl	9	310
<b>19</b>	Ionic V-HCl	16	310
<b>20</b>	V-HCl	16	310

In literature the molecular dynamic studies are simulated for 10 ns.[28][106]. The production time for molecular dynamics simulations should be optimized that if the simulation time is very short it may not be possible to observe the conformational changes in the structure; if the simulation time is very long simulations may cause lots of computing power and computing time. The time interval in this study was chosen to be 22 ns to observe the conformational changes for a longer time than the literature data. However, the first 2 ns were accepted as equilibration run, the remaining 20 ns were production run. Results in this study represent the production run period.

#### 4.1.1. Visual Inspection

Visual inspection of the systems was done with VMD program. The movement of each atom for 5 ns was observed at specified simulation conditions. However this kind of information is subjective without any supporting data or calculation.

The change in the position of  $\text{Cl}^-$  ion, highlighted with yellow circle, can be seen in Fig. 4.1. The ion moves to the middle of the box and the molecule bends to wrap it. This behavior is also observed in all simulations performed in vacuum. It is observed that ionic V-HCl bends more than the V-HCl molecules with visual inspection.

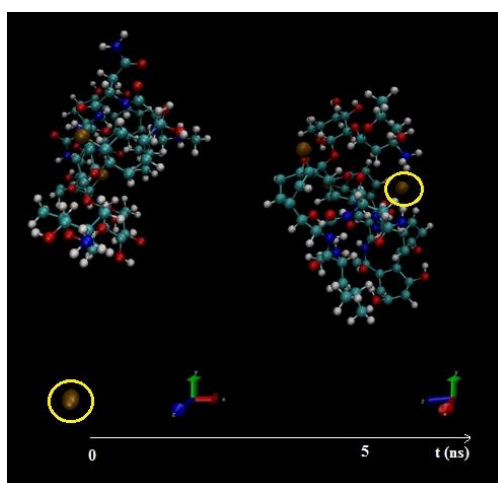


Figure 4.1.  $\text{Cl}^-$  ion position for 1 V-HCl at 310 K vacuum,  $t=0$  and  $t=5$  ns

Fig. 4.2. shows the graphical results of the simulations, where y axis represents the number of V-HCl and ionic V-HCl molecules, x axis shows the simulation time. As seen in the

figure regardless of the number, state of the molecules and temperature, V-HCl molecules approach each other and each molecule bends. To quantify the visual observations and obtain numeric values to compare the systems with each other, radius of gyration, and radial distribution functions are evaluated which can all be found in the following sections.

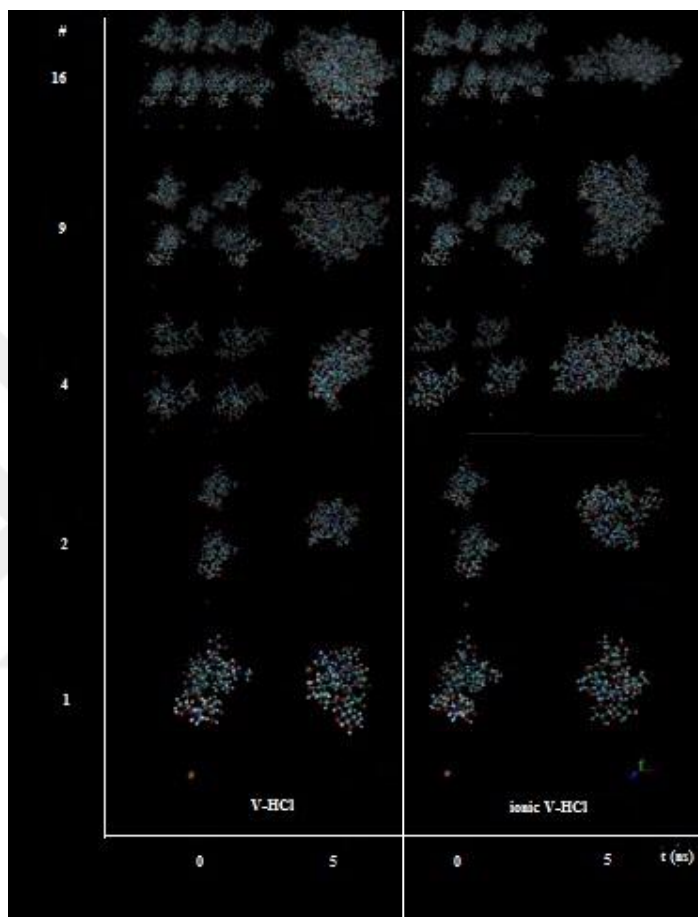


Figure 4.2. Different number of V-HCl and ionic V-HCl molecules at  $t=0$  and  $t=5$  ns

#### 4.1.2. Radius of Gyration of Systems with Vancomycin in Vacuum

The radius of gyration analysis was performed for each system in order to observe the effect of parameters on the behavior of molecules. Comparisons between nonionic and ionic systems, and between simulations performed at room temperature and body temperature were done.



#### 4.1.2.1. Effect of Ionic State on Radius of Gyration in Vacuum

Figures from Fig. 4.3 to Fig. 4.7 represent the comparison between  $R_g$  of ionic and nonionic structures of vancomycin systems in vacuum. The  $R_g$  values are average values for each vancomycin molecules in the systems and represent the behavior of each molecule. The behavior of all molecules in the system is expressed in cluster  $R_g$  profiles, which are performed by considering all atoms in the system as one molecule. Figures from Fig. 4.8 to Fig. 4.11 represent the comparison between cluster  $R_g$  of ionic and nonionic structures. Increase in the cluster  $R_g$  would be an indication of dispersion of V-HCl molecules in the medium. As the cluster  $R_g$  of systems composed of 1 V-HCl are same with the average  $R_g$  results of each molecule, these systems are not considered in cluster  $R_g$  calculations.

As seen in charts at both 298 K and 310 K, ionic V-HCl is more compact than the V-HCl. As the molecule bends to enfold  $\text{Cl}^-$  ion, the charges at the carboxyl and amino terminus attract each other leading to a more compact structure. Visual inspections are validated with these calculations.

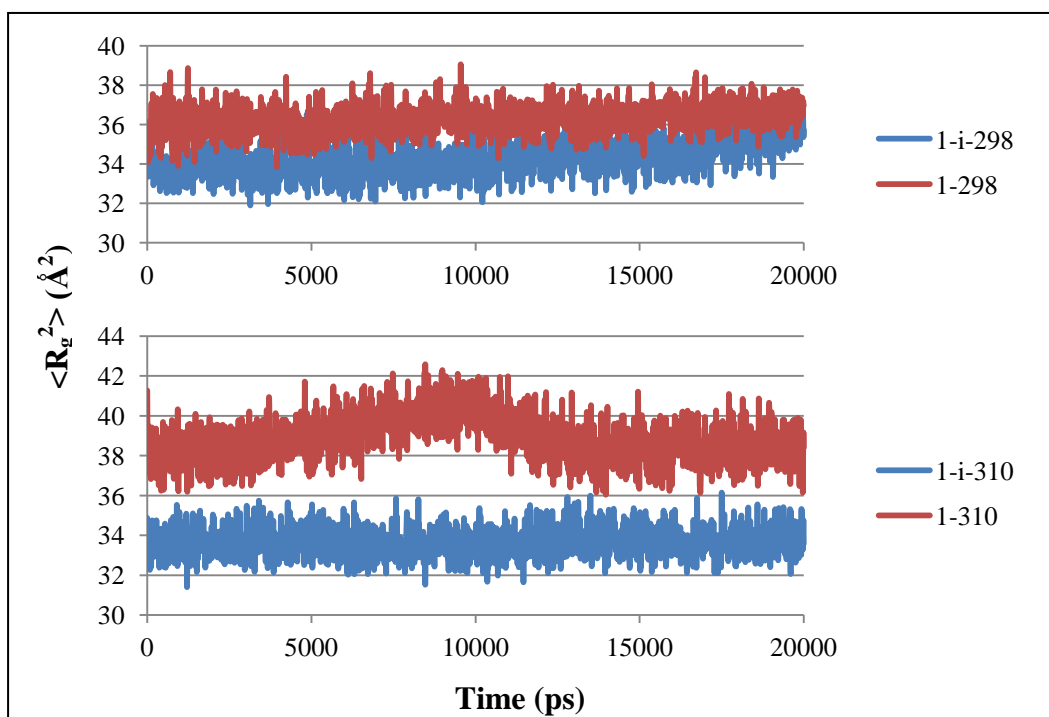


Figure 4.3.  $R_g$  of 1 V-HCl and 1 ionic V-HCl at 298 K and 310 K

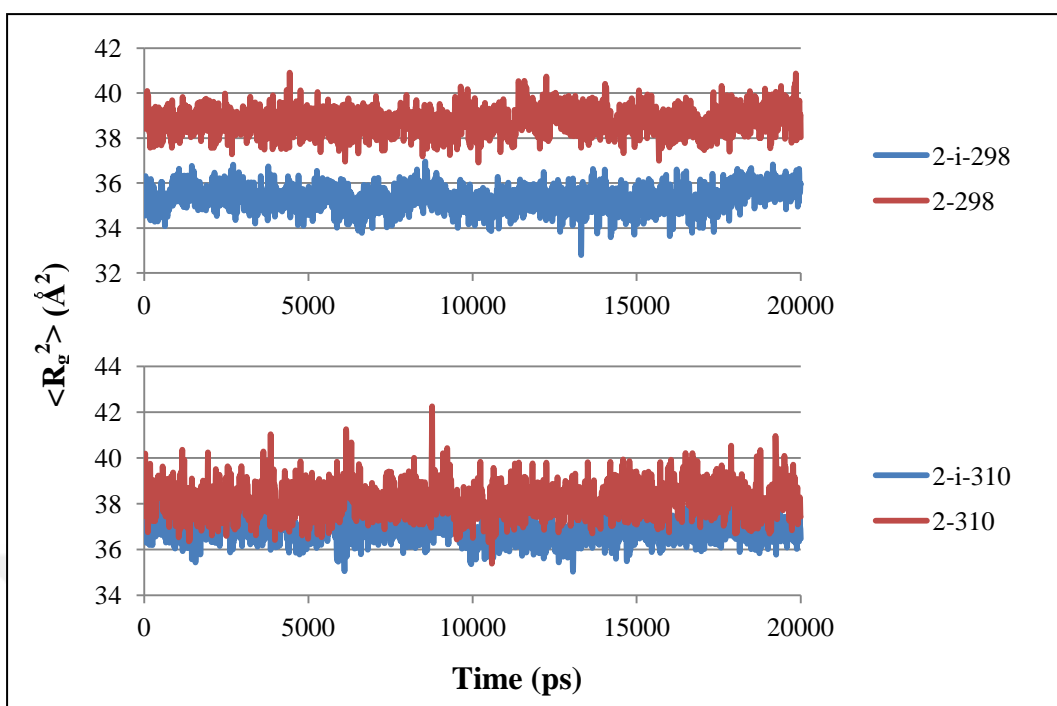


Figure 4.4.  $R_g$  of 2 V-HCl and 2 ionic V-HCl at 298 K and 310 K

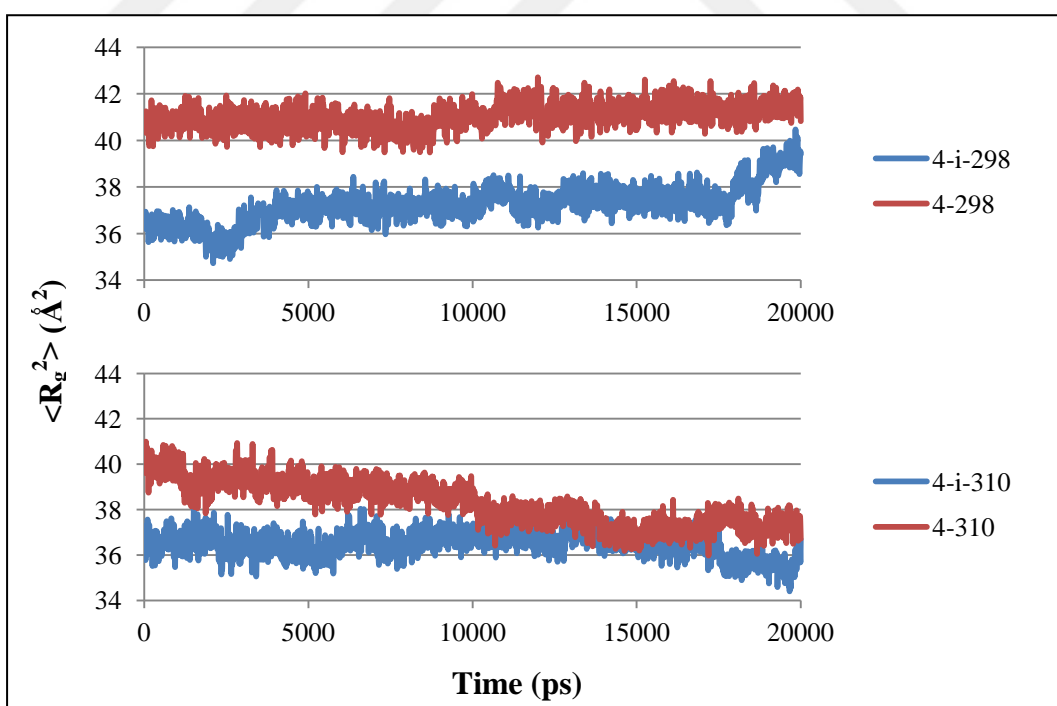
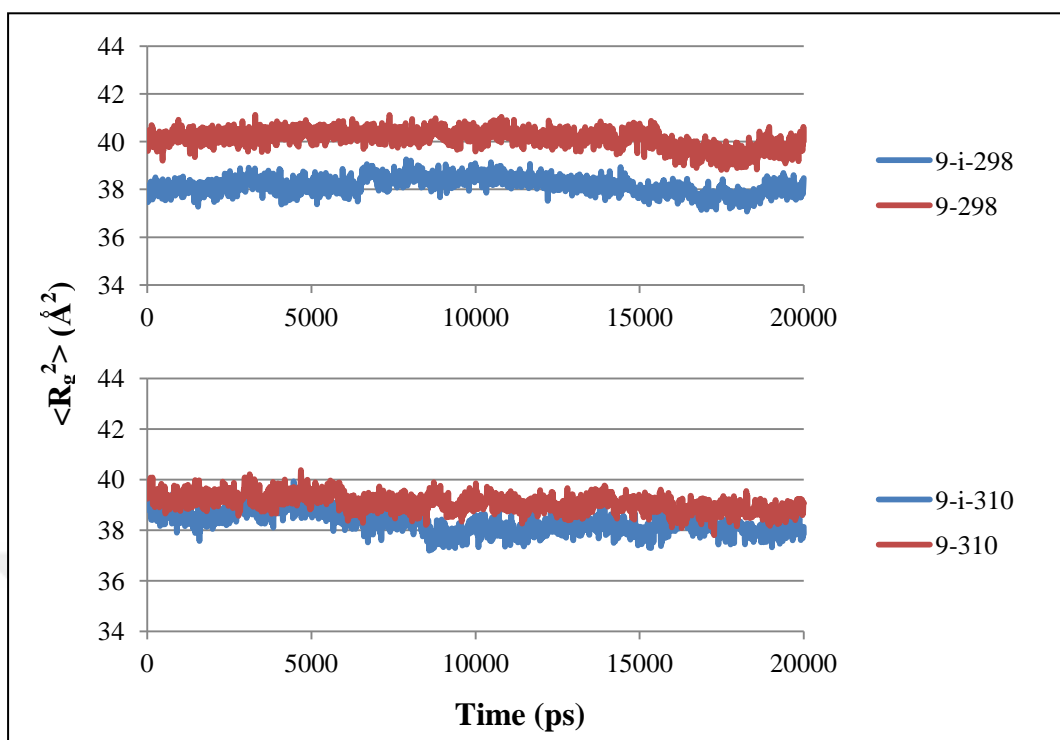
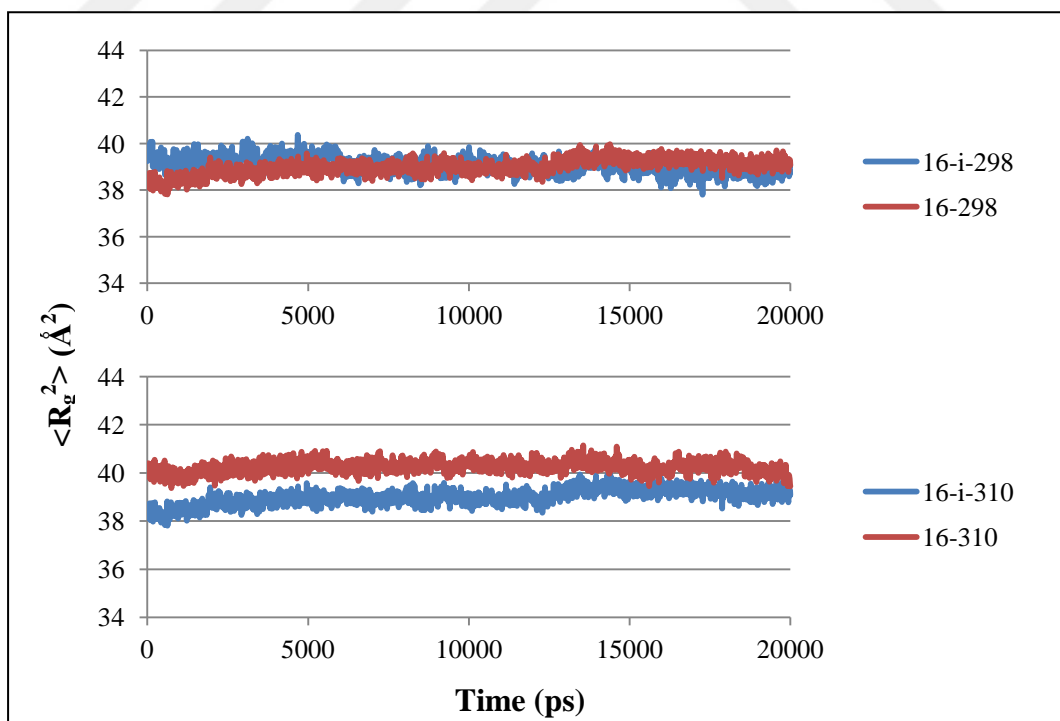


Figure 4.5.  $R_g$  of 4 V-HCl and 4 ionic V-HCl at 298 K and 310 K

Figure 4.6.  $R_g$  of 9 V-HCl and 9 ionic V-HCl at 298 K and 310 KFigure 4.7.  $R_g$  of 16 V-HCl and 16 ionic V-HCl at 298 K and 310 K

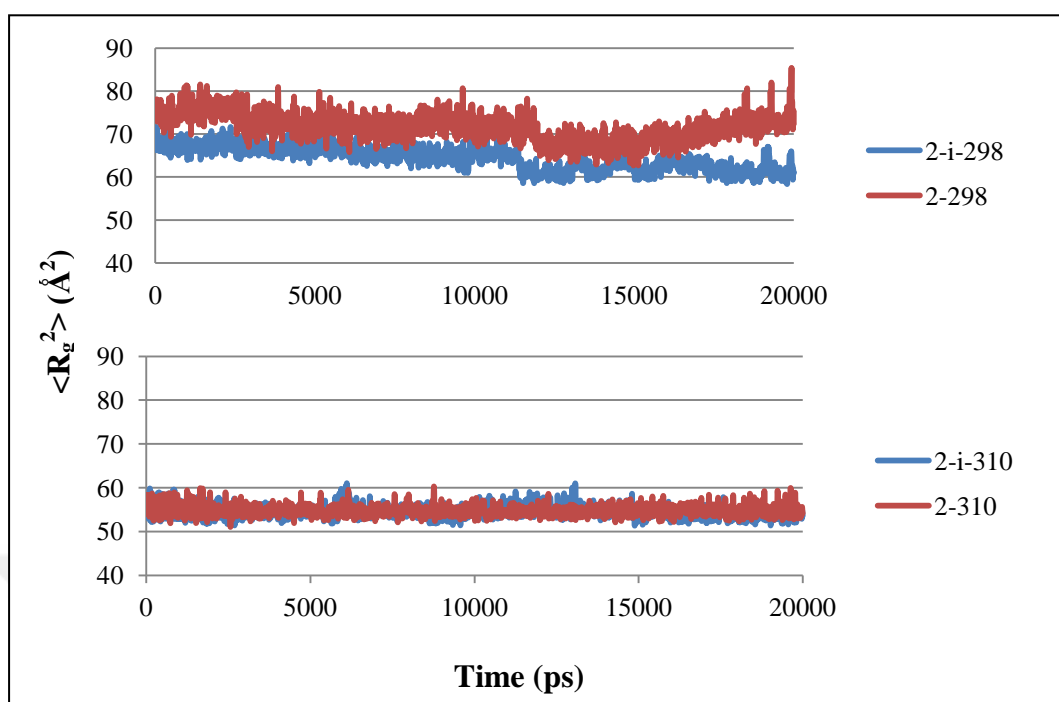


Figure 4.8. Cluster  $R_g$  of 2 V-HCl and 2 ionic V-HCl at 298 K and 310 K

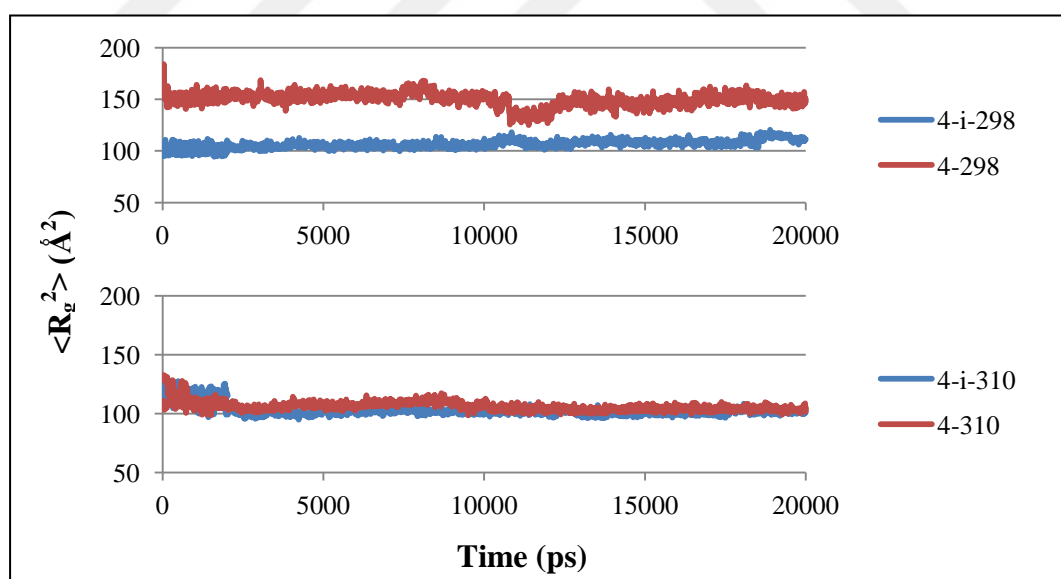


Figure 4.9. Cluster  $R_g$  of 4 V-HCl and 4 ionic V-HCl at 298 K and 310 K

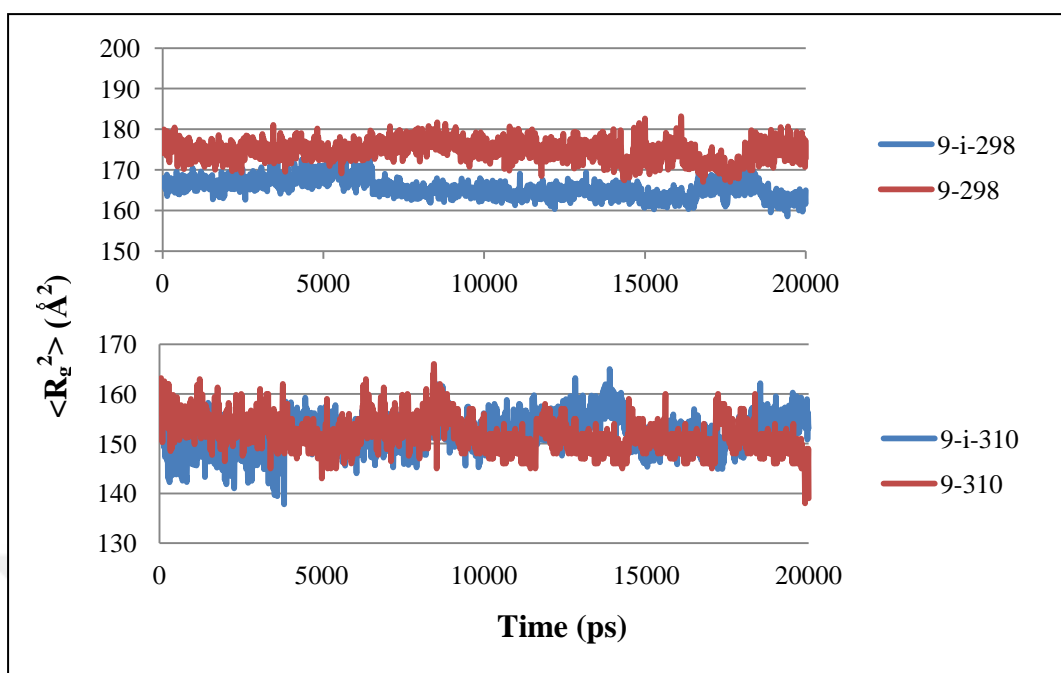


Figure 4.10. Cluster  $R_g$  of 9 V-HCl and 9 ionic V-HCl at 298 K and 310 K

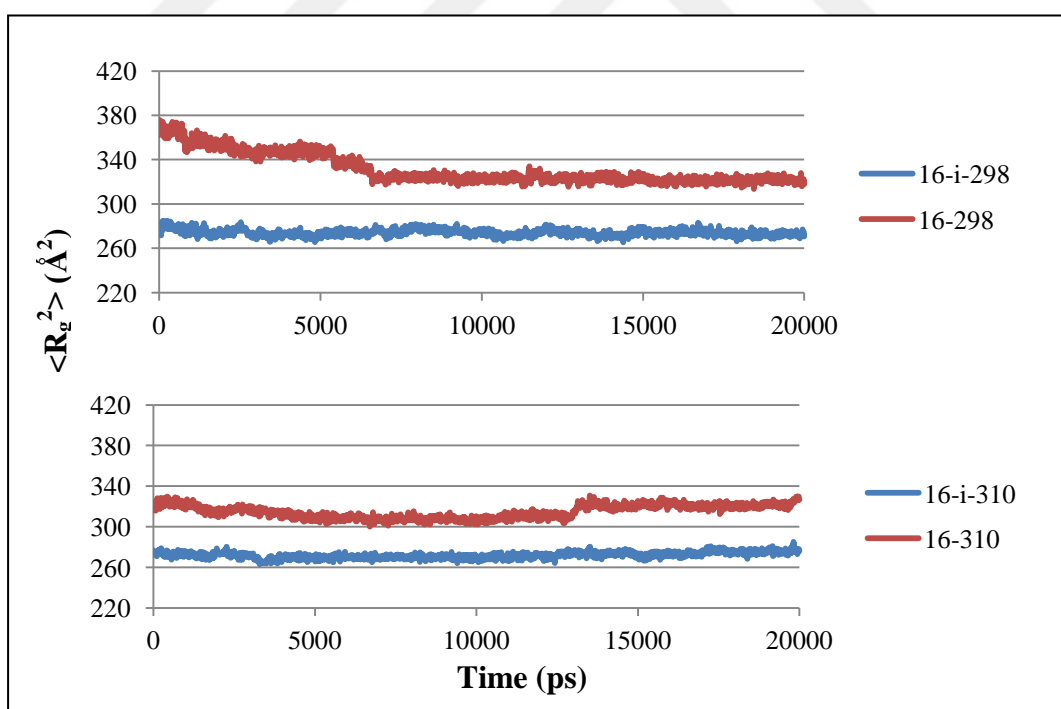


Figure 4.11. Cluster  $R_g$  of 16 V-HCl and 16 ionic V-HCl at 298 K and 310 K

As seen in previous figures cluster  $R_g$  values show oscillations through time. The decrease in the  $R_g$  cluster, which shows the tendency of molecules to come together, is mainly

observed in the equilibration step. After equilibration, the sharp changes in  $R_g$  values may be the indication of conformational changes. With a similar trend with average  $R_g$  values, the ionic V-HCl systems have smaller cluster  $R_g$  with respect to non-ionic V-HCl systems. For all systems, it is observed that at higher temperature the difference in radius of gyration values between ionic states decreases. These results are tabulated in Table 4.2.

Table 4.2. Radius of gyration of all systems at 298 K and 310 K

$R_g$	System	$R_g^2 (\text{Å}^2)$ (298 K)	$R_g^2 (\text{Å}^2)$ (310 K)
average	1 ionic VHCl	$34.2 \pm 0.9$	$33.0 \pm 0.7$
average	1 nonionic VHCl	$36.3 \pm 0.7$	$38.8 \pm 1.1$
average	2 ionic VHCl	$35.3 \pm 0.5$	$36.8 \pm 0.7$
average	2 nonionic VHCl	$38.7 \pm 0.6$	$38.2 \pm 0.7$
average	4 ionic VHCl	$37.3 \pm 0.8$	$36.5 \pm 0.6$
average	4 nonionic VHCl	$41.0 \pm 0.5$	$38.3 \pm 1.0$
average	9 ionic VHCl	$38.2 \pm 0.4$	$38.3 \pm 0.4$
average	9 nonionic VHCl	$40.1 \pm 0.4$	$39.1 \pm 0.4$
average	16 ionic VHCl	$38.4 \pm 0.3$	$39.0 \pm 0.3$
average	16 nonionic VHCl	$40.1 \pm 0.3$	$40.3 \pm 0.4$
cluster	2 ionic VHCl	$64.4 \pm 2.7$	$54.8 \pm 1.4$
cluster	2 nonionic VHCl	$71.7 \pm 3.2$	$56.2 \pm 1.8$
cluster	4 ionic VHCl	$112.6 \pm 2.4$	$101.1 \pm 1.2$
cluster	4 nonionic VHCl	$147.7 \pm 3.7$	$103.6 \pm 1.7$
cluster	9 ionic VHCl	$162.6 \pm 1.4$	$152.1 \pm 3.6$
cluster	9 nonionic VHCl	$175.7 \pm 2.5$	$151.9 \pm 3.5$
cluster	16 ionic VHCl	$273.5 \pm 2.9$	$272.5 \pm 3.0$
cluster	16 nonionic VHCl	$322.3 \pm 2.8$	$317.6 \pm 3.4$

To determine if the ionic states of vancomycin is statistically significant, 2-sample t-test is applied to  $R_g$  values. All systems have normal distribution, so no additional adjustments were applied to have a normal distribution. The tested null hypothesis implies that the difference between the means of  $R_g$  values is zero for ionic and nonionic populations. As shown in Table 3.3, the ionic state of V-HCl molecule is statistically significant with 95% confidence intervals. As mentioned before the difference in average  $R_g$  values between ionic states decreases at higher temperature. However, the difference is still statistically significant due to 2 sample t-test analysis. The difference in cluster  $R_g$  values between

ionic states at high temperature become negligible for systems that have 2, 4 and 9 vancomycins. The differences in the  $R_g$  values between the ionic and nonionic state are statistically significant.

Table 4.3. Significance Test for  $R_g$  Values of Ionic and Non-ionic States of Vancomycin

$R_g$	Sample 1	Sample 2	P-Value
average	1-i-298	1-298	<0.0005
average	1-i-310	1-310	<0.0005
average	2-i-298	2-298	<0.0005
average	2-i-310	2-310	<0.0005
average	4-i-298	4-298	<0.0005
average	4-i-310	4-310	<0.0005
average	9-i-298	9-298	<0.0005
average	9-i-310	9-310	<0.0005
average	16-i-298	16-298	<0.0005
average	16-i-310	16-310	<0.0005
cluster	2-i-298	2-298	<0.0005
cluster	2-i-310	2-310	>0.05
cluster	4-i-298	4-298	<0.0005
cluster	4-i-310	4-310	>0.05
cluster	9-i-298	9-298	<0.0005
cluster	9-i-310	9-310	>0.05
cluster	16-i-298	16-298	<0.0005
cluster	16-i-310	16-310	<0.0005

#### 4.1.2.2. Effect of Temperature on Radius of Gyration in Vacuum

Figures from Fig. 4.12 to Fig. 4.16 represent the comparison between  $R_g$  values of systems at 298 K and 310 K where figures from 4.17 to 4.20 represent cluster  $R_g$  values respectively.

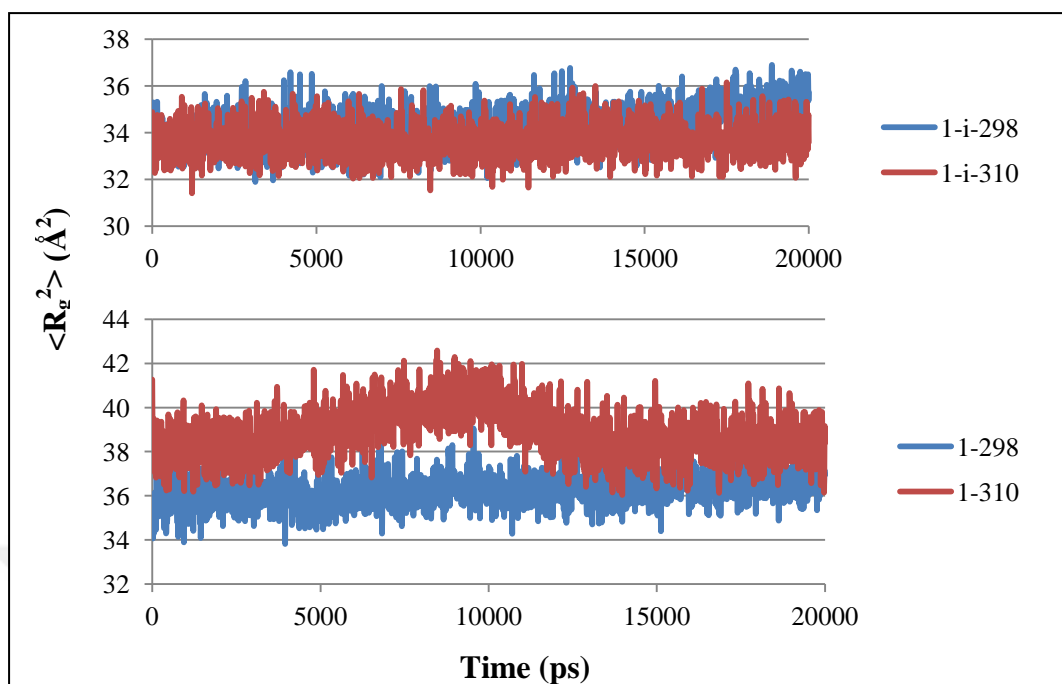


Figure 4.12. Temperature dependence of  $R_g$  of 1 V-HCl and 1 ionic V-HCl

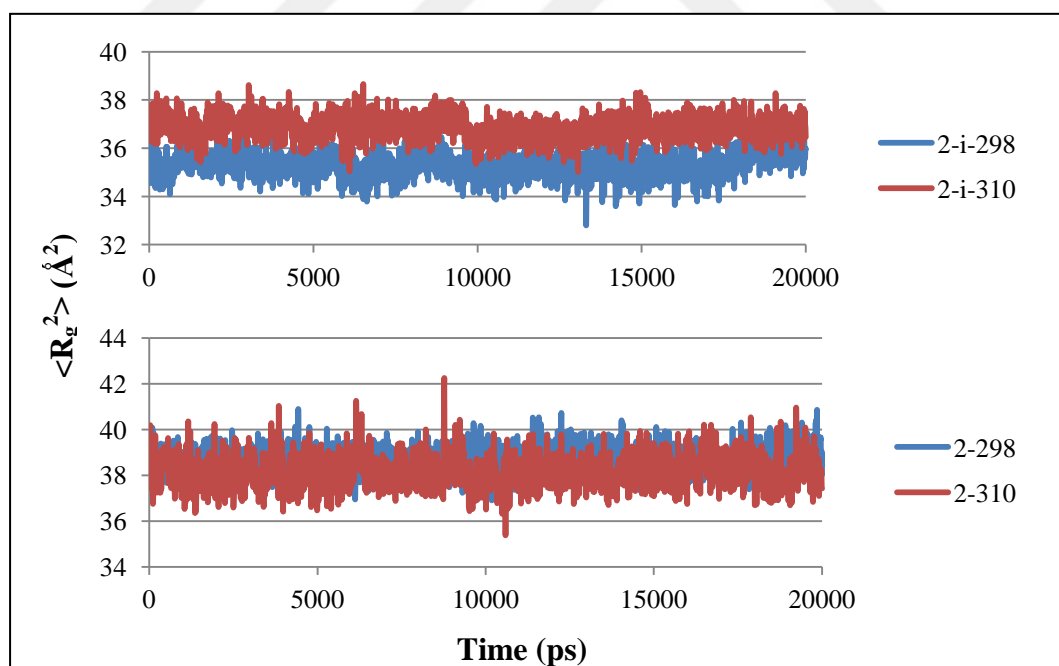


Figure 4.13. Temperature dependence of  $R_g$  of 2 V-HCl and 2 ionic V-HCl



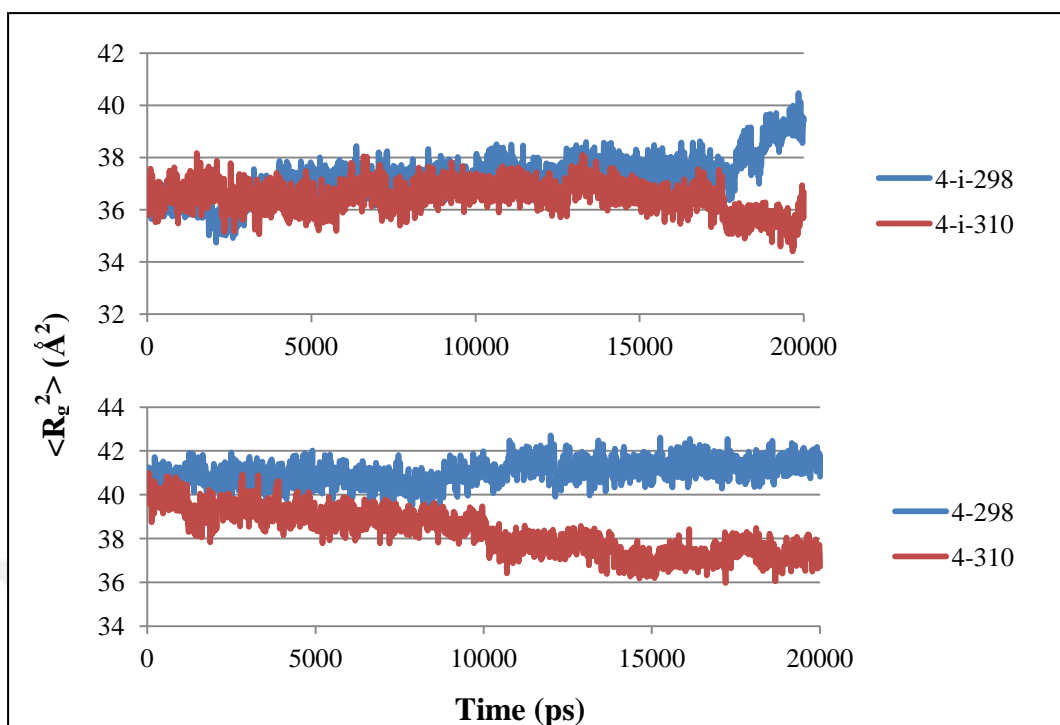


Figure 4.14. Temperature dependence of  $R_g$  of 4 V-HCl and 4 ionic V-HCl

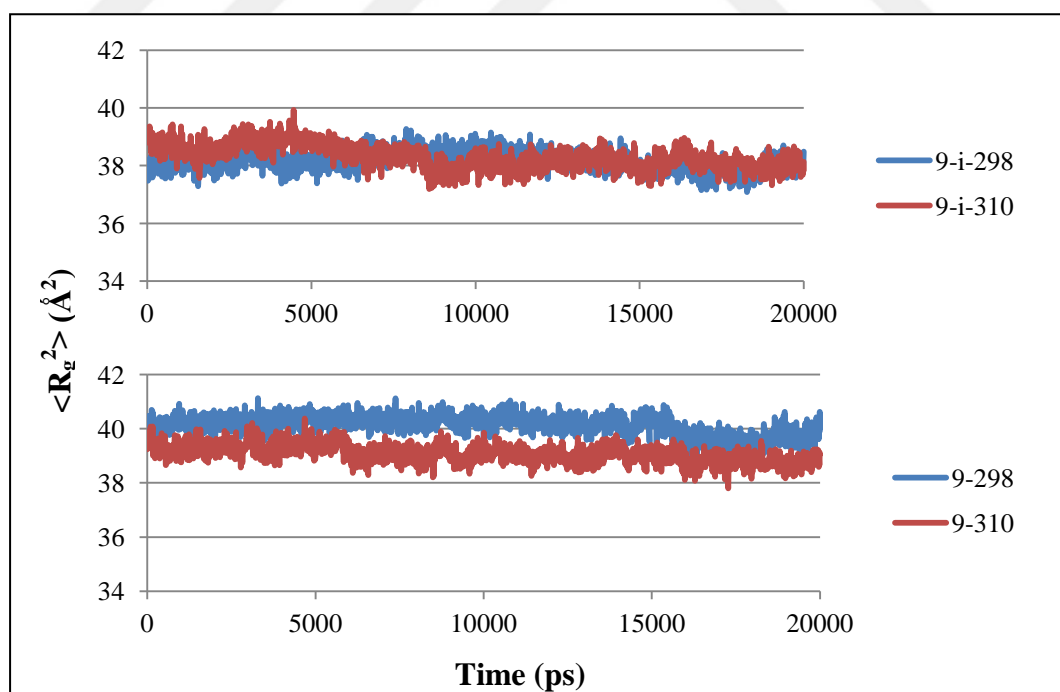


Figure 4.15. Temperature dependence of  $R_g$  of 9 V-HCl and 9 ionic V-HCl

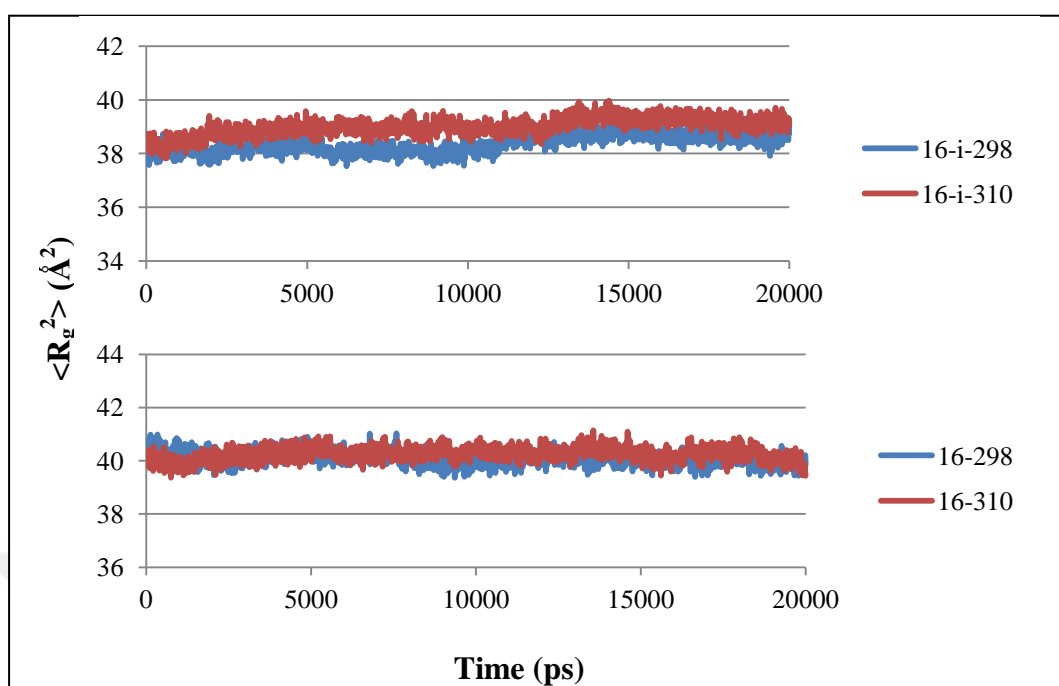


Figure 4.16. Temperature dependence of  $R_g$  of 16 V-HCl and 16 ionic V-HCl

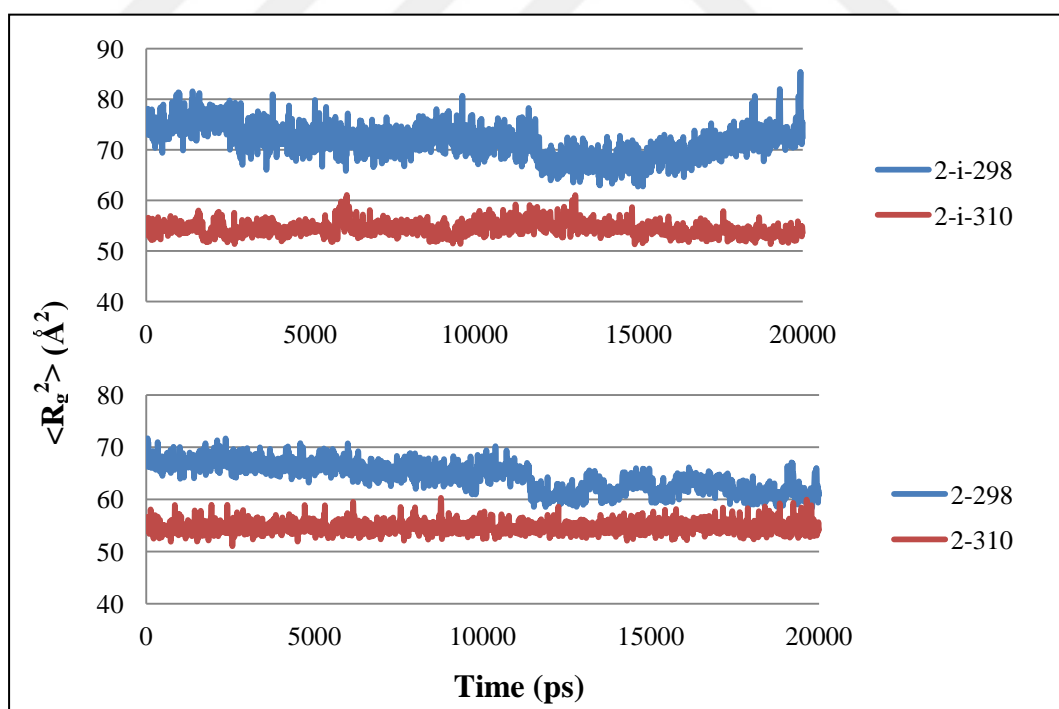


Figure 4.17. Temperature dependence of Cluster  $R_g$  of 2 V-HCl and 2 ionic V-HCl

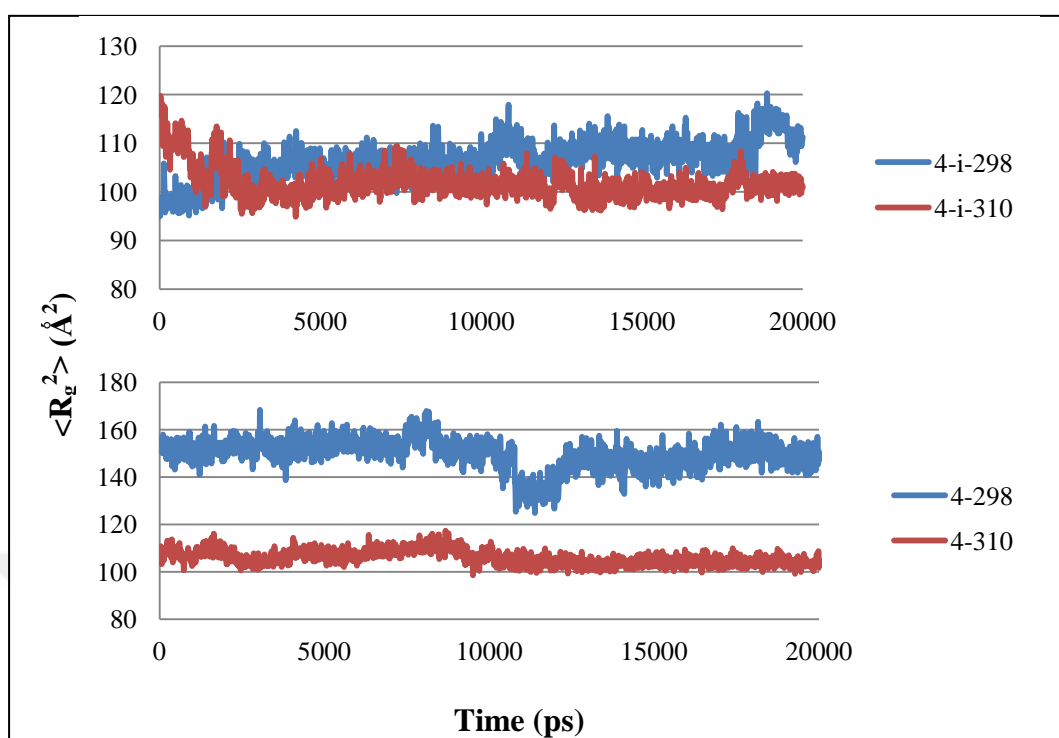


Figure 4.18. Temperature dependence of Cluster  $R_g$  of 4 V-HCl and 4 ionic V-HCl

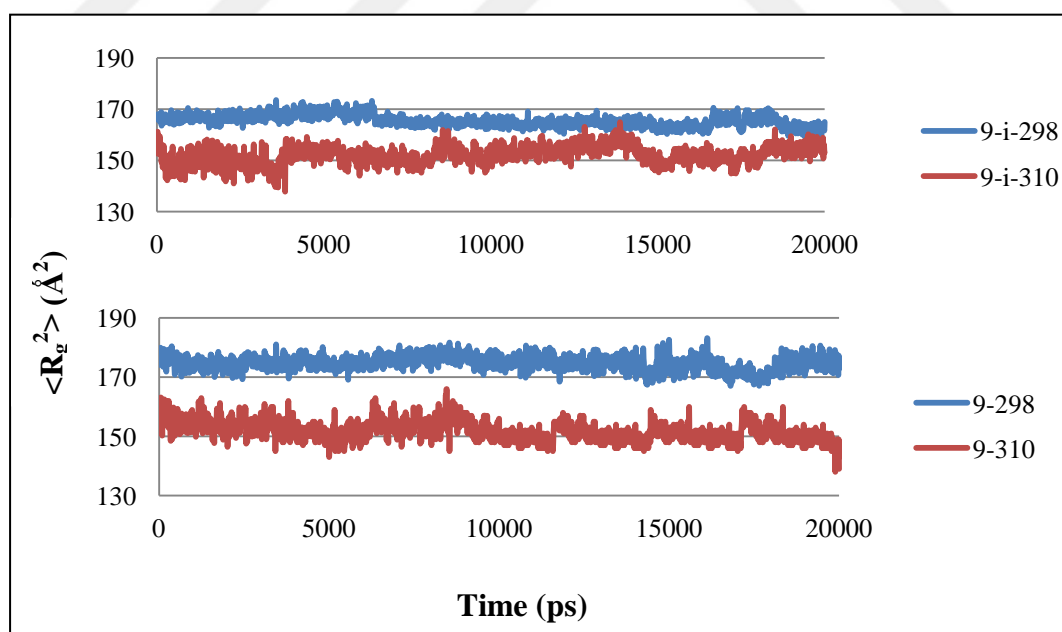


Figure 4.19. Temperature dependence of Cluster  $R_g$  of 9 V-HCl and 9 ionic V-HCl

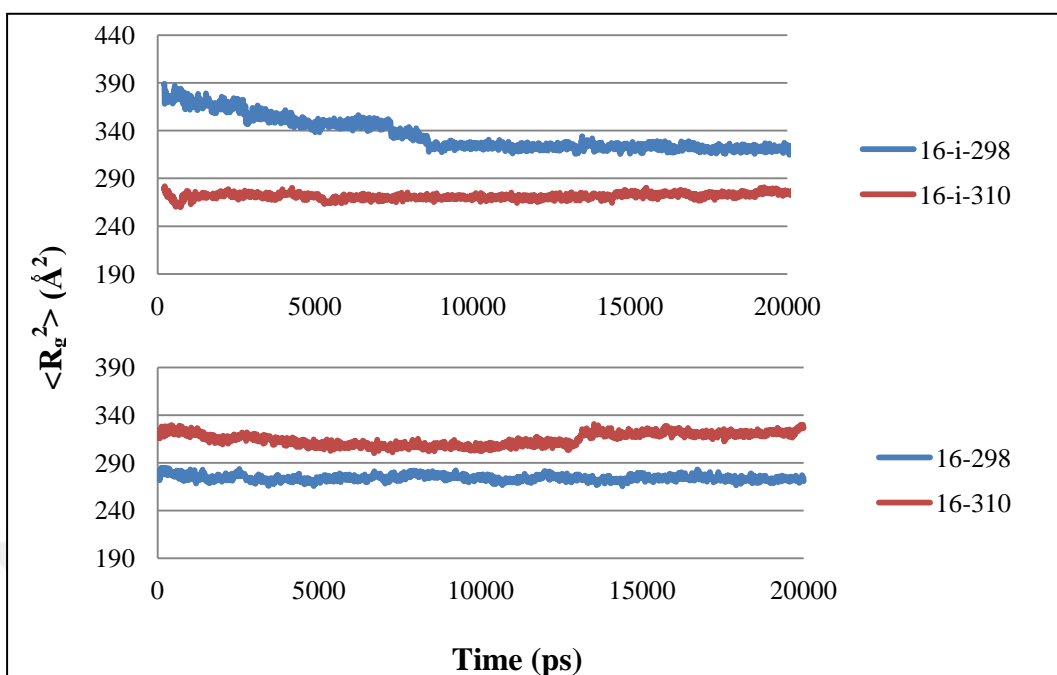


Figure 4.20. Temperature dependence of Cluster  $R_g$  of 16 V-HCl and 16 ionic V-HCl

Table 4.4. Significance Test for  $R_g$  Values of Vancomycin at different temperatures

$R_g$	Sample 1	Sample 2	P-Value
average	1-i-298	1-i-310	<0.0005
average	1-298	1-310	>0.05
average	2-i-298	2-i-310	<0.0005
average	2-298	2-310	>0.05
average	4-i-298	4-i-310	<0.0005
average	4-298	4-310	<0.0005
average	9-i-298	9-i-310	>0.05
average	9-298	9-310	<0.0005
average	16-i-298	16-i-310	<0.0005
average	16-298	16-310	>0.05
cluster	2-i-298	2-i-310	<0.0005
cluster	2-298	2-310	<0.0005
cluster	4-i-298	4-i-310	<0.0005
cluster	4-298	4-310	<0.0005
cluster	9-i-298	9-i-310	<0.0005
cluster	9-298	9-310	<0.0005
cluster	16-i-298	16-i-310	<0.0005
cluster	16-298	16-310	<0.0005

The cluster  $R_g$  values of the system which has 16 V-HCl are not as expected. For this system at higher temperature cluster  $R_g$  values for nonionic V-HCl are higher than the values obtained for 298 K. As seen in the previous charts the system with 16 V-HCl has a different trend from the other systems. However, simulations for this specific system are repeated for 2 times and results are found to be similar.

Generally for average  $R_g$  values nonionic systems temperature seems not to be statistically significant whereas, in ionic systems difference in  $R_g$  due to temperature change is significant. By looking at cluster  $R_g$  values it can be concluded that temperature is statistically significant for all systems.

#### ***4.1.2.3. Effect of Number of Vancomycin on Radius of Gyration in Vacuum***

In order to observe the effect of number of vancomycin molecules on  $R_g$  values in vacuum, the  $R_g$  values of each system is investigated at 5 ns, 10 ns and 20 ns.

In figures from Fig. 4.21 to Fig. 4.23, effect of number of vancomycin molecules on the radius of gyration is investigated at 5 ns, 10 ns and 20 ns respectively. It can be said that, as number of molecules increases the  $R_g$  values calculated per molecule increase as well for systems at 310 K. However, there are some odd data that disturb the trend. These data belong to systems which have 2 or less vancomycin. For simulations at T= 298 K a general trend is observed with respect to the number of vancomycin molecules. There is a sharp increase between 1, 2 and 4 molecules. Then the  $R_g$  values become nearly constant independent of the number of vancomycin molecules, as seen for 9 and 16 molecules. As stated before it can also be easily seen that the  $R_g$  of the V-HCl molecule is higher than that of the ionic one for simulations performed at 298 K, the difference of  $R_g$  values of ionic and nonionic systems seems to be similar in magnitude. However, for systems simulated at 310 K after 2 molecules of vancomycin the  $R_g$  values of ionic and nonionic systems are nearly the same. As  $R_g$  of the system is time dependent due to the conformation of the molecules, it is aimed to see if the resulting trend is spontaneous. If the time dependent behavior is followed through Fig. 4.21, 4.22 and 4.23, it is observed that the difference between the  $R_g$  values of ionic and nonionic systems decreases.

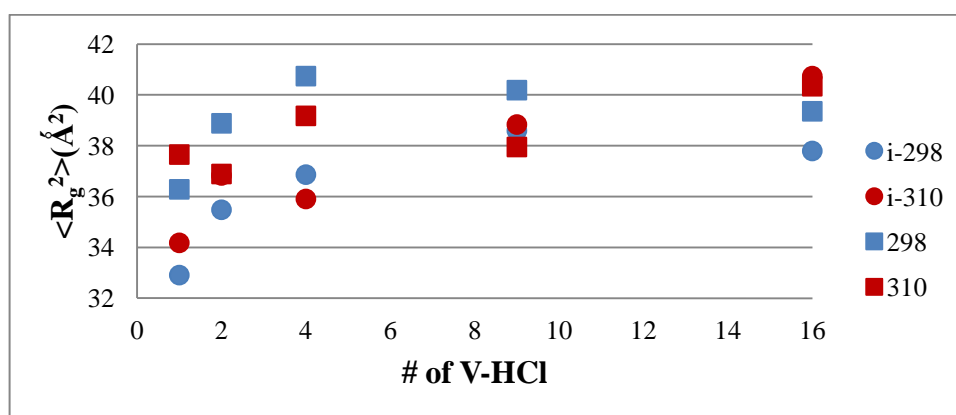


Figure 4.21. Effect of number of vancomycin molecules on  $R_g$  after 5 ns

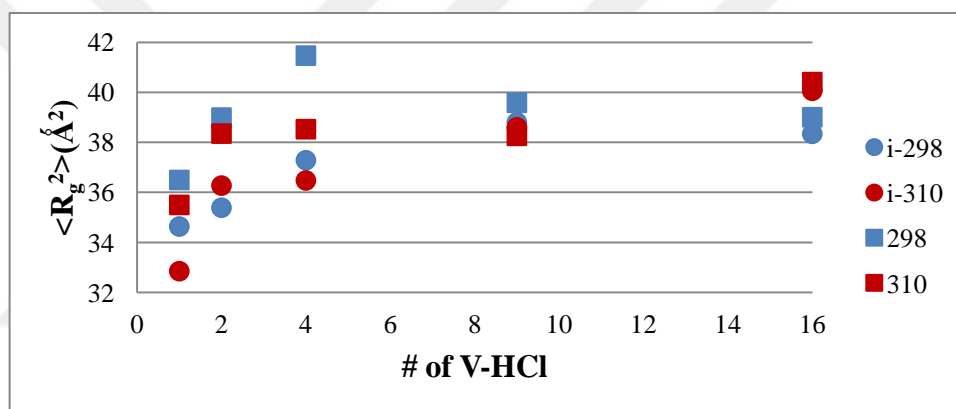


Figure 4.22. Effect of number of vancomycin molecules on  $R_g$  after 10 ns

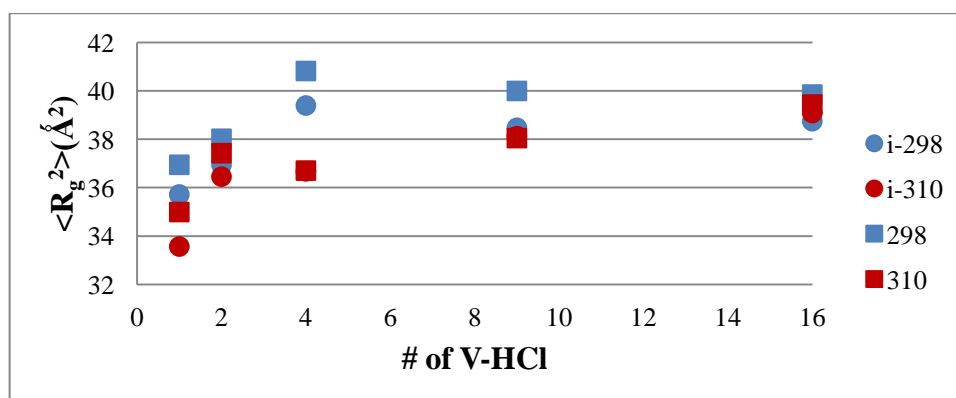


Figure 4.23. Effect of number of vancomycin molecules on  $R_g$  after 20 ns

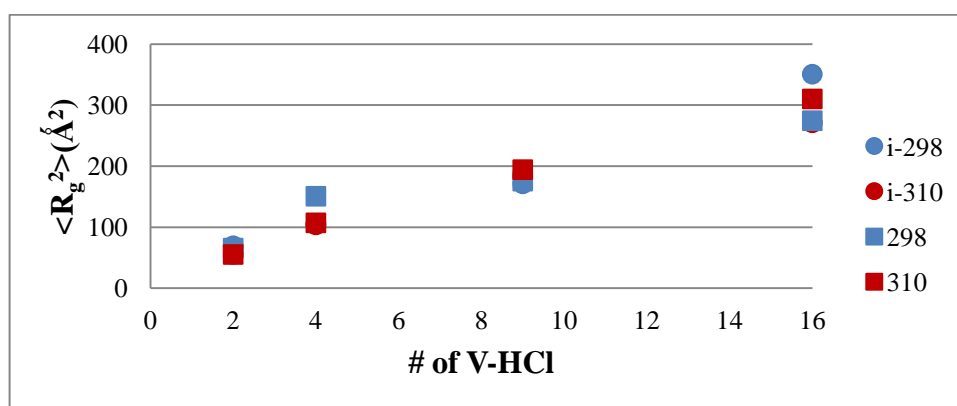


Figure 4.24. Effect of number of the vancomycin molecules on cluster  $R_g$  after 5 ns

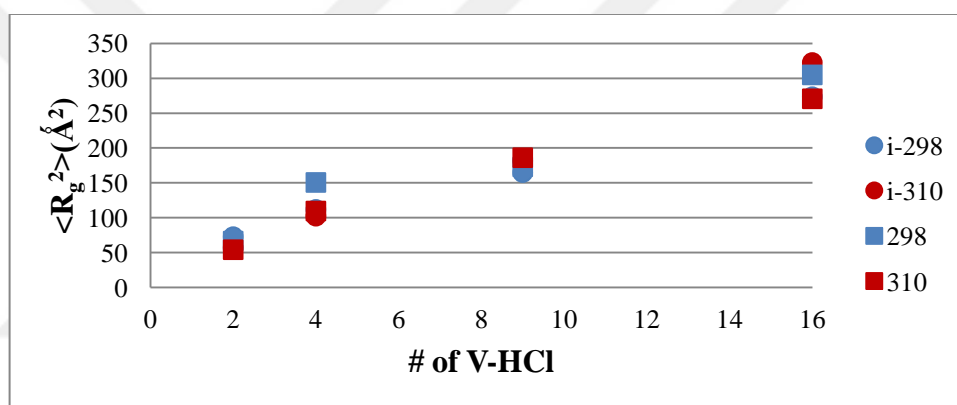


Figure 4.25. Effect of number of the vancomycin molecules on cluster  $R_g$  after 10 ns

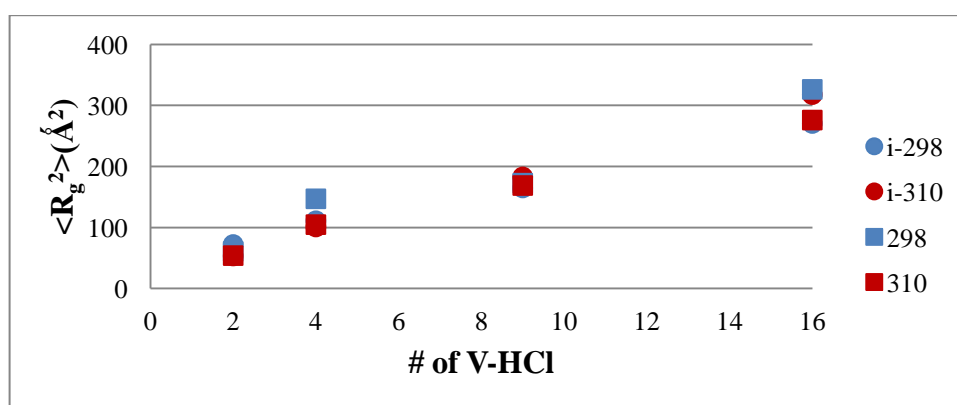


Figure 4.26. Effect of number of the vancomycin molecules on cluster  $R_g$  after 20 ns

The figures from Fig. 4.24 to 4.26 show the effect of number of vancomycin molecules on the cluster  $R_g$  behavior at time 5 ns, 10 ns and 20 ns. For all systems as number of molecules increase in the simulation box the cluster  $R_g$  also increases. This behavior is expected as the in the perspective of cluster  $R_g$  calculations all atoms in the system are assumed to belong to one molecule.

#### 4.2. TREATMENT OF SOLVENT: COMPARISON OF EXPLICIT AND IMPLICIT METHODS

For explicit solvent treatment, 5 different systems were simulated in aqueous conditions. As the number of atoms in the simulation box increase, longer simulations are required to obtain statistically meaningful averages. For this reason, aqueous systems were simulated for 22 ns. And the production run for these systems are accepted as 20 ns. By assigning a dielectric constant of 78.304 to simulation parameters, without adding any solvent molecule, 5 runs were performed. As the systems have same number of atoms with vacuum conditions, 22 ns simulations were performed. The production run was the last 20 ns of the simulations. Table 3.6 represents the simulations treated explicitly and implicitly.

Table 4.5. Simulations treated explicitly and implicitly (total duration= 22 ns)

		# of V-HCl	T (K)	# of water molecules	Total # of atoms
<b>Explicit</b>	Ionic V-HCl	1	298	6776	20506
	Ionic V-HCl	2	298	6696	20444
	Ionic V-HCl	4	298	6553	20371
	Ionic V-HCl	9	298	6159	20079
	Ionic V-HCl	16	298	5611	19681
<b>Implicit</b>	Ionic V-HCl	1	298	0	178
	Ionic V-HCl	2	298	0	356
	Ionic V-HCl	4	298	0	712
	Ionic V-HCl	9	298	0	1602
	Ionic V-HCl	16	298	0	2848



For comparison of the explicit and implicit methods, radius of gyration analysis were applied to each system in order to see if the explicitly and implicitly treated systems with the same number of vancomycin molecules give same or alike results. In explicit systems the water molecules are added to the simulation box in a fully atomistic manner, in implicit systems a dielectric constant which would replace the forces acting on the molecules by the solvent is assigned to the system. First  $R_g$  analysis shows results for average  $R_g$  of the system per molecule, and then  $R_g$  of the cluster are shown.

In Figures Fig. 4.27 to Fig. 4.31 it is seen that the  $R_g$  of the implicit solvent treated systems is initially smaller than the explicitly treated systems. For implicit systems initial values are close to the systems in vacuum as the energy minimization of the systems are done due to vacuum conditions in Xenoview. As simulations start there is an immediate change in the average  $R_g$  values, which shows that the system runs in the effect of assigned dielectric constant. When the  $R_g$  values of vancomycin in both treatments are compared, there is an obvious difference in the trends of the systems. For further investigation,  $R_g$  of the clusters in each system is investigated. For the implicit systems the  $R_g$  values are represented in the secondary axis on the right hand side. Primary axis, on the left corresponds to explicit systems.

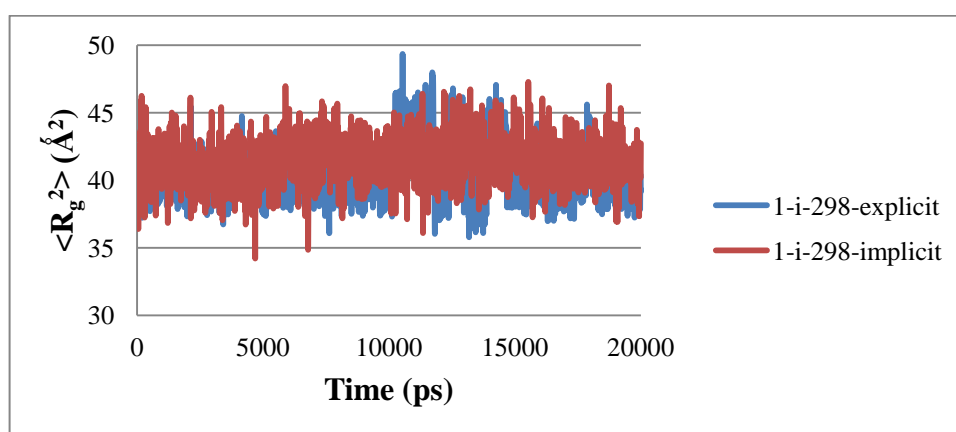


Figure 4.27.  $R_g$  of 1 ionic V-HCl at 298 K, water solvent treated explicitly and implicitly

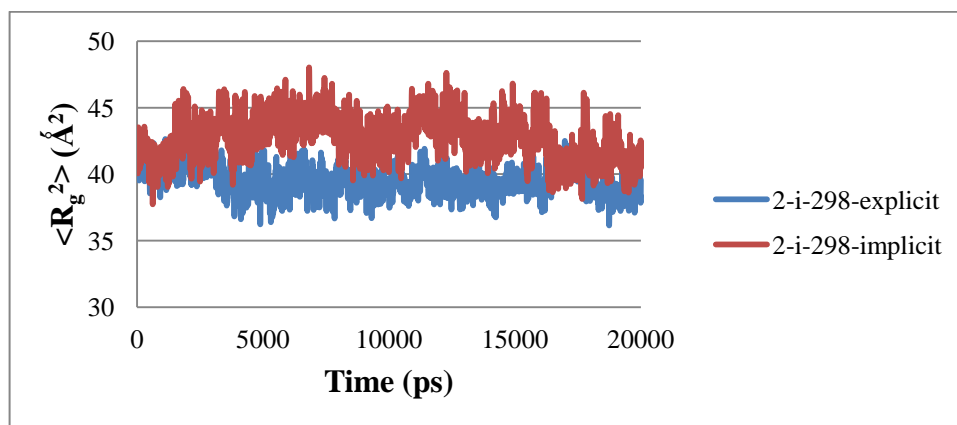


Figure 4.28.  $R_g$  of 2 ionic V-HCl at 298 K, water solvent treated explicitly and implicitly

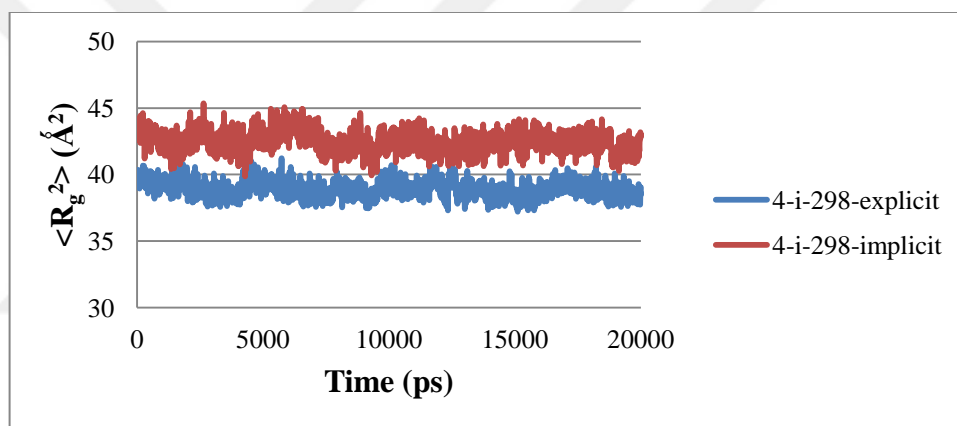


Figure 4.29.  $R_g$  of 4 ionic V-HCl at 298 K, water solvent treated explicitly and implicitly

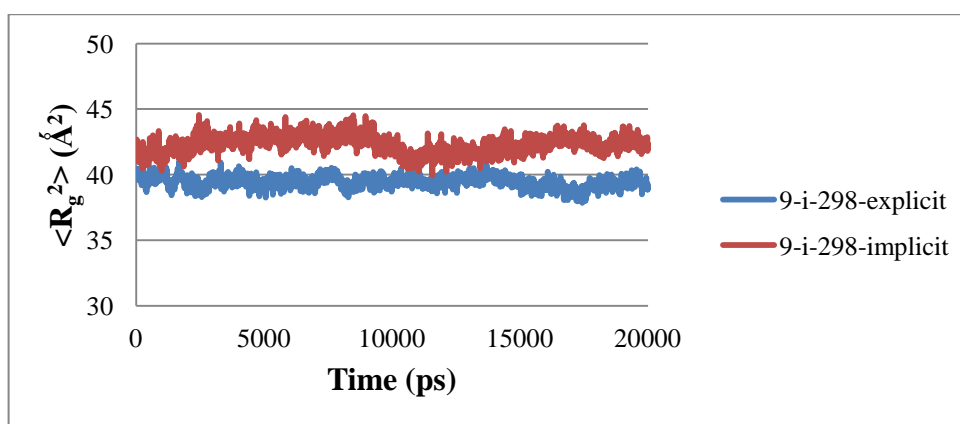


Figure 4.30.  $R_g$  of 9 ionic V-HCl at 298 K, water solvent treated explicitly and implicitly

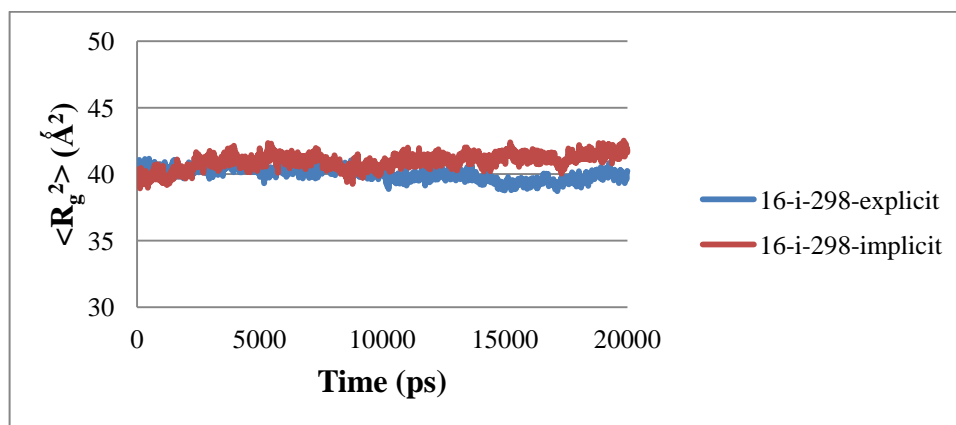


Figure 4.31.  $R_g$  of 16 ionic V-HCl at 298 K, water solvent treated explicitly and implicitly

Following figures represent cluster  $R_g$  comparison of explicit and implicit treatment of water in simulations. In the figures 4.32 to 4.35 shown above, there is a large difference between the cluster  $R_g$  values of solvated systems treated implicitly and explicitly. Although study of Anandakrishnan and coworkers with protein structures shows implicit treatment speeds the simulations up to even 60 folds for systems having low solvent viscosity, when a dielectric constant assigned for Coulombic interactions in a simulation, it is used to reduce the strength of the interactions as the value is used as denominator of the formulas used for Coulombic interactions [91]. Dielectric field being a continuum model reduces all interactions in the system, e.g. interactions of solvent and solute, interactions of solute and solute etc. So it is investigated that implicit method can give an idea on behavior of each molecule, this is also seen in the calculations of average  $R_g$  for each molecule as seen in figures 4.27 to 4.31. However, this kind of treatment is insufficient to reflect cluster behavior of the systems due to the induced electrostatic interactions between solvent molecules, as seen in cluster  $R_g$  data. The  $R_g$  values of implicitly solvated systems show very small differences from the ones of vacuum simulations. Therefore, it was concluded that for these systems treatment of the solvent explicitly is more suitable and further studies will be continued as such. Also the conformational changes in the vancomycin cluster is observed via the fluctuations occurred during the simulations. Vancomycin is known to be a water soluble chemical. In the explicit simulations there are lots of water molecules that tends to move to the gaps between the vancomycin molecules. As the number of vancomycin molecules decreases, the density of vancomycin in the simulation box also decreases. This allows water molecules to move more freely across the

vancomycin molecules and the interaction between vancomycin and water molecules may hinder the intermolecular forces in vancomycin. The vancomycin itself tends to close its structure by approaching the active sites. These complex forces acting on the molecules cause the time dependent conformational changes. So the synchronized changes in each molecule have a bigger effect on the cluster e.g. each molecule bends to its active terminus which simultaneously yields a decrease in cluster  $R_g$ .

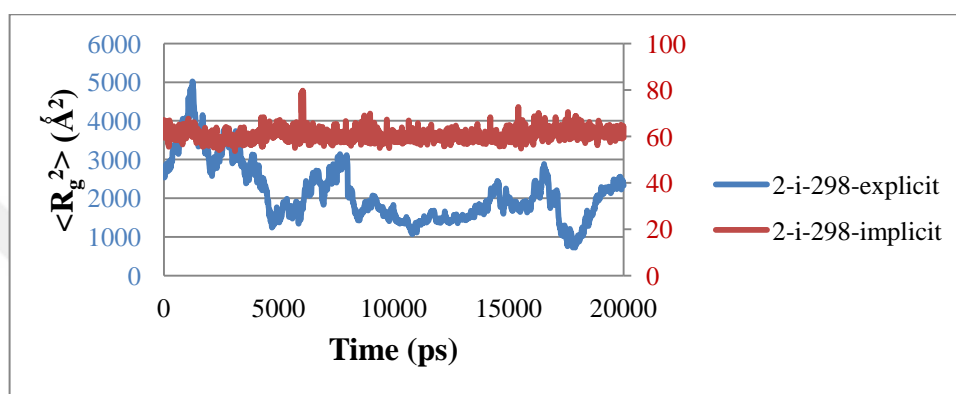


Figure 4.32. Cluster  $R_g$  of 2 ionic V-HCl at 298 K, water solvent treated explicitly and implicitly

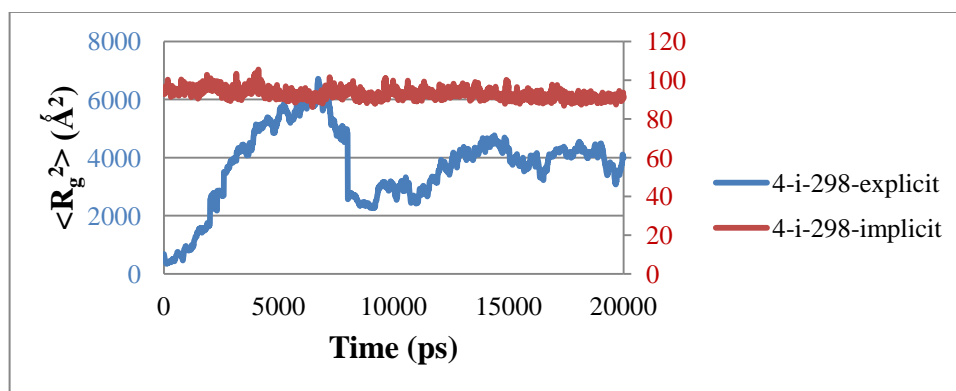


Figure 4.33. Cluster  $R_g$  of 4 ionic V-HCl at 298 K, water solvent treated explicitly and implicitly

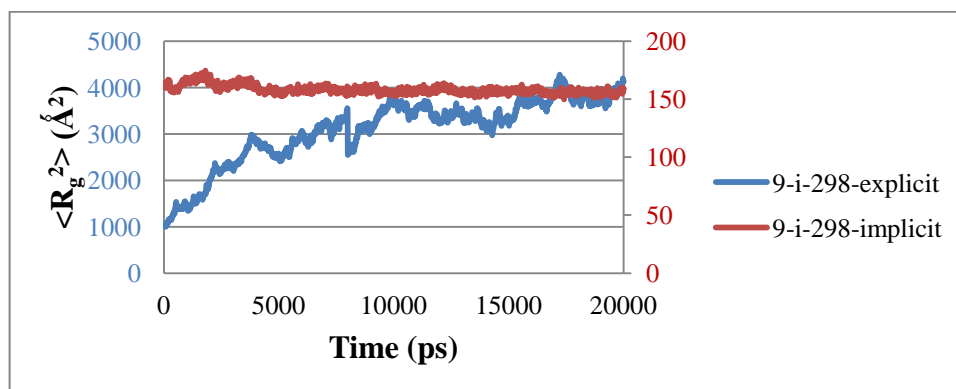


Figure 4.34. Cluster  $R_g$  of 9 ionic V-HCl at 298 K, water solvent treated explicitly and implicitly

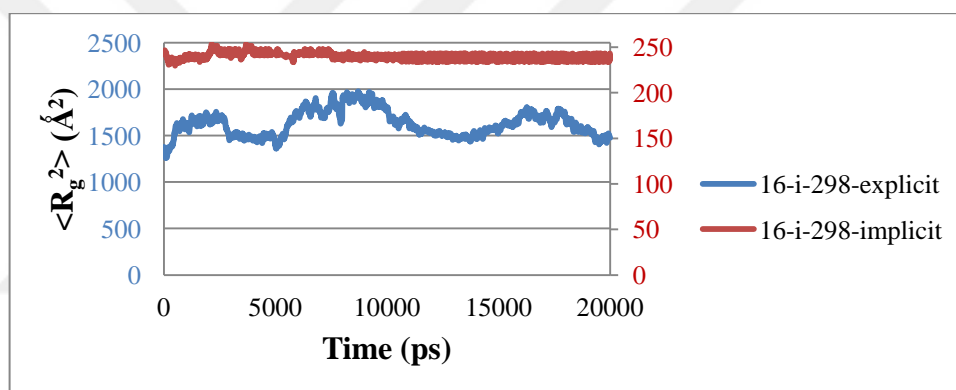


Figure 4.35. Cluster  $R_g$  of 16 ionic V-HCl at 298 K, water solvent treated explicitly and implicitly

In the study of Herlambang and Saleh, the movements of pathogenic viruses (high pathogenic and low pathogenic) and their complexes with neuraminidase and sialic acid are investigated with implicit and explicit treatment of water molecules. The structural changes during the simulation is screened through root mean square deviation and showed that explicitly solvated complexes show better stability than implicitly solvated complexes. In the simulations the activity of high pathogenic virus show higher activity in both explicitly and implicitly treated systems with respect to low pathogenic virus. However, the structural changes showed significant changes. The implicit method was adequate to identify their research but it is also their experience and advice to use explicitly solvated systems for precise results. [107]

In this work, although an attempt to use implicit solvent was made, it is concluded that for this particular system, explicit treatment of the solvent would be more appropriate.

### 4.3. SIMULATIONS IN AQUEOUS MEDIUM WITH VANCOMYCIN

The vancomycin structures were placed in a simulation box at the same initial positions with the systems performed at vacuum. Then the simulation box was filled with water molecules to observe the behavior of vancomycin molecules in aqueous medium. The solvent, water molecules in this study, were treated explicitly that the clustral movements can not be observed with implicit methods. Also zwitter ionic state of vancomycin was chosen. Table 4.6 shows the systems performed with vancomycin in aqueous medium.

Table 4.6. Simulations performed in aqueous medium (total duration= 22 ns)

		# of V-HCl	T (K)
<b>1</b>	Ionic V-HCl	1	298
<b>2</b>	Ionic V-HCl	2	298
<b>3</b>	Ionic V-HCl	4	298
<b>4</b>	Ionic V-HCl	9	298
<b>5</b>	Ionic V-HCl	16	298
<b>6</b>	Ionic V-HCl	1	310
<b>7</b>	Ionic V-HCl	2	310
<b>8</b>	Ionic V-HCl	4	310
<b>9</b>	Ionic V-HCl	9	310
<b>10</b>	Ionic V-HCl	16	310

#### 4.3.1. Effect of Temperature on Radius of Gyration for Simulations in Aqueous Medium

In order to mimic body conditions solvated systems are also simulated at 310 K. It is aimed to see if temperature affects the arrangement of vancomycin molecules in the simulation box. Average and cluster  $R_g$  of the molecules obtained from the simulations are investigated.

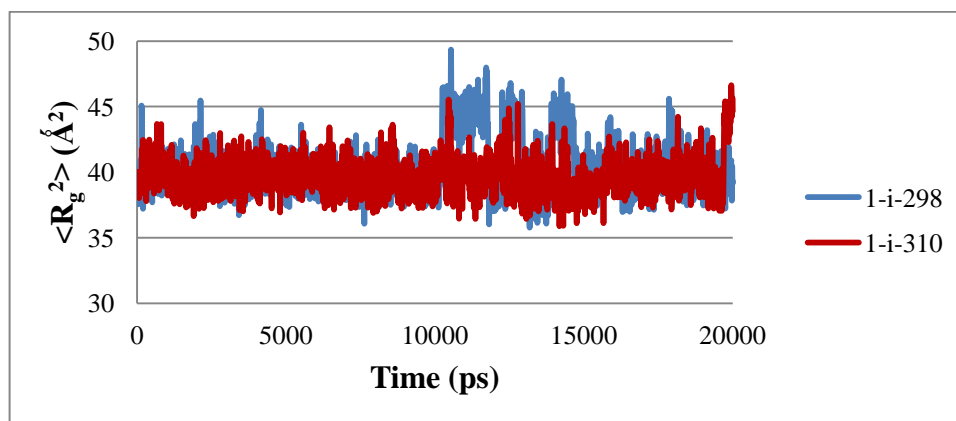


Figure 4.36.  $R_g$  of 1 ionic V-HCl explicitly solvated at 298 K and 310 K

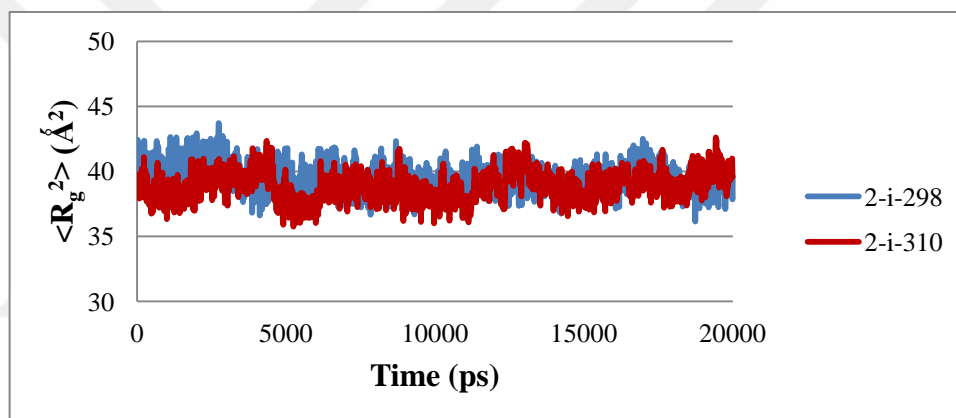


Figure 4.37.  $R_g$  of 2 ionic V-HCl explicitly solvated at 298 K and 310 K

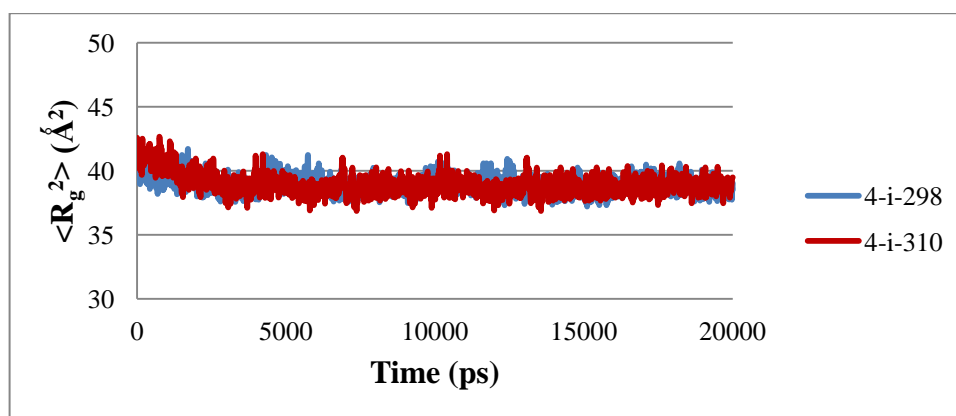


Figure 4.38.  $R_g$  of 4 ionic V-HCl explicitly solvated at 298 K and 310 K

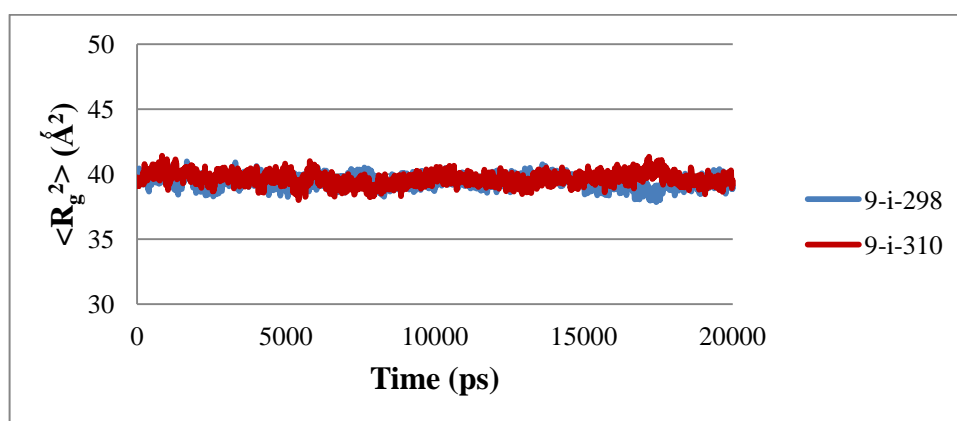


Figure 4.39.  $R_g$  of 9 ionic V-HCl explicitly solvated at 298 K and 310 K

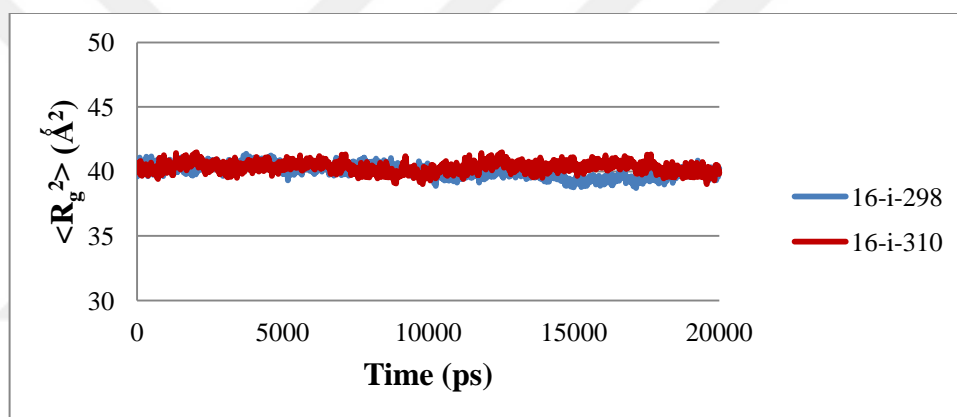


Figure 4.40.  $R_g$  of 16 ionic V-HCl explicitly solvated at 298 K and 310 K

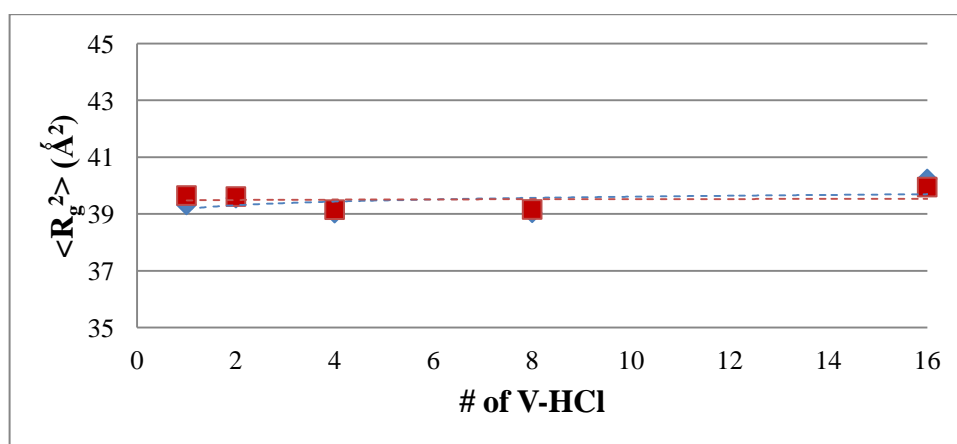


Figure 4.41. Effect of number of the vancomycin molecules on  $R_g$  of systems explicitly solvated at 298 K and 310 K after 20 ns



The figures from Fig. 4.36 and 4.41 show that the average  $R_g$  of the systems are not affected by temperature. The oscillation band width and the values seem similar at both temperatures. In vacuum media interaction of the vancomycin atoms are at maximum degree as the media has no force to prevent or decrease the forces due to increasing kinetic energy between the atoms at different temperature levels. In aqueous media the water molecules absorb the kinetic energy and prevent vancomycin atoms to move freely. In the study of Srivastava, a linear polymer is investigated under dynamic strain in terms of structure by molecular dynamics. It is observed that the change in temperature does not have a significant effect on radius of gyration that at constant strain loads with increasing temperature calculated radius of gyration values for the polymer remains nearly same. [108]. However in the study of Sargolzaei and coworkers, it is observed that in the temperature range of 300 to 344 K, the calculated  $R_g$  values remained constant, whereas at temperatures higher than 400 K the radius of gyration of spinach plastocyanin is increased [109].

The cluster  $R_g$  values are shown in figures between Fig. 4.42 and 4.45. Cluster  $R_g$  of the systems at high temperature have an increasing trend through the simulations. Despite all systems have fluctuations, cluster  $R_g$  of systems at low temperature do not increase continuously with respect to time.

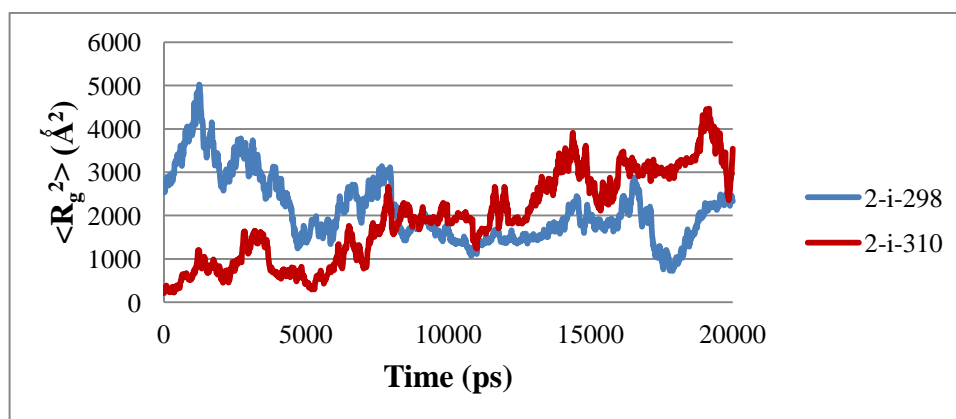


Figure 4.42. Cluster  $R_g$  of 2 ionic V-HCl explicitly solvated at 298 K and 310 K

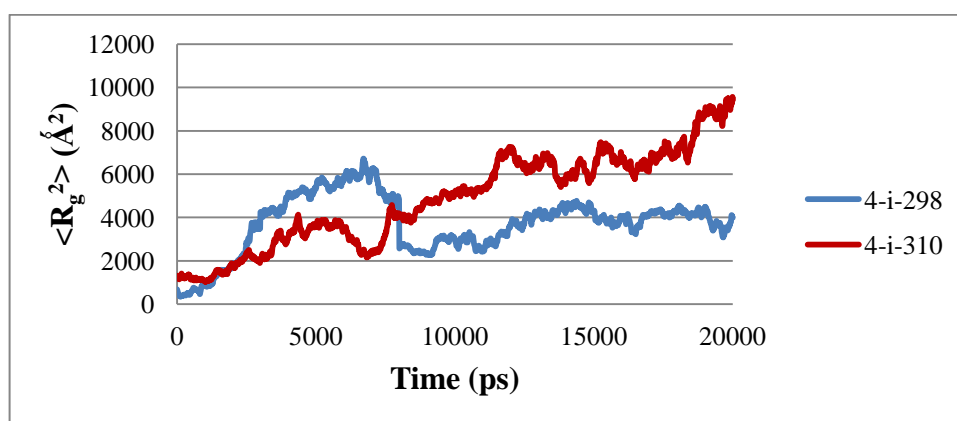


Figure 4.43. Cluster  $R_g$  of 4 ionic V-HCl explicitly solvated at 298 K and 310 K

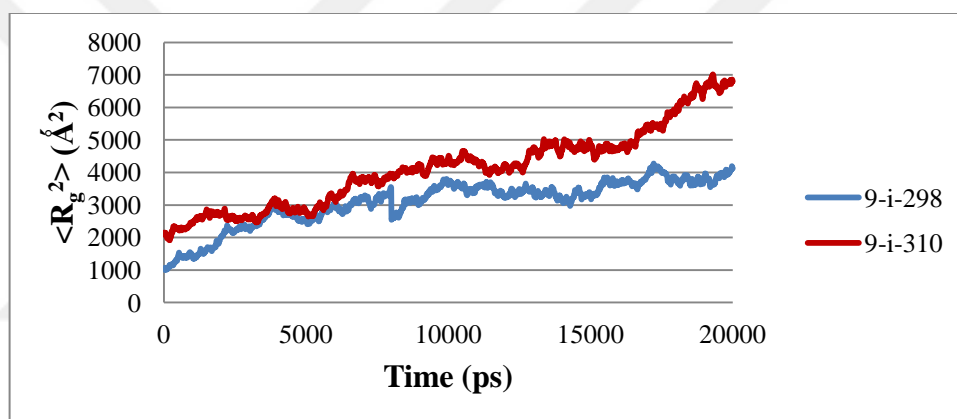


Figure 4.44. Cluster  $R_g$  of 9 ionic V-HCl explicitly solvated at 298 K and 310 K

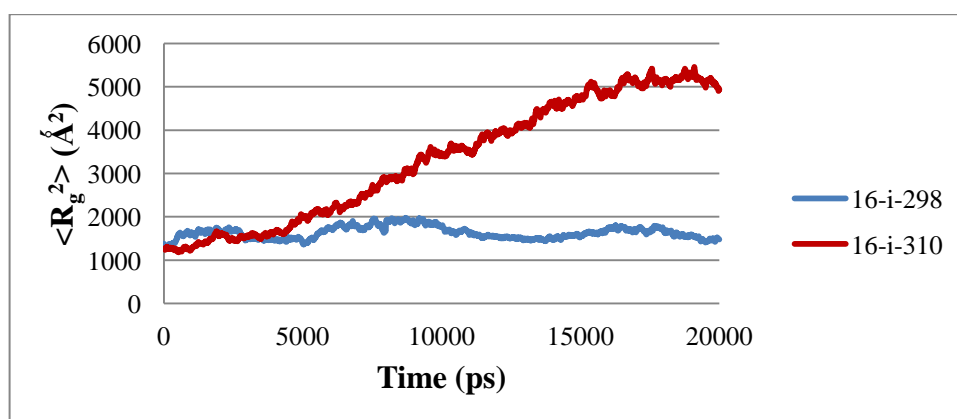


Figure 4.45. Cluster  $R_g$  of 16 ionic V-HCl explicitly solvated at 298 K and 310 K

Despite the seemingly similar general trend, the statistical difference and if this difference is significant can be investigated via statistical analysis shown in Table 4.7. As the number of molecules increases in the system temperature seems to be ineffective on the individual  $R_g$  of vancomycin molecules. According to significance test results, it is observed that the temperature has an effect on cluster  $R_g$  behavior of the systems. The observation that the individual  $R_g$  remains constant while the cluster  $R_g$  increases with increasing temperature is possibly caused by the weakening of the intermolecular forces between vancomycin molecules while water-vancomycin interaction becomes more amicable (entropy contribution increases), making the molecule more water soluble upon increase in temperature.

Table 4.7. Significance Test for  $R_g$  Values of Vancomycin at different temperatures

$R_g$	Sample 1	Sample 2	P-Value
average	1-i-298	1-i-310	>0.05
average	2-i-298	2-i-310	>0.05
average	4-i-298	4-i-310	>0.05
average	9-i-298	9-i-310	>0.05
average	16-i-298	16-i-310	>0.05
cluster	2-i-298	2-i-310	<0.0005
cluster	4-i-298	4-i-310	<0.0005
cluster	9-i-298	9-i-310	<0.0005
cluster	16-i-298	16-i-310	<0.0005

#### 4.3.2. Radial Distribution Function (RDF)

In this study RDF is used to investigate the behavior of water molecules around V-HCl. For the first inspections ions in the active sites of vancomycin are selected. The data represented show the average value over simulation time. Also for same type of atoms in the simulation the method calculates the average value per atom. If simulation has two nitrogen atoms having a positive charge then the distribution is represented for the average of two atoms.

The ordered arrangement of water molecules around a structure is defined as a hydration shell. Hydration shells can be obtained in an RDF analysis with local minimums in  $g(r)$ . As

represented in Fig. 4.46, after some distance from the structure, randomly distributed water molecules can be obtained. This random arrangement of water molecules are referred as bulk solvent. The first hydration shells must be treated in a fully atomistic manner to interpret the special arrangement of hydrogen bonds around the structure. Whereas, for bulk solvent a coarse model might be employed.

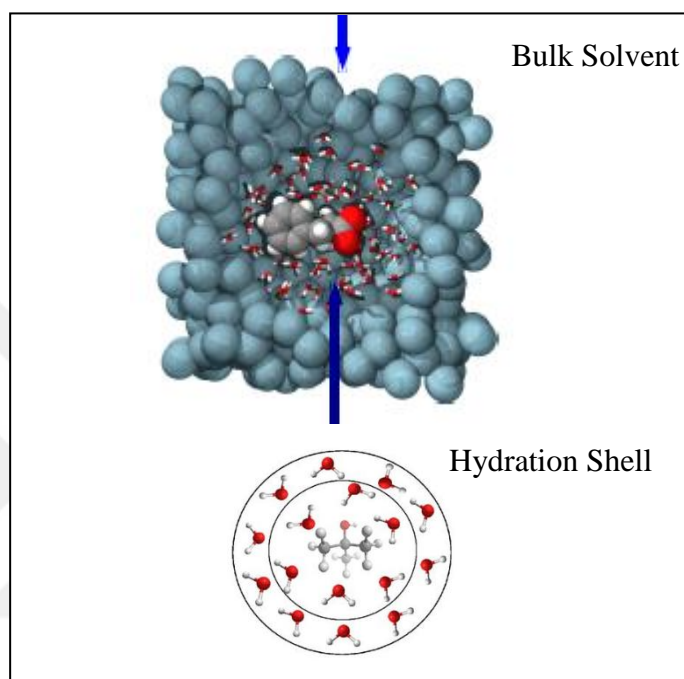
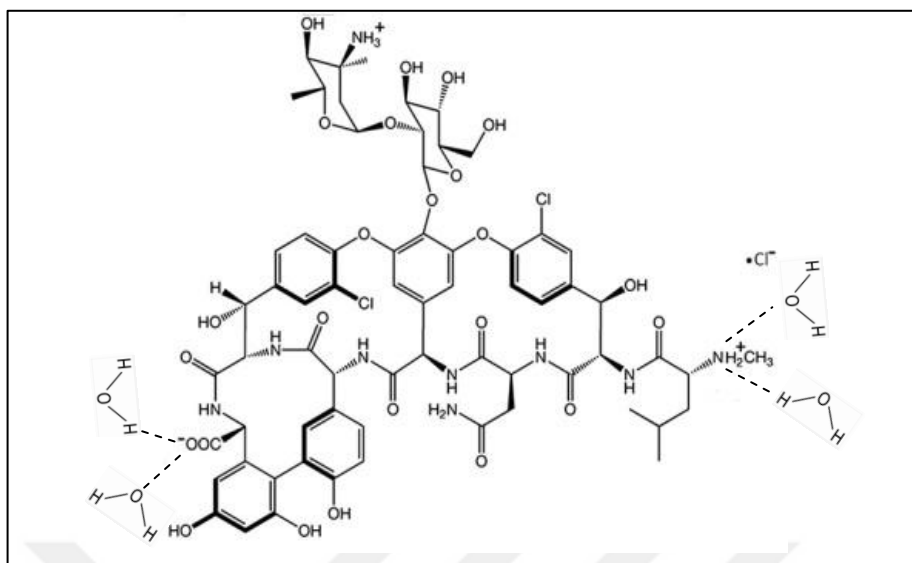


Figure 4.46. Hydration Shell and Bulk Solvent around a molecule

Glycopeptides are the class of proteins which have carbohydrate groups bound covalently to polypeptide chain. And for a protein hydration shell has a critical influence on structure and function. In particular, the dynamic properties of the hydration shell play a role in biochemical processes including protein folding, enzyme function, and molecular recognition. [110] Indeed, proteins lack activity in the absence of hydrating water. The aqueous structuring around proteins found at least 1 - 1.5 nm from its surface or 2 - 3 nm between neighboring proteins. Additionally, the presence of glycans attached to (glyco)proteins impose a long-range order on the water structure out to several nanometers, dependent on the orientation of the glycan [111]

The distribution of water molecules are investigated around amino (nitrogen ion) and carboxy (oxygen ion) terminus of vancomycin molecule.



4.47. Interaction of water molecules to amino and carboxy terminus of vancomycin molecule [99]

In Figure 4.48 pairwise radial distribution of nitrogen ion in vancomycin and hydrogen atom in water is represented. A clear structure can be seen starting at 2.25 Å and ending at 4.25 Å, which is centered at 3.25 Å. This corresponds to hydrogen bonding between nitrogen ions of vancomycin and water for the distances  $r(\text{n-h}) \leq 3.25$  Å [100]. However as mentioned before it can not be assured that all water molecules in these regions are hydrogen bonded to vancomycin. Previous discussions in literature are based on the analysis of the nitrogen and oxygen RDF, which shows a distinct first maximum at about 2.80 Å corresponding to apparently strong N–H•••O and N•••H–O hydrogen bonds [99].

The integration of RDF, which gives the number of atoms at distances  $r$  and shown with the red curve in charts, yields 4 in figure 4.48 and 1 in figure 4.49. Near nitrogen ion there are 4 hydrogen atoms implying 2 water molecules and near oxygen ion there are 2 hydrogen atoms representing 1 water molecule. The water molecules calculated for the first peak represents the first hydration shell.

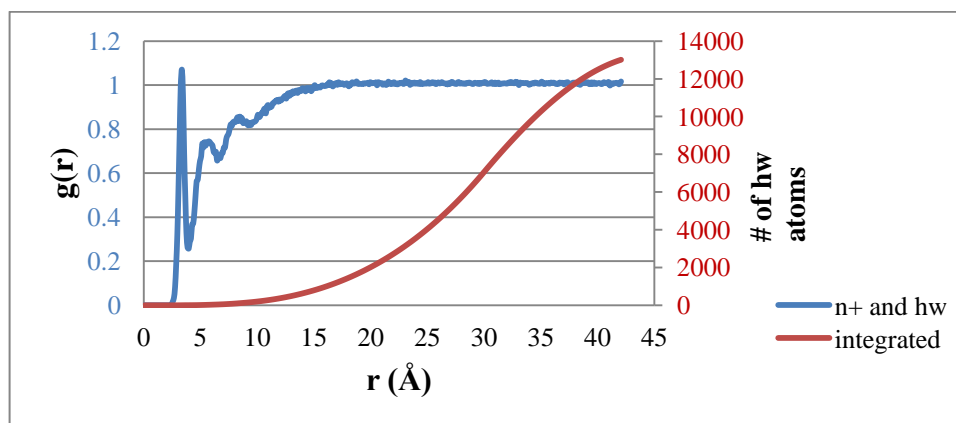


Figure 4.48. Pairwise Radial Distribution Function of nitrogen ion (n+) of 1 ionic V-HCl and hydrogen (hw) of water between 0-1 ns

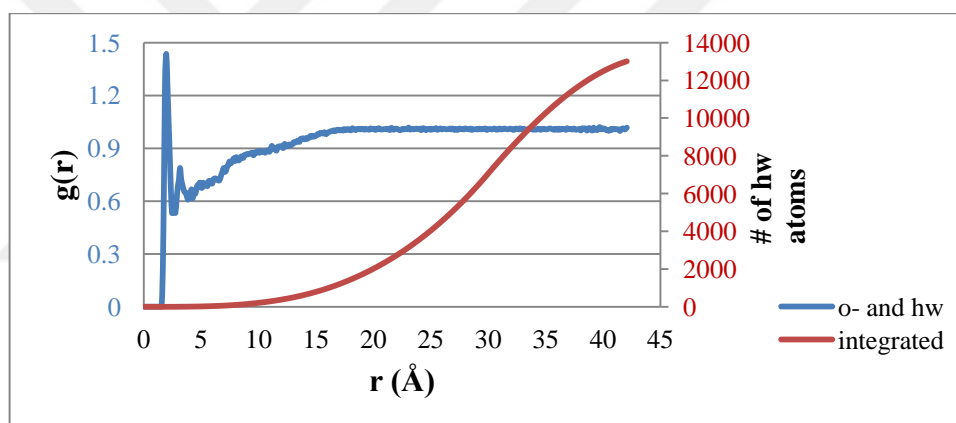


Figure 4.49. Pairwise Radial Distribution Function of oxygen ion (o-) of 1 ionic V-HCl and hydrogen (hw) of water between 0-1 ns

In Fig. 4.50 the first peak starts at 2.35 Å and ends at 3.65 Å, giving a maximum value of 2.5 at  $r=2.65$  Å, which means there is a chance of finding oxygen of water at this distance is 2.5 times of the chance finding it anywhere else. Integrated value gives the number of oxygen atoms of water molecules at this distance, it is 2, implying 2 water molecules. According to this RDF plot hydrogen bonds can be located for the distance  $r(n-o) \leq 3.25$  Å. In Fig. 4.41 the first peak starts at 2.45 Å and ends at 3.65 Å, giving a maximum value of 1.7 at  $r=2.85$  Å, which means there is a chance of finding oxygen of water at this distance is 1.7 times of the chance finding it anywhere else. Integrated value gives the number of oxygen atoms of water molecules at this distance, it is 1, implying 1 water molecule. In

experimental studies of radial distribution functions obtained by X-ray method, because of the difficulties in observing the hydrogen atoms of water, radial distribution functions of solute and oxygen of water are used as complementary [112]. These complementary data are expected to give the same or similar results. As validated from previous figures calculations for hydrogen and oxygen of water molecules give same number of water molecules.

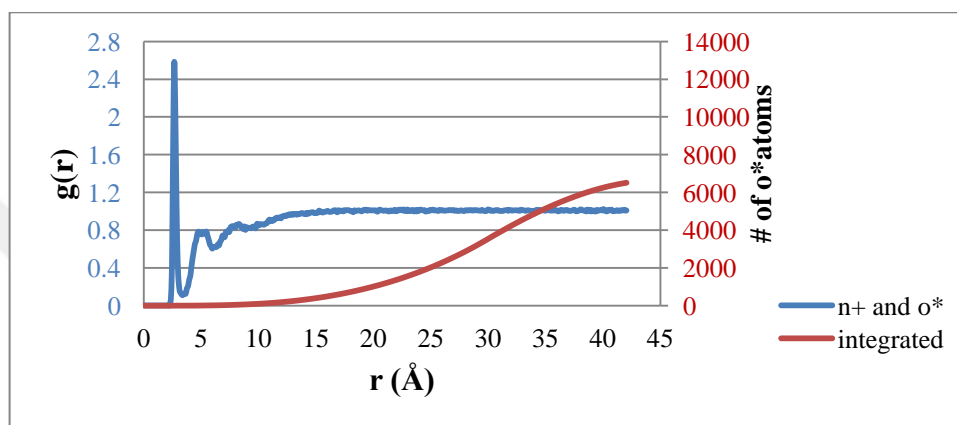


Figure 4.50. Pairwise Radial Distribution Function of nitrogen ion ( $n+$ ) of 1 ionic V-HCl and oxygen ( $o^*$ ) of water between 0-1 ns

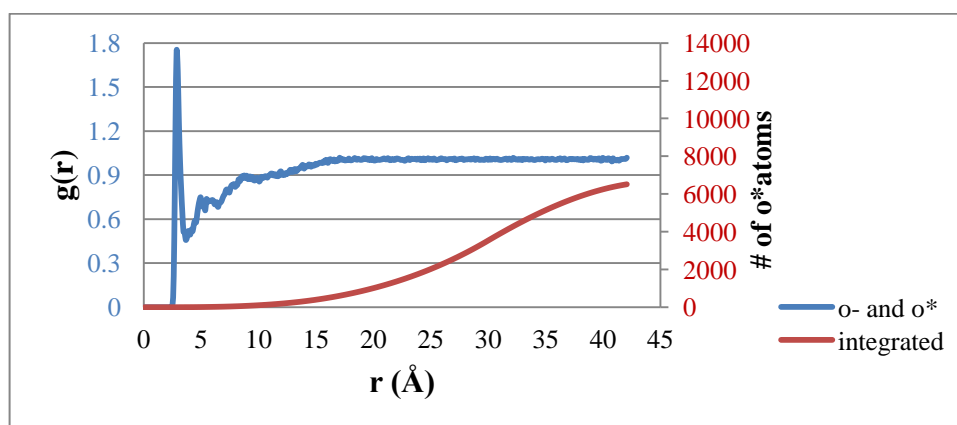


Figure 4.51. Pairwise Radial Distribution Function of oxygen ion ( $o^-$ ) of 1 ionic V-HCl and oxygen ( $o^*$ ) of water between 0-1 ns

When figure 4.50 and 4.51 are treated together, it is seen that for distances up to 15 Å, the oxygen density varies from bulk solvent and also varies from different sites of vancomycin

(as amino terminus and carboxyl terminus). This is an indication of specific solvent structure around vancomycin molecule [98]. The positively charged part of the vancomycin molecule, i.e. nitrogen atom of the amino terminus, attracts mostly the electronegative charged oxygen of water molecule. Therefore probability of finding oxygen of water is higher for positively charged amino terminus than negatively charged carboxy terminus.

For ease of interpretation of the results pairwise radial distribution is calculated for oxygen atom of water molecules for the rest of the study.

Also in order to see the time dependent behavior of atoms of the water molecules RDF analysis can be performed for certain time intervals. The figures 4.52 to 4.57 represent time dependent RDF of the systems. First analysis is performed for 0-1 ns interval for production run. Then last 19-20 ns interval of the simulations is investigated. With this time dependent results the interaction between oxygen/hydrogen atoms of water and selected vancomycin atoms will be observed. The interaction between active sites of vancomycin and oxygen atom of water is investigated due to the reason explained above.

As seen in Fig. 4.52 at time interval 0-1 ns first peak of the RDF analysis has the maximum value of 2.58 at 298 K, at time interval 19-20 ns first peak has the maximum value of 2.61 at  $r = 2.65 \text{ \AA}$ . And between 0-1 ns and 19-20 ns number of oxygen atom of water molecules remains same. Assembling of water molecules and probability of finding them around amino terminus of vancomycin shows hydrophilicity but the change in number of oxygen atoms is small. At all time intervals number of hydration shells are same. At the latest time interval amino terminus has 2 water molecules at first, 15 water molecules at second, 78 water molecules at third hydration shell. These clusters present sphere-like hydrated shells, ordered due to water–water hydrogen bonding formation. At time interval 0-1 ns first peak of the RDF analysis has the maximum value of 2.56 at 310 K, at time interval 19-20 ns first peak has the maximum value of 2.66 at  $r = 2.65 \text{ \AA}$ .



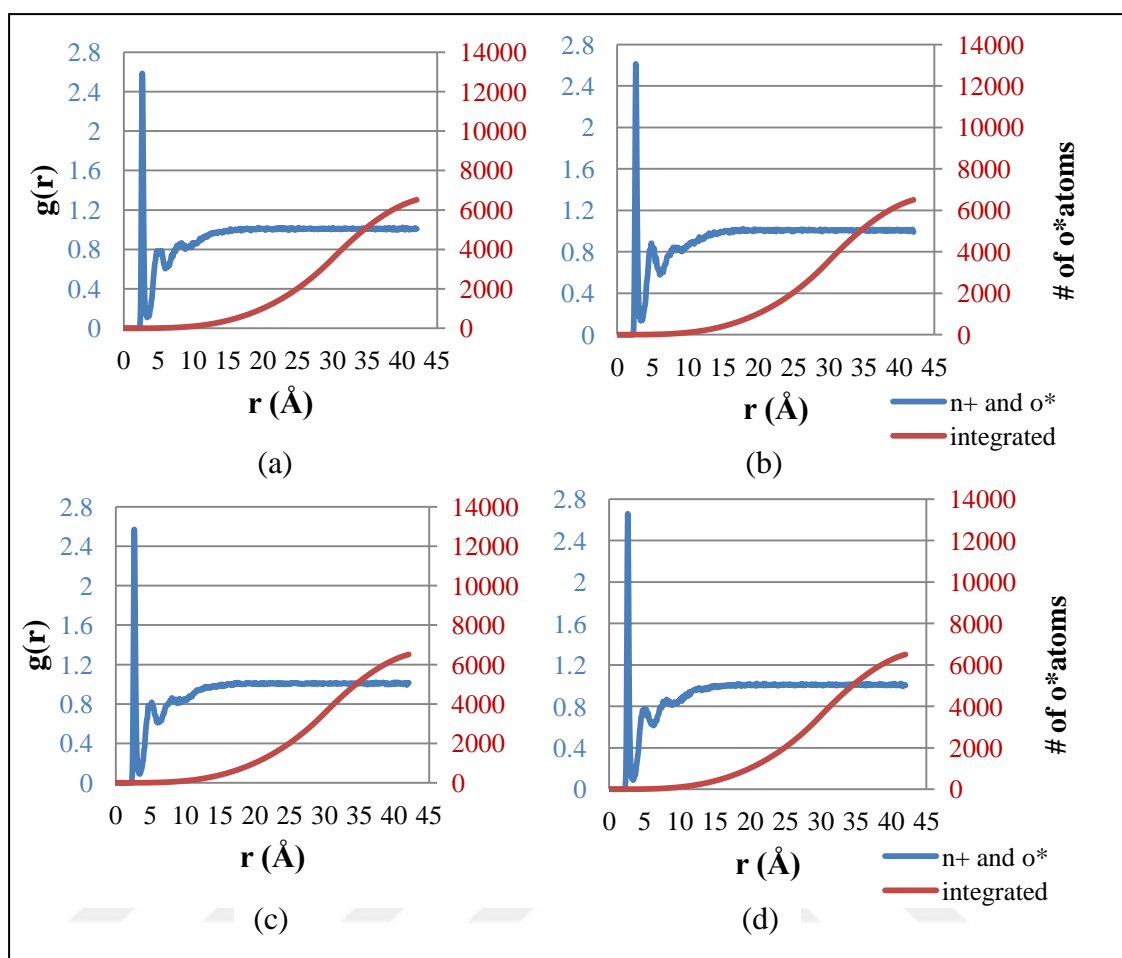


Figure 4.52. Pairwise Radial Distribution Function of nitrogen ion ( $n^+$ ) of 1 ionic V-HCl and oxygen ( $o^*$ ) of water between a) 0-1 ns at 298 K and b) 19-20 ns at 298 K c) 0-1 ns at 310 K and b) 19-20 ns at 310 K

As seen in Fig. 4.53 at time interval 0-1 first peak of the RDF analysis has the maximum value of 1.74 at 298 K and at time interval 19-20 ns first peak has the maximum value of 1.67 at  $r = 2.75 \text{ \AA}$ . At time interval 0-1 ns first peak of the RDF analysis has the maximum value of 1.63 at 310 K, at time interval 19-20 ns the maximum value of first peak is same as previous time interval.

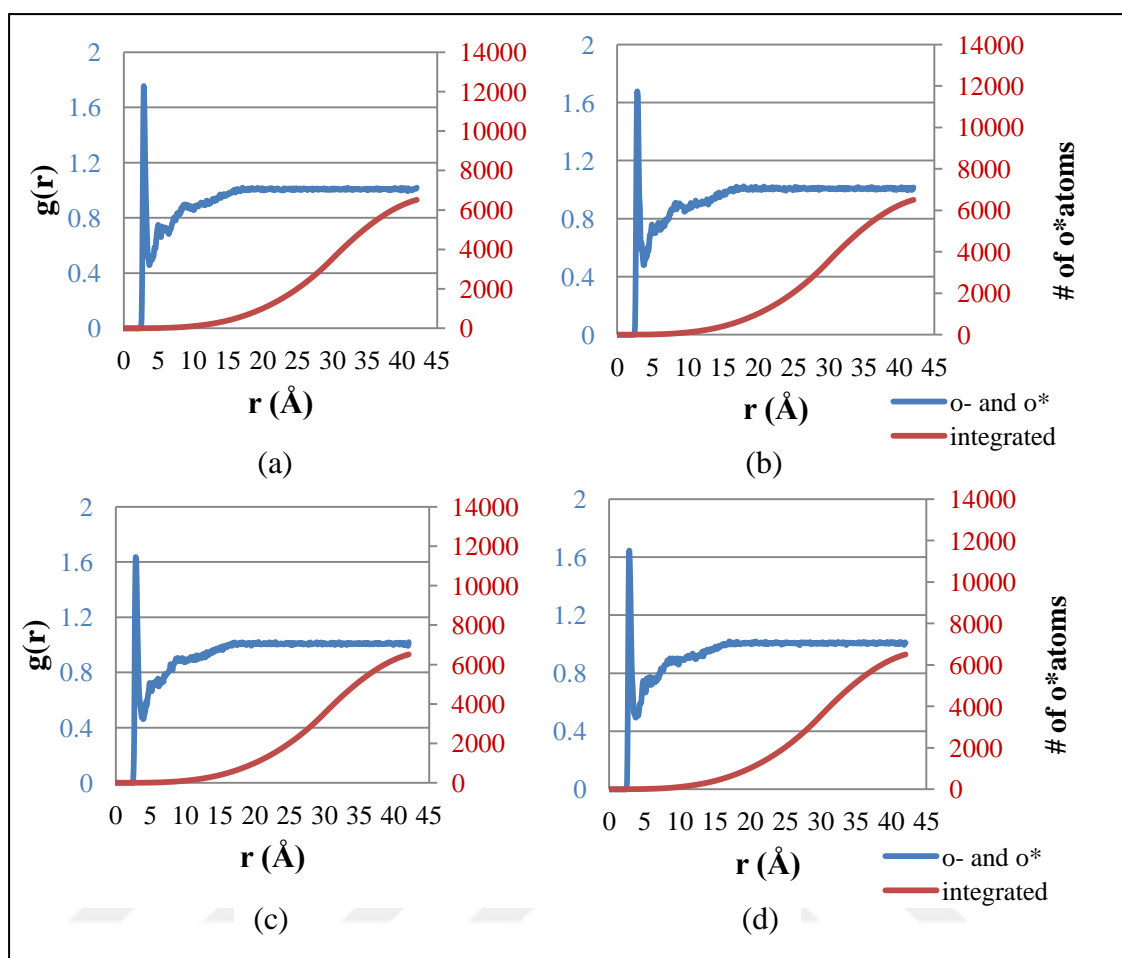


Figure 4.53. Pairwise Radial Distribution Function of oxygen ion (o-) of 1 ionic V-HCl and oxygen (o\*) of water between a) 0-1 ns at 298 K and b) 19-20 ns at 298 K c) 0-1 ns at 310 K and b) 19-20 ns at 310 K

From previous two figures, Fig 4.52 and Fig. 4.53 it can be concluded that amino terminus of vancomycin has more water molecules in its first hydration shell. Also the width of the first peak of  $g(r)$  function is an indication of hydrogen bond strength. As seen first peak of carboxy terminus is wider than first peak of amino terminus, which indicates carboxy terminus has weaker hydrogen bonds [99]. However the bond strength represented is between selected atoms that nitrogen ion and oxygen of water and oxygen ion and oxygen of water. It is known that positively charged ions tend to attract oxygen of the water molecule whereas the negatively charged ions tend to attract and form stronger bonds with hydrogen of water molecule This is also observed from figures 4.37 to 4.40. The first peak of nitrogen ion and hydrogen of water (figure 4.37) is weaker than the first peak of oxygen ion and hydrogen of water (figure 4.38) where the first peak of nitrogen ion and oxygen of

water (figure 4.39) is stronger than the first peak of oxygen ion and oxygen of water (figure 4.40).

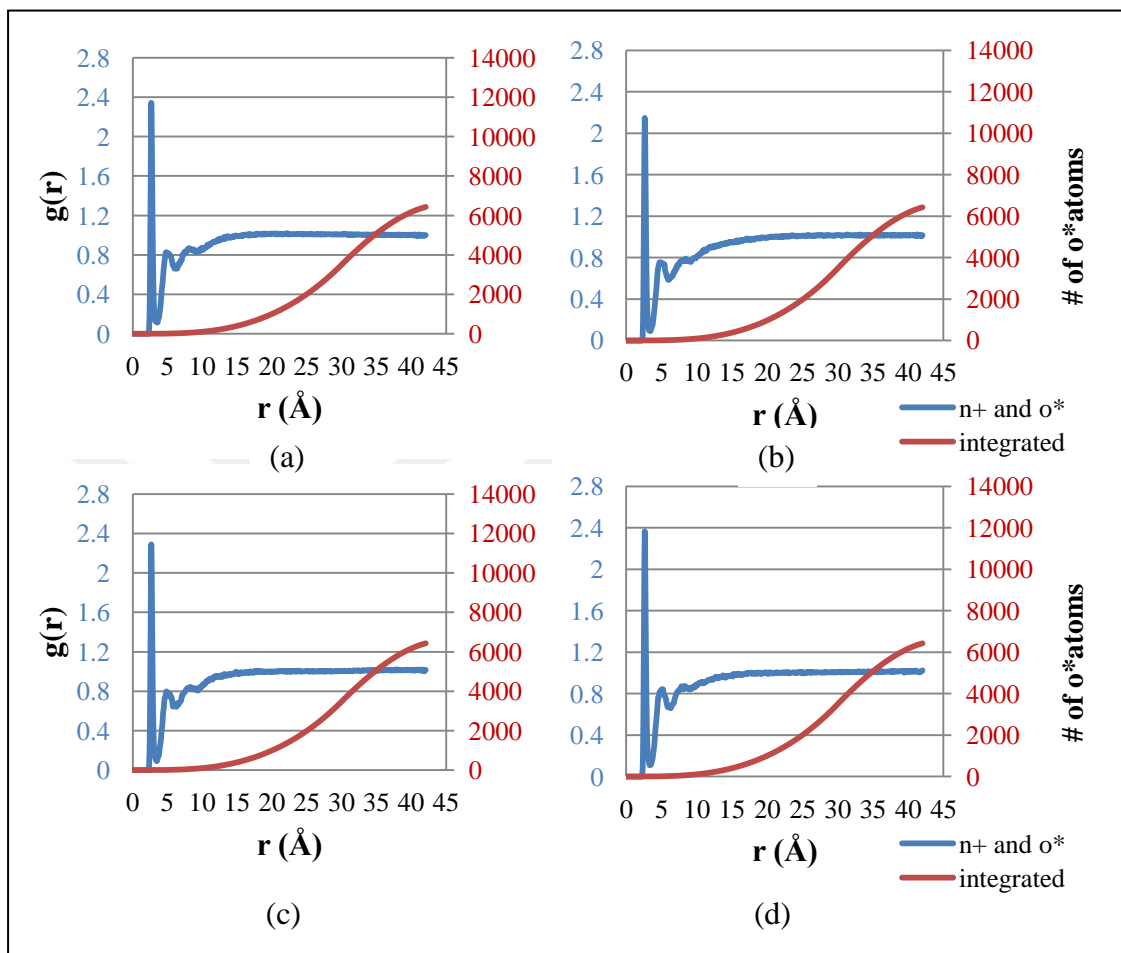


Figure 4.54. Pairwise Radial Distribution Function of nitrogen ion ( $n^+$ ) of 2 ionic V-HCl and oxygen ( $o^*$ ) of water between a) 0-1 ns at 298 K and b) 19-20 ns at 298 K c) 0-1 ns at 310 K and b) 19-20 ns at 310 K

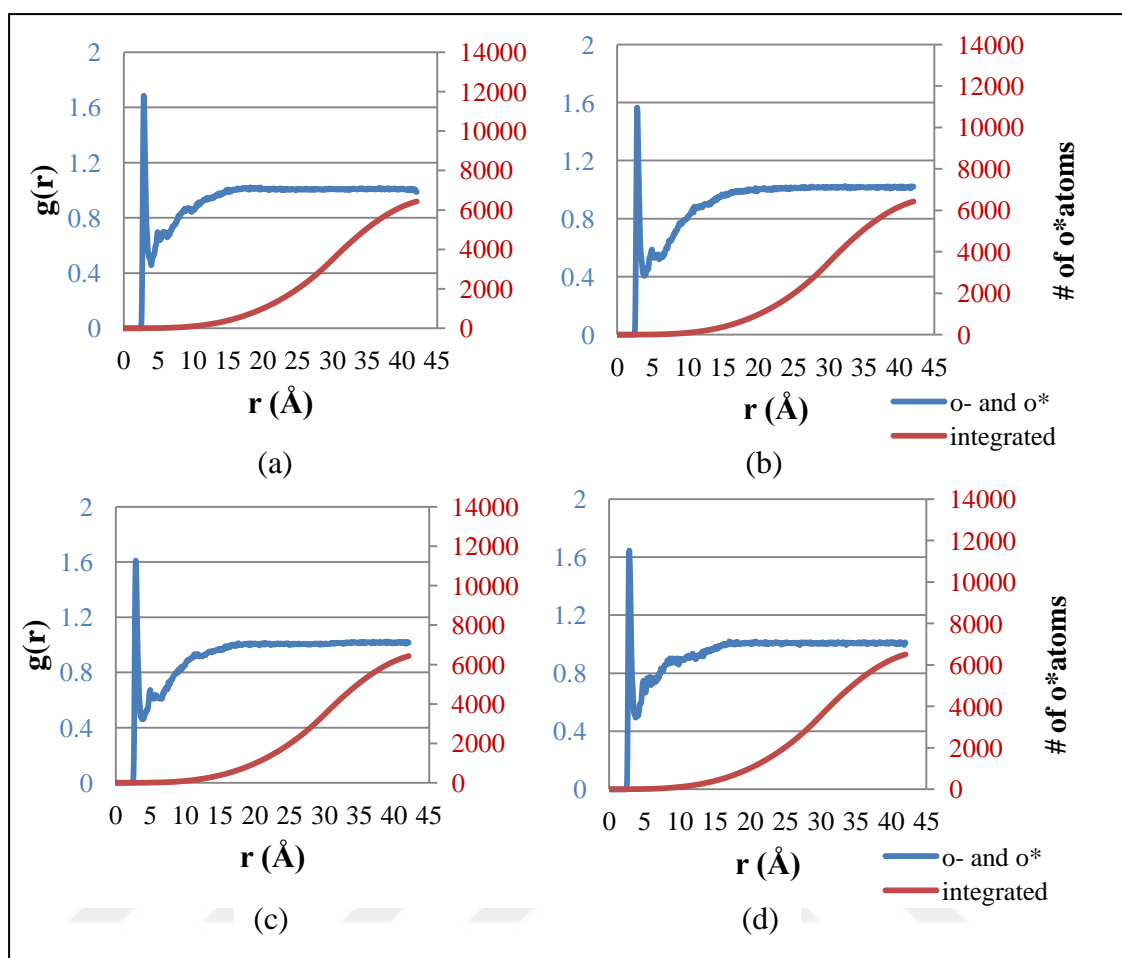


Figure 4.55. Pairwise Radial Distribution Function of oxygen ion (o-) of 2 ionic V-HCl and oxygen (o\*) of water between a) 0-1 ns at 298 K and b) 19-20 ns at 298 K c) 0-1 ns at 310 K and b) 19-20 ns at 310 K

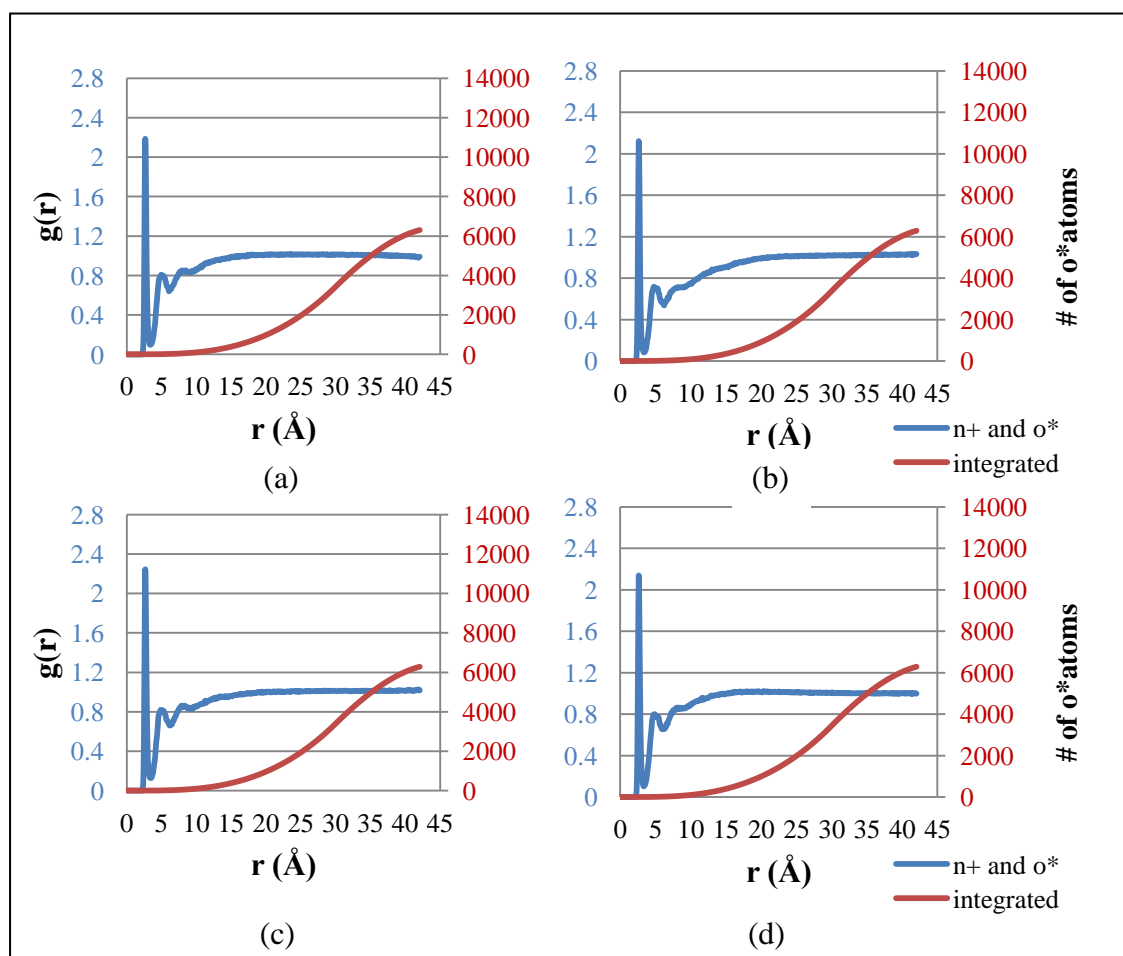


Figure 4.56. Pairwise Radial Distribution Function of nitrogen ion ( $n^+$ ) of 4 ionic V-HCl and oxygen ( $o^*$ ) of water between a) 0-1 ns at 298 K and b) 19-20 ns at 298 K c) 0-1 ns at 310 K and b) 19-20 ns at 310 K

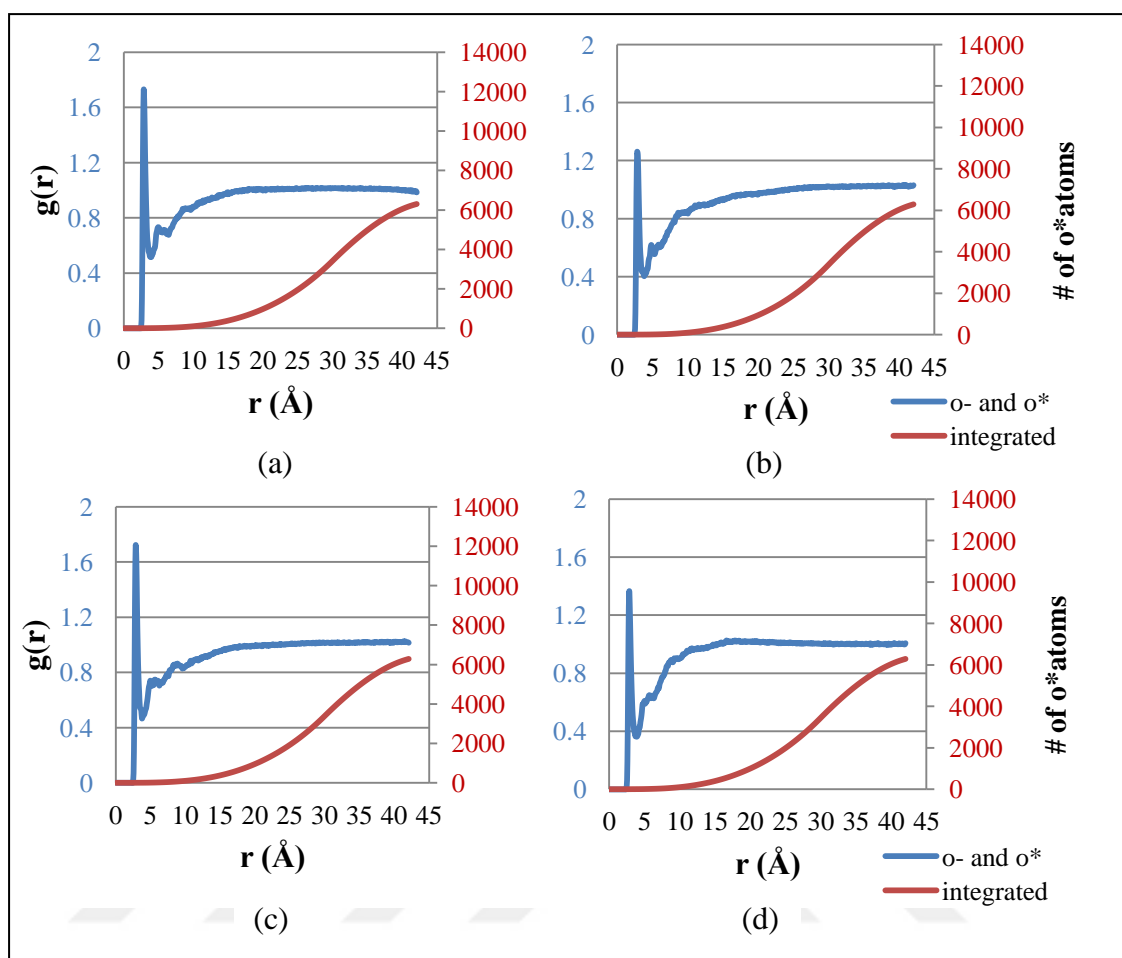


Figure 4.57. Pairwise Radial Distribution Function of oxygen ion ( $o^-$ ) of 2 ionic V-HCl and oxygen ( $o^*$ ) of water between a) 0-1 ns at 298 K and b) 19-20 ns at 298 K c) 0-1 ns at 310 K and b) 19-20 ns at 310 K

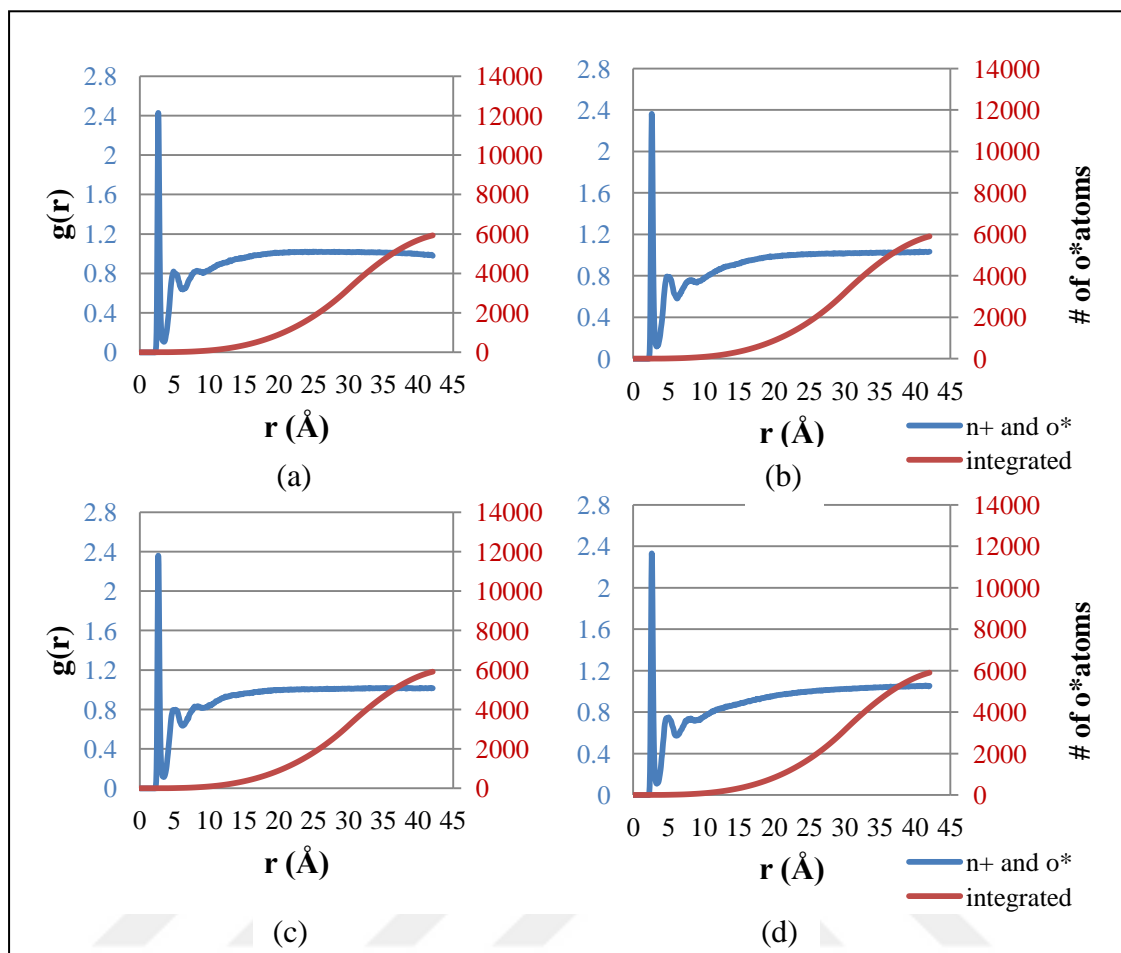


Figure 4.58. Pairwise Radial Distribution Function of nitrogen ion ( $n^+$ ) of 9 ionic V-HCl and oxygen ( $o^*$ ) of water between a) 0-1 ns at 298 K and b) 19-20 ns at 298 K c) 0-1 ns at 310 K and b) 19-20 ns at 310 K

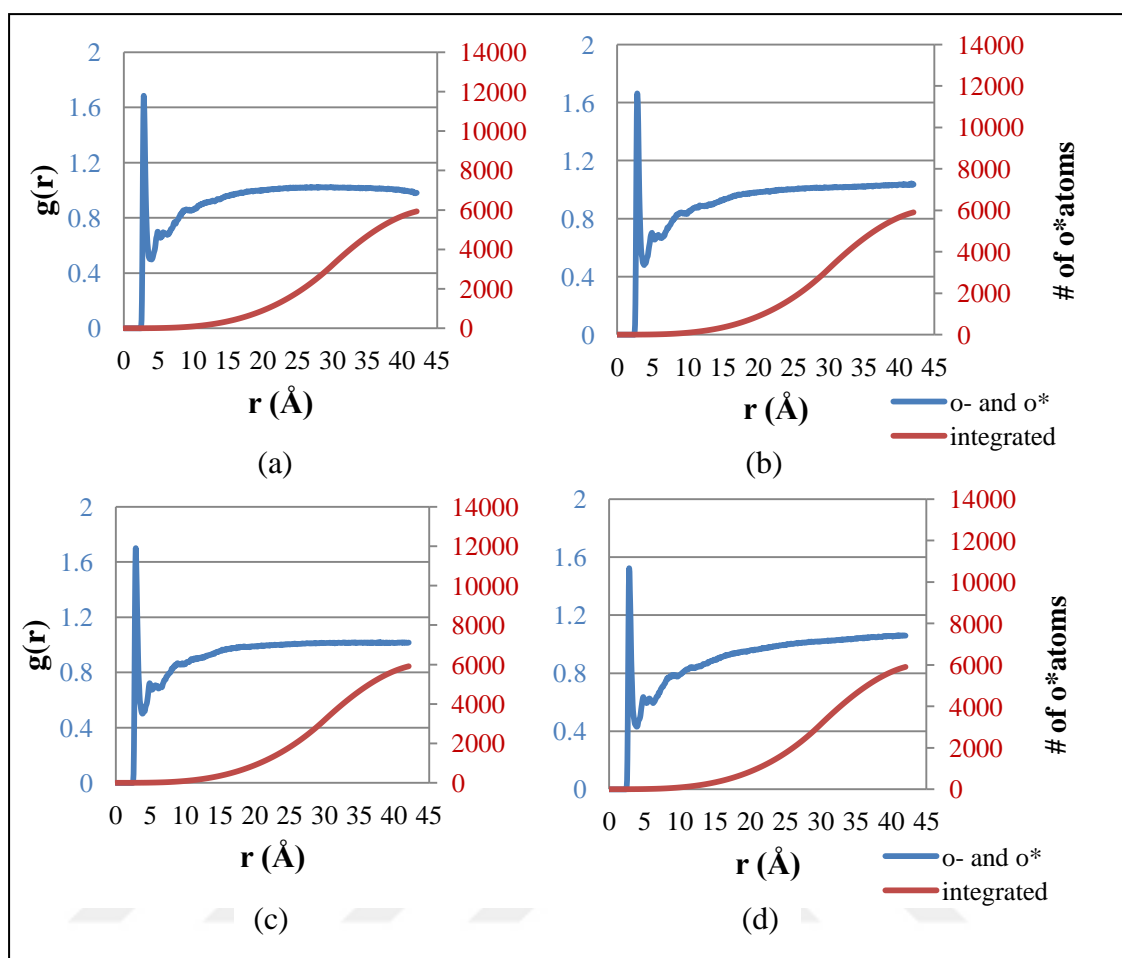


Figure 4.59. Pairwise Radial Distribution Function of oxygen ion (o-) of 9 ionic V-HCl and oxygen (o\*) of water between a) 0-1 ns at 298 K and b) 19-20 ns at 298 K c) 0-1 ns at 310 K and b) 19-20 ns at 310 K



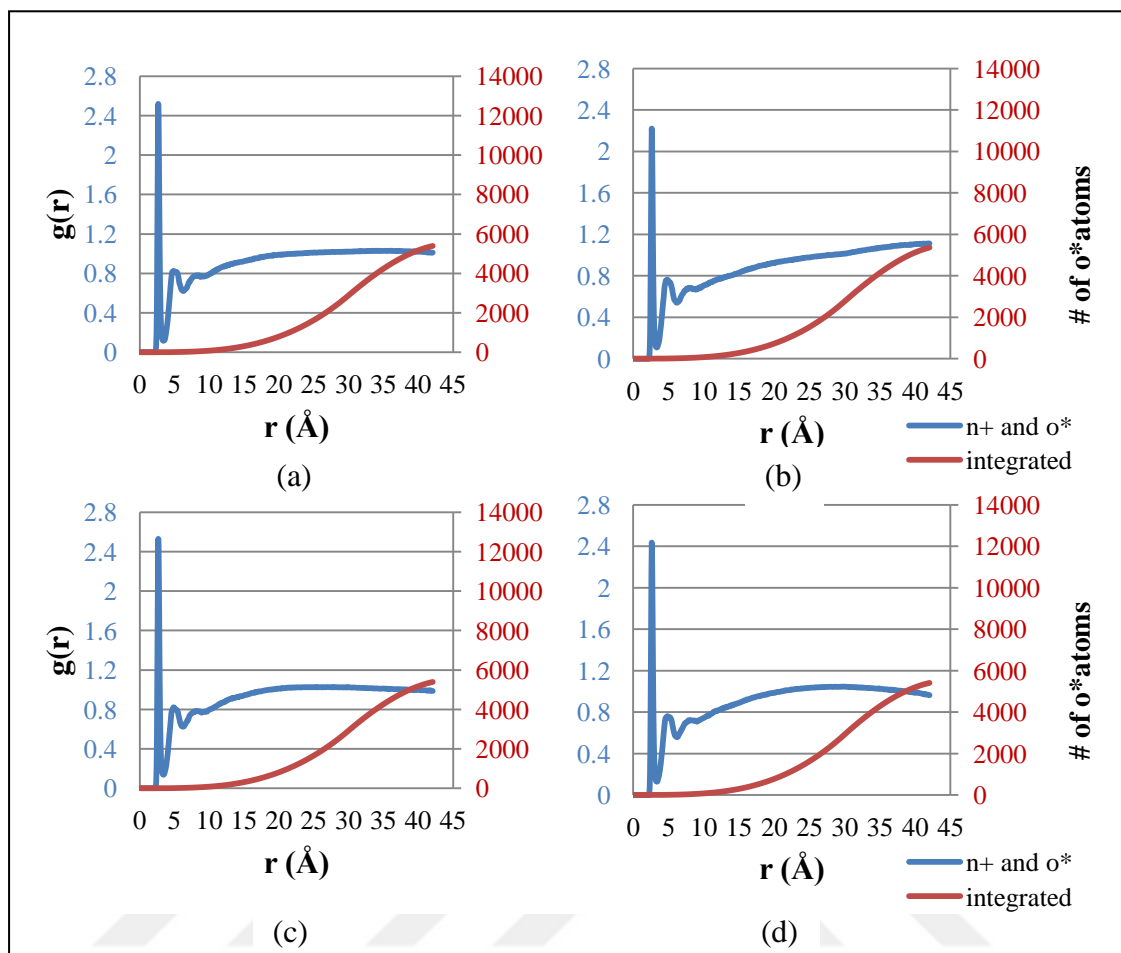


Figure 4.60. Pairwise Radial Distribution Function of nitrogen ion ( $n^+$ ) of 16 ionic V-HCl and oxygen ( $o^*$ ) of water between a) 0-1 ns at 298 K and b) 19-20 ns at 298 K c) 0-1 ns at 310 K and b) 19-20 ns at 310 K

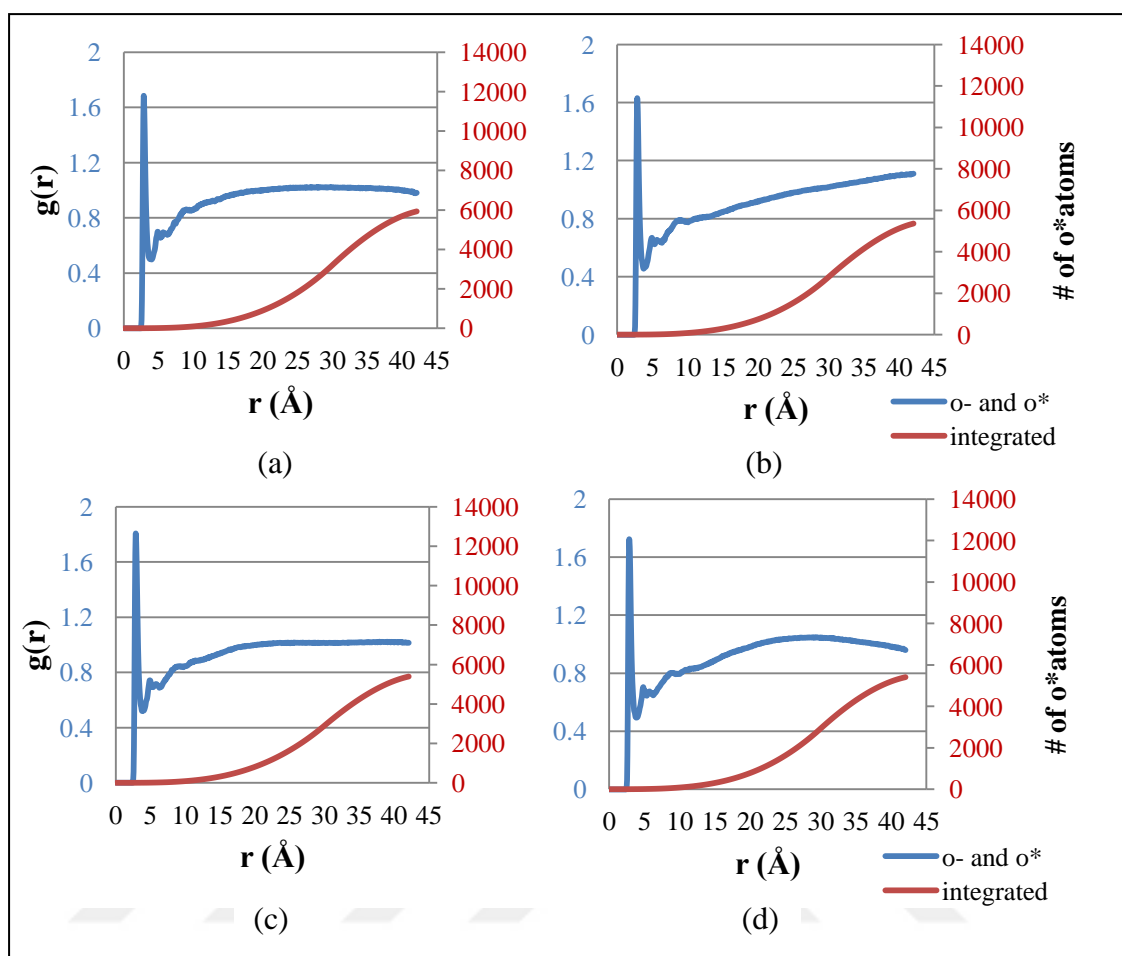


Figure 4.61. Pairwise Radial Distribution Function of oxygen ion (o-) of 16 ionic V-HCl and oxygen (o\*) of water between a) 0-1 ns at 298 K and b) 19-20 ns at 298 K c) 0-1 ns at 310 K and b) 19-20 ns at 310 K

It is observed for the systems having 2 to 16 vancomycin, for amino and carboxy terminus as simulation proceeds the probability of finding an oxygen atom which belongs to water molecule decreases slightly for both 298 K and 310 K. The pairwise radial distribution function of the systems including vancomycin in aqueous medium was investigated for simulations performed at 310 K. For amino terminus at higher temperature the probability of finding water molecules at a distance of 2.75 Å is higher than 298 K. The radial distribution function parameter, the probability of finding of oxygen of water are listed for amino and carboxy terminus of vancomycin for all systems in Table 4.8.

Table 4.8. Radial Distribution Function of amino and carboxy terminus of vancomycin for all systems

	Temperature (K)	298		310	
	Time (ns)	0-1	19-20	0-1	19-20
# of VHCl	type of interacting atoms				
1	n+ - o*	2.61	2.58	2.66	2.56
	o- - o*	1.74	1.67	1.69	1.63
2	n+ - o*	2.3	2.14	2.36	2.29
	o- - o*	1.67	1.56	1.6	1.46
4	n+ - o*	2.18	2.12	2.24	2.13
	o- - o*	1.71	1.25	1.71	1.36
9	n+ - o*	2.42	2.36	2.36	2.33
	o- - o*	1.67	1.65	1.68	1.52
16	n+ - o*	2.53	2.22	2.52	2.43
	o- - o*	1.82	1.62	1.79	1.71

Aforementioned systems in section 4.3.2. were already simulated in a simulation box full of water. As the distances of each molecule is long even at the beginning, the water molecules are already dispersed around each molecule. Thus number of oxygen atoms which belong to water molecules do not change significantly during the simulations.

#### 4.4. SIMULATIONS IN VACUUM WITH VANCOMYCIN AND LEVAN

In order to observe the behavior of vancomycin molecule in the same simulation box with levan molecule, 6 simulations were performed. It was aimed to see if vancomycin and levan have a specific interaction with each other that is orientation dependent. In these simulations vancomycin molecule was fixed at the center of the box and in each simulation levan molecule was placed at different positions. Levan polymer used in the simulations has 12 fructose rings, 255 atoms. Table 4.9 represents the simulations performed.

The following tables show the results of each simulation on the basis of closest 10 atoms after 20 ns of production run. Initial distances of the closest atoms and also atom types are listed. A small graphical representation is given for each table, showing the initial positions of levan and V-HCl, and the red lines connect the closest atoms. These figures are only used to see which sites of V-HCl are favored. As levan polymer have conformational

changes through the simulation, figures are not appropriate to investigate the shape of the cluster at the end of the simulation. This kind of information will be given on the basis of cluster  $R_g$  analysis.

Table 4.9. Simulations performed in vacuum with 1 ionic V-HCl and 1 Levan  
(total duration= 22 ns)

		# of V-HCl	# of Levan	Position of Levan	T (K)
<b>1</b>	Ionic V-HCl	1	1	above	298
<b>2</b>	Ionic V-HCl	1	1	below	298
<b>3</b>	Ionic V-HCl	1	1	behind	298
<b>4</b>	Ionic V-HCl	1	1	in front	298
<b>5</b>	Ionic V-HCl	1	1	left	298
<b>6</b>	Ionic V-HCl	1	1	right	298

Table 4.10. Distance Data Obtained, Levan Position: above

V-HCl Atom #	V-HCl Atom Type	Levan Atom #	Levan Atom Type	Distance at 5 ns	Initial Distance
142	h+	194	oh	1.72	21.60
145	ho	299	oh	1.93	22.77
154	hc	315	hc	2.00	22.27
164	h+	249	oh	2.04	15.18
138	ho	252	oh	2.18	15.54
159	hn	314	ho	2.29	23.84
56	c	260	hc	2.35	26.71
34	hc	335	ho	2.48	18.73
176	h+	253	hc	2.49	14.59
33	hn	313	oh	2.56	20.44

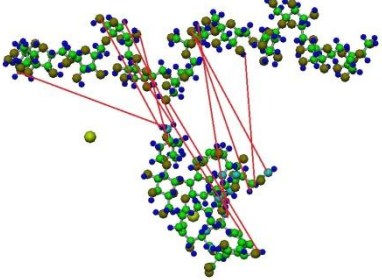


Table 4.11. Distance Data Obtained, Levan Position: below

V-HCl Atom #	V-HCl Atom Type	Levan Atom #	Levan Atom Type	Distance at 5 ns	Initial Distance
142	h+	431	ho	1.66	39.40
176	h+	426	oh	1.82	39.08
83	o-	364	ho	1.87	12.98
94	oh	196	ho	1.98	19.39
145	ho	405	oh	2.02	13.34
152	hc	367	hc	2.09	12.80
72	oh	419	ho	2.16	20.22
110	hc	315	hc	2.26	16.66
105	hc	320	hc	2.39	13.62
164	h+	431	ho	2.42	39.49

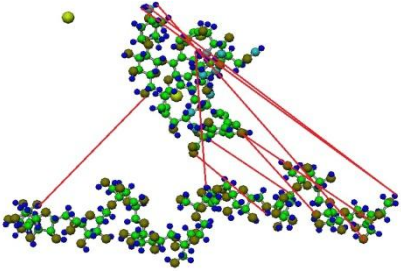


Table 4.12. Distance Data Obtained, Levan Position: behind

V-HCl Atom #	V-HCl Atom Type	Levan Atom #	Levan Atom Type	Distance at 5 ns	Initial Distance
142	h+	186	oh	1.79	25.98
82	o-	419	ho	2.09	22.01
164	h+	196	ho	2.19	21.10
171	hc	253	hc	2.23	20.98
173	hc	339	hc	2.23	15.97
129	ho	376	oh	2.23	24.37
125	hc	383	hc	2.28	21.30
81	c-	419	ho	2.43	20.96
68	o=	424	hc	2.44	15.64
176	h+	196	ho	2.48	20.76

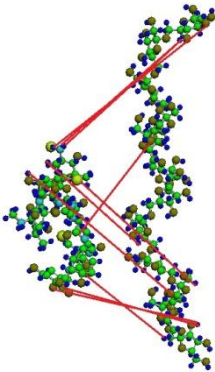


Table 4.13. Distance Data Obtained, Levan Position: in front

V-HCl Atom #	V-HCl Atom Type	Levan Atom #	Levan Atom Type	Distance at 5 ns	Initial Distance
82	o-	419	ho	1.91	11.01
54	oh	217	ho	1.92	35.45
144	ho	257	oh	1.92	24.53
176	h+	342	oh	1.94	21.71
153	ho	236	oh	1.97	35.96
77	oh	344	ho	1.99	15.16
175	hc	338	hc	2.13	20.30
139	hc	380	hc	2.14	23.09
83	o-	386	ho	2.14	15.78
113	hc	320	hc	2.26	14.32

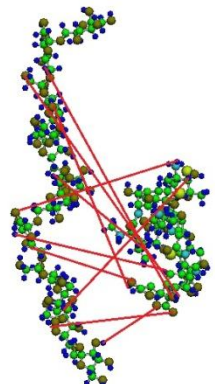


Table 4.14. Distance Data Obtained, Levan Position: left

V-HCl Atom #	V-HCl Atom Type	Levan Atom #	Levan Atom Type	Distance at 5 ns	Initial Distance
164	h+	301	ho	1.77	16.99
133	ho	313	oh	1.93	11.11
142	h+	293	hc	1.95	17.23
163	hc	319	hc	2.20	11.47
173	hc	275	hc	2.21	21.26
158	hc	259	ho	2.30	25.31
30	o=	259	ho	2.41	27.22
137	hc	315	hc	2.42	11.74
98	n+	293	hc	2.43	17.49
27	o=	280	ho	2.50	29.25

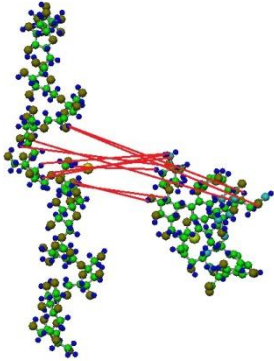
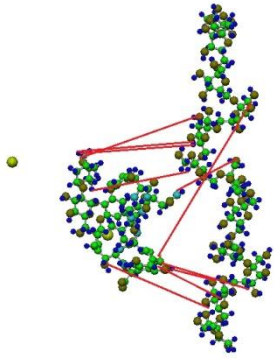


Table 4.15. Distance Data Obtained, Levan Position: right

V-HCl Atom #	V-HCl Atom Type	Levan Atom #	Levan Atom Type	Distance at 5 ns	Initial Distance
153	ho	397	oh	1.96	5.94
33	hn	321	oh	2.08	9.47
160	hc	399	hc	2.13	9.52
142	h+	280	ho	2.14	15.56
138	ho	270	oh	2.15	17.79
164	h+	280	ho	2.25	15.90
172	hc	240	hc	2.31	22.20
165	hc	256	hc	2.39	25.15
55	c	381	hc	2.42	13.16
70	oh	407	ho	2.43	15.37



It is observed that independent of the position, positively charged sites of vancomycin have tendency to interact with levan. These sites attract the atoms of levan so much that the approach of two atoms can be up to 93 % from initial positions of the atoms. Also negatively charged site of the V-HCl has tendency to interact with levan as seen in below, behind and in front simulations. It can be concluded that the active sites mentioned in the literature review are observed and validated by molecular dynamics simulations. However, short-range interactions are also observed depending on the position of levan. These kinds of behavior show that higher polymer concentrations would be more effective in the encapsulation process. As the molecules would be packed tightly short-range interactions

would provide attraction to the atoms of vancomycin rather than just the active site atoms. Similar approach can be applied for more than one levan molecules. Also this would give an estimate on how many levan molecules are approximately required to encapsulate one vancomycin molecule. Also to include the effect of environment, same simulations will be performed in aqueous medium.

Time dependent cluster  $R_g$  values of 1 V-HCl and 1 Levan systems at 298 K in vacuum are shown in Fig.4.62. As seen in the graph all cluster  $R_g$  values tend to decrease from initial states. This can be explained with several reasons. At time = 0, levan is a linear polymer, as time passes levan polymer tends to fold so the atoms will be closer to the center of mass of the cluster with respect to the linear state of levan.

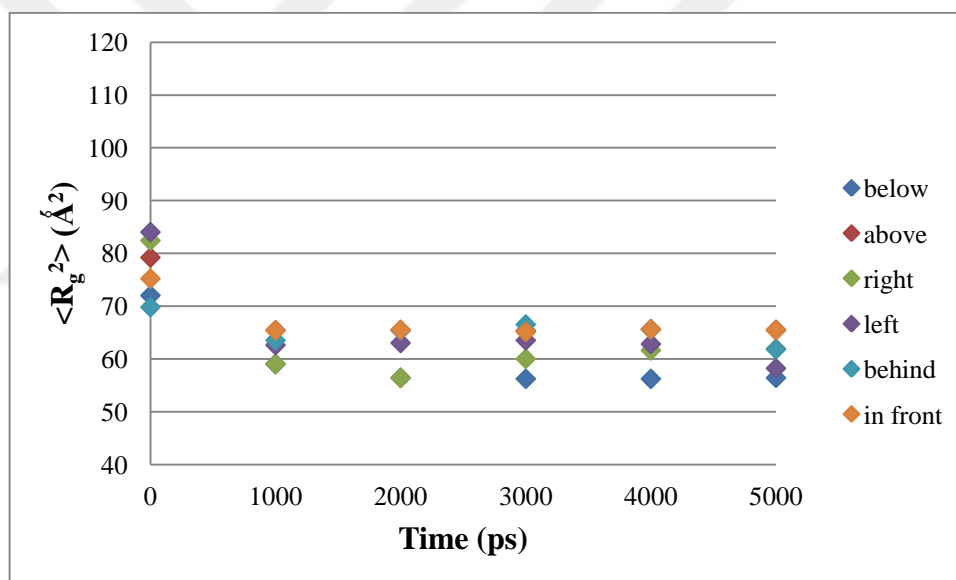


Figure 4.62. Cluster  $R_g$  of V-HCl and Levan systems at 298 K in vacuum

Also it was observed in the simulations that V-HCl and levan has an attraction and tend to come closer, which would again cause a decrease in cluster  $R_g$ . The smallest value belongs to the system including levan below the vancomycin, which shows at that position the system is in most packed form with respect to other systems. However, other systems with levan at different positions also have a similar cluster  $R_g$ . This result shows that the position of levan does not affect the system significantly.

#### 4.5. ENCAPSULATION AND RELEASE OF VANCOMYCIN

In experimental studies [64] vancomycin encapsulated particles were obtained by precipitation method and then freeze-dried. As both vancomycin and levan are hydrophilic structures, water molecules in the environment should be avoided. This procedure was assumed to be identical to vacuum conditions in MD simulations as no water molecules are represented in the system. Systems were run 20 ns for production stage then the coordinates of each atom in the system after 20 ns, are transferred to a new simulation box and box is filled with water molecules. Temperature for the new system was chosen to be 310 K in order to simulate body conditions. Cluster radius of gyration calculations, showing the dispersion of each molecule, for the systems are performed to have an idea for release of vancomycin through polymers. Table 4.16 represents the systems performed first at vacuum at 298 K and then solvated at 310 K.

Simulations performed have only one vancomycin with varying levan amount. The systems represent a small portion of whole system as real time systems have much more vancomycin molecules. Figure 4.63 represents how a macro system was reduced to a micro system.

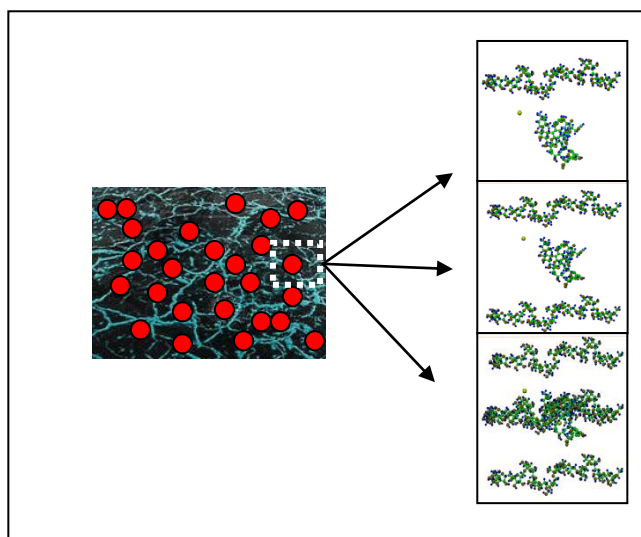


Figure 4.63. Representation of Simulated Systems with one vancomycin and varying number of levan molecules



Table 4.16. Vancomycin/Levan simulations performed in vacuum at 298 K and solvated at 310 K (total duration= 44 ns)

		# of V-HCl	# of Levan	Vancomycin/Levan
<b>1</b>	Ionic V-HCl	1	1	1
<b>2</b>	Ionic V-HCl	1	2	0.5
<b>3</b>	Ionic V-HCl	1	4	0.25

The encapsulation process occurs at the beginning of the simulations in equilibration steps. The equilibration of the systems are represented in the following figures from Figure 4.64 to 4.66.

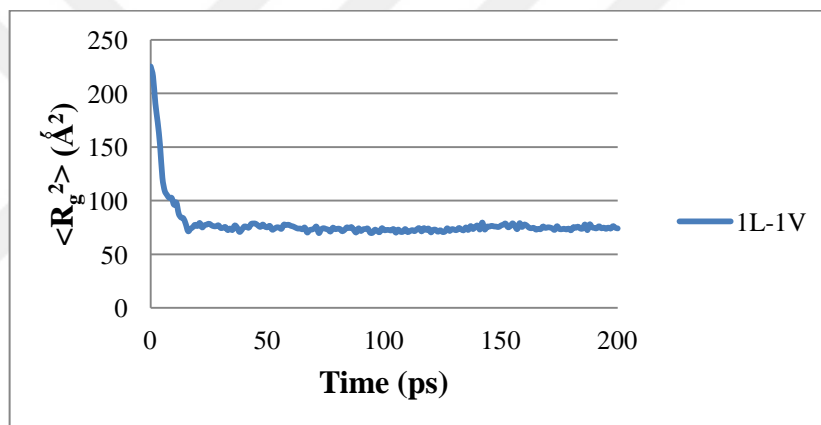


Figure 4.64. Encapsulation of 1 levan 1 vancomycin system

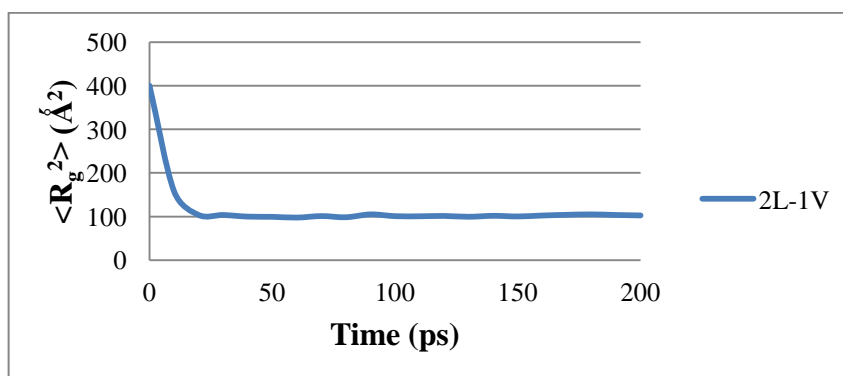


Figure 4.65. Encapsulation of 2 levan 1 vancomycin system

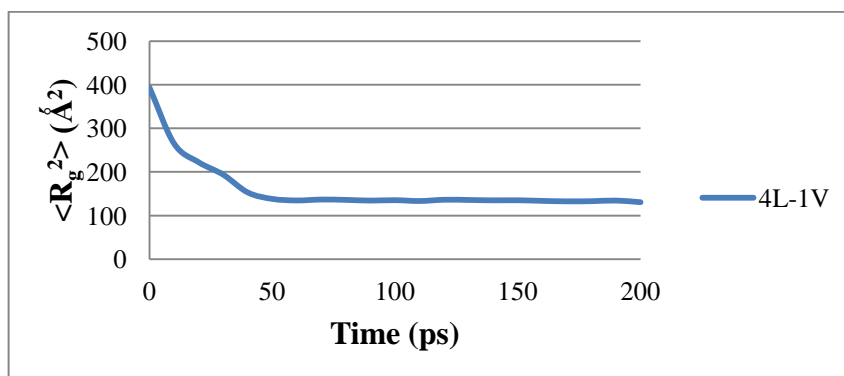


Figure 4.66. Encapsulation of 4 levan 1 vancomycin system

The sharp decrease in the cluster  $R_g$  of previous charts shows the encapsulation of levan molecules and vancomycin molecule. As the number of levan molecules increases in the system the encapsulation process takes more time. It takes 16 ps, 22 ps and 48 ps for systems having 1, 2 and 4 levan molecules respectively.

The figures Fig. 4.67 to 4.69 show the cluster  $R_g$  of the systems. Vancomycin molecules used in the simulations are in ionic form. The data represented in the charts for 0-20 ns time interval belongs to simulations performed at vacuum, 298 K. Remaining data for 20–40 ns time interval shows the simulations performed in aqueous medium, 310 K. As observed in all charts the cluster  $R_g$  values increases immediately with the presence of water molecules. The most dispersed system after 40 ns production run was observed to be 2 levan, 1 vancomycin system. In the system consisting of 4 levan and 1 vancomycin has the lowest dispersion through time as the water molecules needs to go across the levan and vancomycin molecules by disturbing their attraction. In this system levan molecules are placed on top, below, right and left handside of vancomycin, where in system consisting of 2 levan and 1 vancomycin levan molecules are placed on top and below the vancomycin. When the systems are solvated, water molecules readily filled the right and left hand side the vancomycin in 2 levan, 1 vancomycin system where water molecules directly interact with vancomycin. For encapsulation process to release the vancomycin in a more controlled manner, all sides of vancomycin should be coated with polymer. The amount of polymer should be decided with respect to the amount of drug to be encapsulated. The experimental study was performed by Sezer and coworkers and they found that encapsulation capacity increases with increasing concentrations of levan when vancomycin

has constant concentration. [64] System having 4 levans and 1 vancomycin would yield encapsulation capacity more than other studied systems as the vancomycin concentration is same and levan concentration is highest. In the study of Sezer et al. in vitro vancomycin release through levan shows that systems having higher concentration of levan needs more time for diffusion. MD simulations represented in this study confirm the validity of these results.

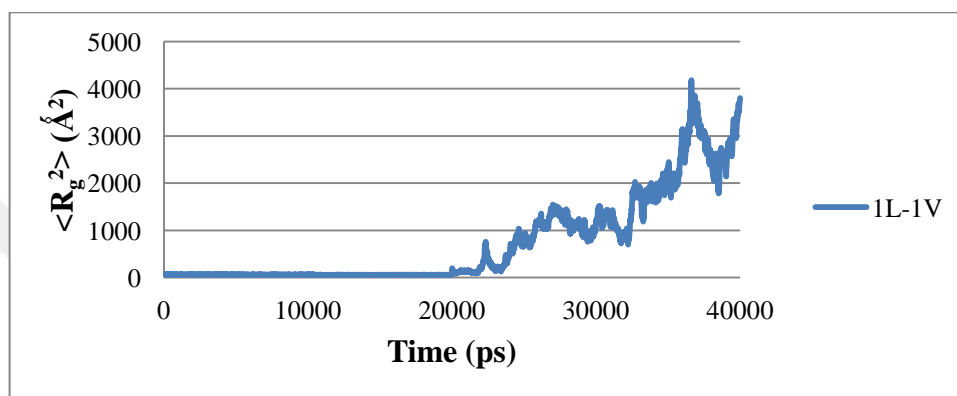


Figure 4.67. Cluster  $R_g$  of 1 Levan – 1 Vancomycin System

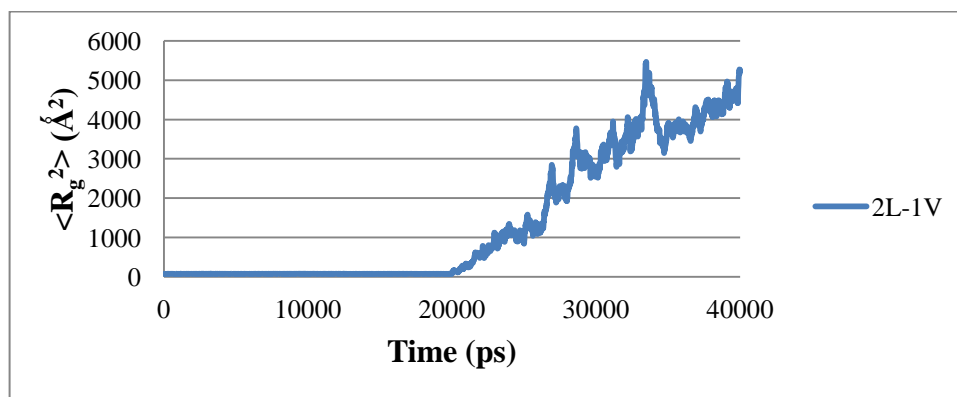


Figure 4.68. Cluster  $R_g$  of 2 Levan – 1 Vancomycin System

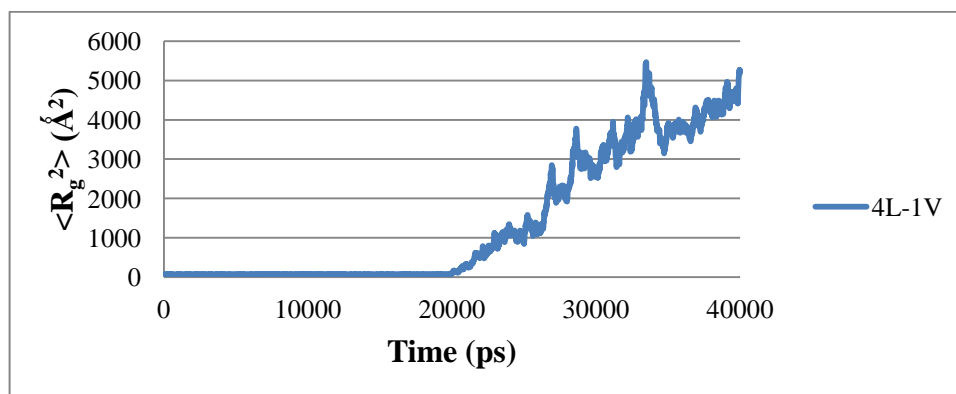


Figure 4.69. Cluster  $R_g$  of 4 Levan – 1 Vancomycin System

As next step systems with 1 vancomycin and 1, 2 and 4 levans respectively were simulated in aqueous conditions. In this step the simulations were performed for 120 ns without encapsulation process. The initial conditions of the molecules are arranged to be the same as the with initial conditions of systems performed in vacuum to simulate the encapsulation phase. The trends of radius of gyrations of the systems are shown in Figure 4.70.

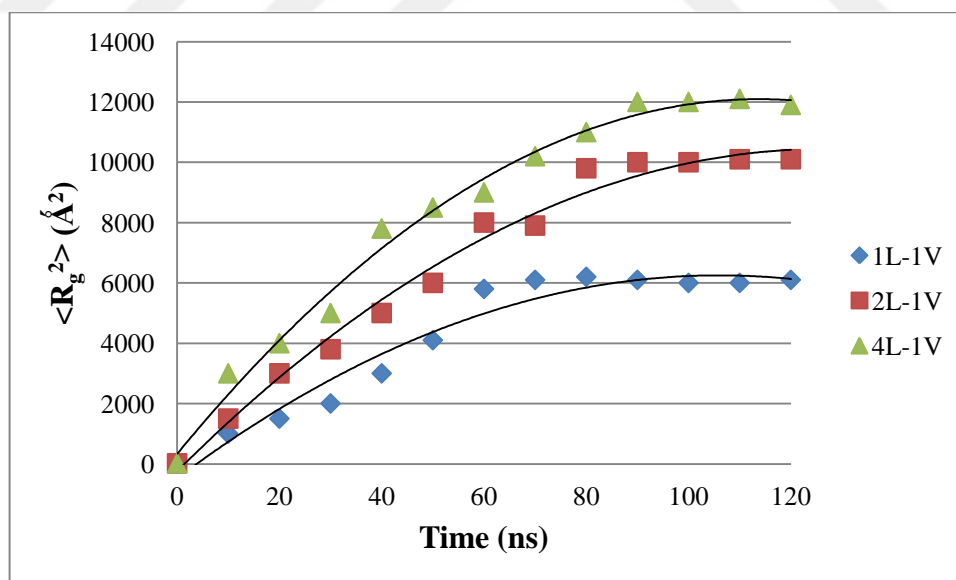


Figure 4.70. Cluster  $R_g$  of 1,2 and 4 Levan – 1 Vancomycin Systems at steady state

The percent release of the systems are calculated due to steady state radius of gyration values of systems having same number of molecules that. After 40 ns of production run of

systems 58%, 46% and 31% release for systems 1 vancomycin and 1,2,4 levan molecules respectively.

Branching and also the molecular weight of levan biopolymer depend on the production route and source of levan. Branching and molecular weight play an important role to express biological activities of levan. In the study of Yoon and coworkers the antitumor activity of levans secreted from four different bacteria was investigated and *Microbacterium* levan was found to have the strongest antitumor activity over other bacterial levans. [113] And in the study of Calazans, the antitumor activity of *Zymomonas* levan was found to be related to the specific class of molecular weight [114].

It is known, that biological and pharmacological properties of polysaccharides can be increased by chemical modifications [115]. From literature data the  $\beta$ -D-fructofuranosic ring C3-C4 region and also C6 region were shown to be important for immunological properties. [116].

Gonta has modified levan in aforementioned sites with various types of sub groups such as hydrazine, glycine, diglycine triglycine and iodine groups. It was found that the chemical modification of the C3-C4 region of the levan increase the possibilities of modified form to stimulate the unspecific immunities of organism [62]. Also it was suggested by Nakapong and coworkers that increasing the molecular weight of levan would yield higher encapsulation efficiency [117]. This may rather be enhanced by adding more fructose units to the polymer or adding sub groups to various sites.

Novel derivatives of levan including levan sulfates, phosphates, and acetates are being utilized in medicine as anti-AIDS agents; food processing as food additive with prebiotic and hypocholesterolemic effects. [118].

Carbohydrate polymers, such as heparin, alginate, and pectin, have been shown to express biological activities [119] Among others heparin is a animal sourced, naturally sulfated polysaccharide which inhibit clot formation in blood. Heparin is known to be most used anticoagulant. However the difficulties of obtaining heparin and also its structural beingheterogeneity have lead researchers to develop novel anticoagulant molecules which can mimic heparin [120]. Due to the properties of bacterial levan as being water soluble, and non-toxic potential use of modified levan structures, sulfated levan molecules, are being investigated to be new alternatives of anticoagulant heparin-like structures.

In order to observe the effect of sub groups attached to polymer on encapsulation and release process, levan polymers were sulfated. Sulfate groups were attached to C6 region of each fructose unit as shown in Figure 4.71. Figures from Fig 4.73 to 4.75 represent comparison of cluster  $R_g$  of the systems with modified levan molecule and vancomycin, levan molecule and vancomycin, levan molecule and vancomycin molecule. Same results as unmodified levan systems are obtained as general trend.

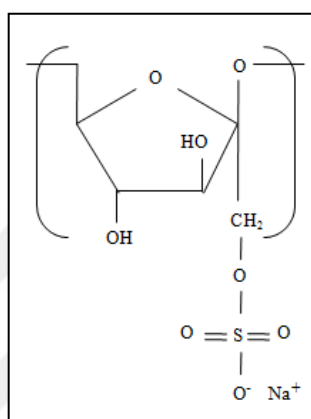


Figure 4.71. Sulfated levan structure

The encapsulation process of modified systems are shown in Figure 4.72.

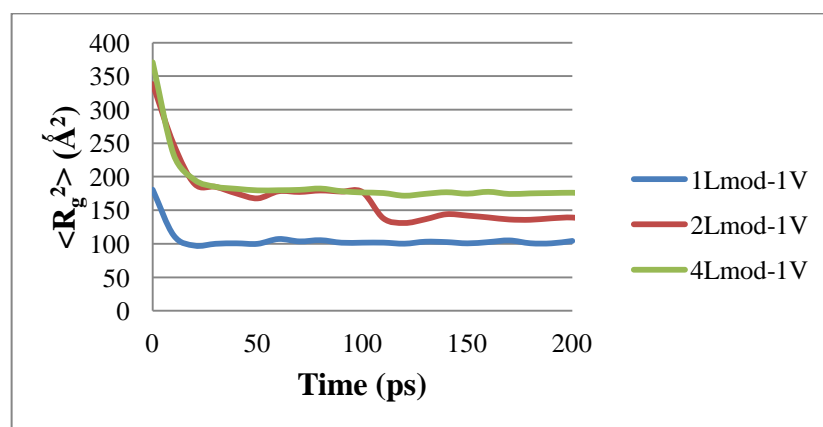


Figure 4.72. Encapsulation of Sulfated levan and vancomycin systems

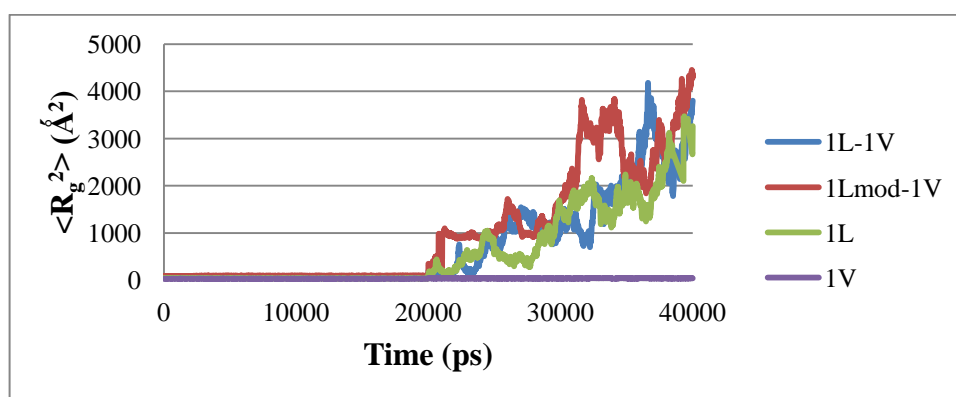


Figure 4.73. Comparison of Cluster  $R_g$  of 1 sulfated Levan – 1 Vancomycin System with 1 Levan – 1 Vancomycin system

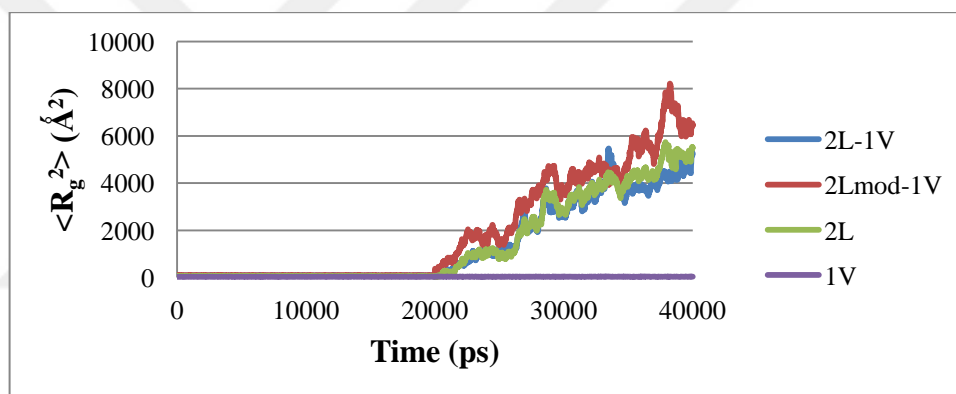


Figure 4.74. Comparison of Cluster  $R_g$  of 2 sulfated Levan – 1 Vancomycin System with 2 Levan – 1 Vancomycin system

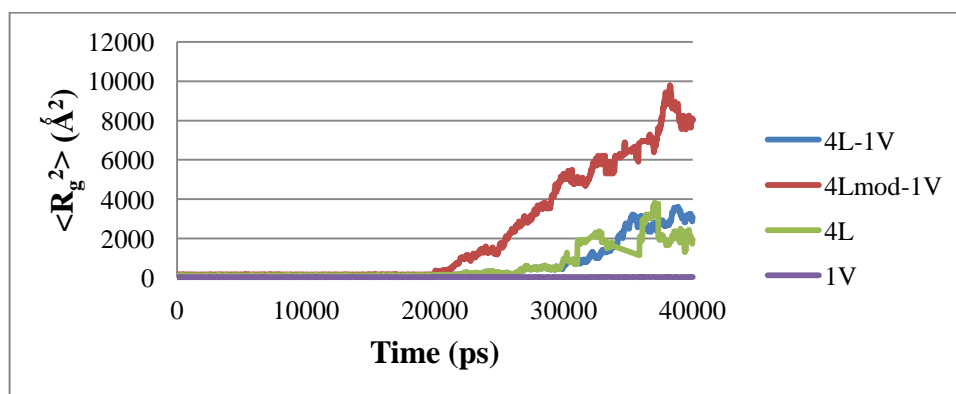


Figure 4.75. Comparison of Cluster  $R_g$  of 4 sulfated Levan – 1 Vancomycin System with 4 Levan – 1 Vancomycin system

In fig. 4.76 the simulations at vacuum were compared. It is observed that in sulfated levan systems have higher cluster  $R_g$  with respect to systems with unmodified levan. The reason of this result may be that the modification at each fructose unit behaves as a steric barrier for the molecule itself, which prevents the folding up to a certain point. Also for simulations in aqueous medium as seen in fig. 4.77 for both unmodified and sulfated systems the rapid release observed from systems with 2 levan molecules. And again sulfated systems have larger cluster  $R_g$  values. No negative effect of modification was observed in terms of release profile for levan.

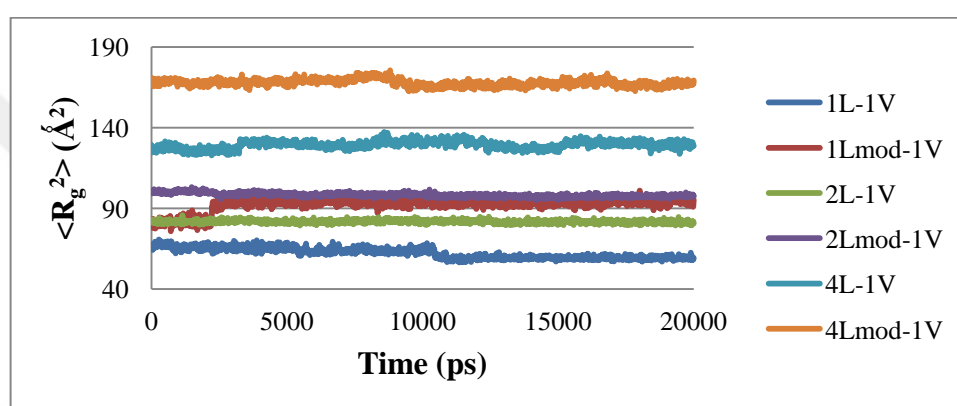


Figure 4.76. Cluster  $R_g$  comparison of systems with unmodified and sulfated levan at vacuum

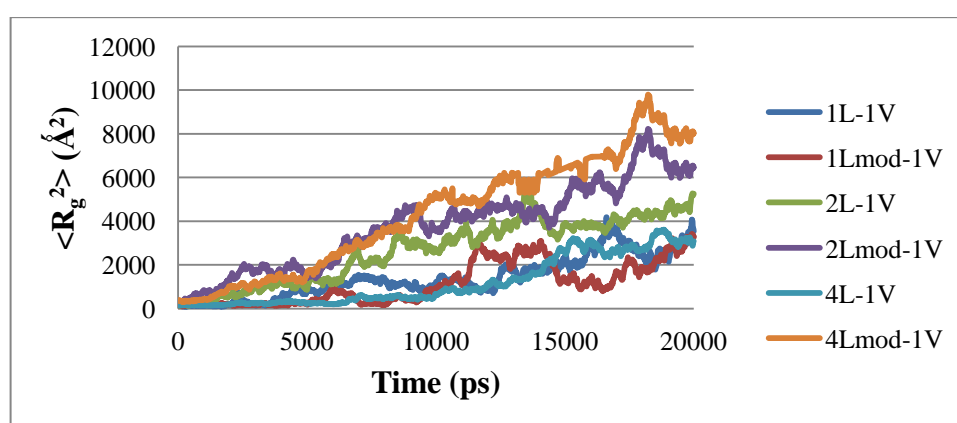


Figure 4.77. Cluster  $R_g$  comparison of systems with unmodified and sulfated levan in aqueous medium



#### 4.6. ENCAPSULATION OF VANCOMYCIN WITH POLYSTYRENE

A control study for the encapsulation and release mechanism of vancomycin was performed with 4 polystyrene molecules each consisting of 9 monomer units. Polystyrene is a hydrophobic polymer as represented in fig. 4.78.

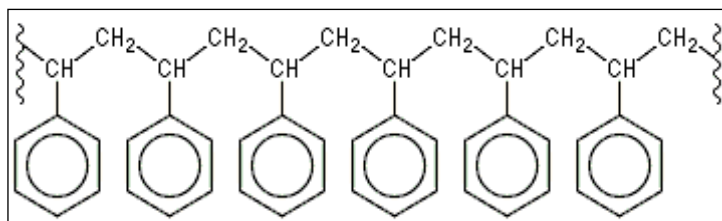


Figure 4.78. Structure of polystyrene

Figure 4.79 represents the cluster  $R_g$  of the system with 4 polystyrene and 1 vancomycin molecule. The first 20 ns time interval corresponds to simulation performed at vacuum and remaining 20 ns interval (from 20 ns to 40 ns) defines the simulation performed in aqueous medium. As seen in the chart no release mechanism is observed with polystyrene. A slight increase in fluctuations after 0-20 ns period is observed. As polystyrene is a hydrophobic polymer having aromatic monomer units, when the system is solvated at 310 K polymers which are folded at encapsulation step has no or slight tendency to disperse in aqueous phase, preventing vancomycin to be released from the encapsulated structure.

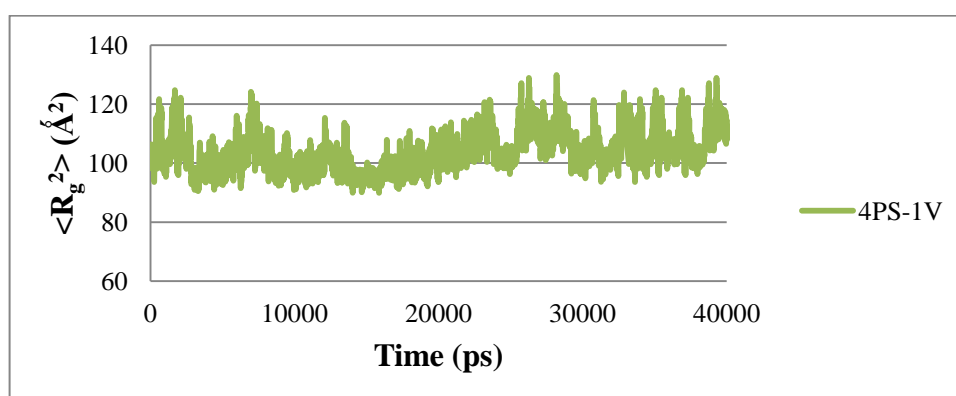


Figure 4.79. Cluster  $R_g$  of 4 Polystyrene – 1 Vancomycin System

With the control test performed, it can be said that the molecular dynamics simulations can be used as complementary or as a leading method for experimental drug delivery studies.



## 5. CONCLUSION AND FUTURE WORK

Vancomycin is a large glycopeptide compound which is active against gram-positive bacteria. The use of vancomycin had been restricted due to its toxic properties. However, as bacteria get resistant to conventional antibiotics, new ways to introduce drugs especially antibiotics which may have toxic or adverse effects on human health, to body have become a popular research area. Among traditional routes such as intravascular dosing, encapsulation of active matter with different kinds of materials are being investigated. Encapsulation may be achieved with nano particles, polymeric or liposomal carriers.

The goal of this study is to investigate the behavior of vancomycin molecules in different media and to suggest levan-biopolymer as vancomycin carrier to body based on MD simulations.

First, behavior of vancomycin was studied in vacuum conditions in terms of radius of gyration to see the intra- and intermolecular behaviour of vancomycin molecules. For this part of the study 20 simulations were performed. Effects of ionic state, number of molecules and temperature were investigated.

Zwitter-ionic form, which is known to be more biologically active was compared with the nonionic form of vancomycin at different temperatures, varying number of molecules present. With a similar trend with average  $R_g$  values, the ionic V-HCl systems have smaller cluster  $R_g$  with respect to non-ionic V-HCl systems. For all systems, it is observed that at higher temperature the difference in radius of gyration values between ionic states decreases. 2-sample t-test was applied to  $R_g$  values to see the statistical significance of ionic states of vancomycin and the differences in the  $R_g$  values between the ionic and nonionic state are statistically significant.

In order to explore the effect of temperature, simulations were performed at 298 K and 310 K. 310 K was chosen to mimic body temperature. Effect of temperature on average  $R_g$  values seems insignificant in systems which have nonionic vancomycin. However, in terms of cluster  $R_g$ , the temperature is statistically significant. On the other hand, zwitter-ionic vancomycin molecules tend to result in smaller  $R_g$  values at higher temperature.

Effect of number of vancomycin molecules on the radius of gyration is investigated at 5 ns, 10 ns and 20 ns. It can be said that, as number of molecules increases the  $R_g$  values calculated per molecule increase as well for systems at 310 K. For simulations at  $T=298$  K there is a sharp increase between 1, 2 and 4 molecules. For systems that have 9 and 16 molecules, the  $R_g$  values become nearly constant independent of the number of vancomycin molecules. For cluster  $R_g$  comparison the expected behavior was observed that as number of molecules increase in the simulation box the cluster  $R_g$  also increases.

In the second part of the study simulations were performed in aqueous condition. The treatment of solvent, water was selected to be atomistic as assigning dielectric constant of water to simulations do not give reliable values of cluster  $R_g$ . All aqueous systems were treated explicitly through the study. Also as zwitter-ionic form of vancomycin is known to be more active than nonionic form, the rest of the simulations were performed with the ionic state.

In aqueous systems, effect of temperature was investigated and it is concluded with  $R_g$  values and oscillation band of these values that the average  $R_g$  of the systems are not affected by change in temperature. For cluster  $R_g$  of the systems at high temperature an increasing trend was observed through the simulations. Despite all systems have fluctuations, cluster  $R_g$  of systems at low temperature do not increase continuously with respect to time. With statistical significance test also these results are validated that difference due to temperature on cluster  $R_g$  values are statistically significant.

The behavior of water molecules around vancomycin molecules are studied in terms of pairwise radial distribution function  $g(r)$ . It can be concluded that amino terminus of vancomycin has more water molecules in its first hydration shell and carboxy terminus has weaker hydrogen bonds. It is observed for the systems having 2 to 16 vancomycin, for amino and carboxy terminus as simulation proceeds the probability of finding an oxygen atom which belongs to water molecule decreases slightly for both 298 K and 310 K.

To introduce vancomycin to body a novel carrier, levan was suggested. With simulations in vacuum where levan biopolymer is positioned different sides of simulation box with respect to vancomycin, it is concluded that active sites, which are carboxy and amino terminus, of vancomycin tend to interact with polymer. However, also short range

interactions, indicating the concentration of polymer might be important in encapsulation process.

To see the encapsulation, systems with varying number of levan molecule and one vancomycin were simulated in vacuum and systems were analyzed in terms of cluster  $R_g$  values. The sharp decrease in cluster  $R_g$  values at the beginning of the simulations show the tendency of molecules to come together. As number of levan molecules increase in the simulation box more time is required to come to equilibrium. To mimic the release of the drug, vancomycin, to body encapsulated systems were again simulated in a simulation box with water molecules. The percent release of the systems are calculated with the ratio of steady state  $R_g$  values and  $R_g$  values at the end of production run for all systems. After 40 ns of production run, 58%, 46% and 31% release is observed for systems with 1 vancomycin and 1, 2 and 4 levan molecules respectively.

Levan polymers were sulfated in order to observe the effect of sub groups attached to polymer on encapsulation and release process. Sulfation of levan was suggested to obtain a heparin like molecule, which was suggested experimentally. Similar general trend of cluster  $R_g$  with higher values with respect to systems having unmodified levan in encapsulation and release processes was obtained.

At the last part encapsulation and release steps were repeated for vancomycin and polystyrene to verify the method of simulations. It was aimed to have compact systems which do not release voncomycin in aqueous medium as polystyrene is an insoluble polymer and is not expected to release vancomycin. With the control experiment performed, it can be said that the molecular dynamics simulations can be used as complementary or as a leading method for experimental drug delivery studies.

For future studies blood conditions might be adapted to simulation conditions. Salt molecules might be added to the system and concentration might be adjusted to blood levels. To find novel ways to deliver vancomycin different types of polymers might be used before experimental studies. Jia and coworkers stated that the dimerization and the type of dimers formed could be functionally significant[28]. Dimers of vancomycin might be used to see the effect of dimerization on encapsulation and release mechanism.

## REFERENCES

1. U.S. Department of Health and Human Services, Infectious Diseases, <http://www.niaid.nih.gov/topics/antimicrobialresistance/Pages/default.aspx> [retrieved 30 April 2012].
2. G. L. Armstrong, L. A. Conn and R. W. Pinner. Trends in Infectious Disease Mortality in the United States During the 20th Century. *The Journal of the American Medical Association*, 281:61-66, 1999.
3. K. Todar, Bacterial Resistance to Antibiotics, Todar's Online Textbook for Bacteriology, <http://textbookofbacteriology.net/resantimicrobial.html> [retrieved 12 December 2012]
4. B. S. Weeks, *Alcamo's Microbes and the Society*, 3rd Edition, Jones and Bartlett Learning, USA, 2011.
5. J. C. Pommerville, *Alcamo's Fundamentals of Microbiology*, 2nd Edition, Jones and Bartlett Learning, USA, 2012.
6. G. Seltmann and O. Holst, *The Bacterial Cell Wall*, Springer, Germany, 2002.
7. M. C. Lawson, Structure-Function Relationships of Polymerizable Vancomycin Derivatives for the Antimicrobial Surface Modification of Orthopedic Devices, PhD Thesis, University of Colorado, 2008.
8. T. Jin, M. Bokarewa, T. Foster, J. Mitchell, J. Higgins and A. Tarkowski. Staphylococcus aureus Resists Human Defensins by Production of Staphylokinase, a Novel Bacterial Evasion Mechanism. *The Journal of Immunology*, 172:1169-1176, 2004.
9. A. Schmidtchen, I. M. Frick, E. Andersson, H. Tapper, and L. Björck. Proteinases Of Common Pathogenic Bacteria Degrade and Inactivate The Antibacterial Peptide LL-37. *Molecular Microbiology*, 46:157-168, 2002.

10. J. Diana, D. Visky, J. Hoogmartens, A. Van Schepdael and E. Adams. Investigation of Vancomycin and Related Substances by Liquid Chromatography/Ion Trap Mass Spectrometry. *Rapid Communications In Mass Spectrometry*, 20:685-693, 2006.
11. R. C. Moellering. Vancomycin: A 50-Year Reassessment. *Clinical Infectious Diseases*, 42:3-4, 2006.
12. M. J. Rybak. The Pharmacokinetic and Pharmacodynamic Properties of Vancomycin. *Clinical Infectious Diseases*, 42:35-39, 2006.
13. K. Koteva, H. J. Hong, X. D. Wang, I. Nazi, D. Hughes, M. J. Naldrett, M. J. Buttner, and G. D. Wright. A Vancomycin Photoprobe Identifies The Histidine Kinase Vanssc As A Vancomycin Receptor. *Nature Chemical Biology*, 6:327-329, 2010.
14. M. Schäfer, T. R. Schneider, and G. M. Sheldrick. Crystal Structure of Vancomycin. *Structure*, 4:12-23, 1996.
15. M. C. Harris, H. Kopecka, and T. M. Harris. Vancomycin: Structure and Transformation to CDP-I. *Journal of American Chemical Society*, 105:23-28, 1983.
16. R. R. Pfeiffer. Structural Features of Vancomycin. *Clinical Infectious Diseases*, 3:205-209, 1981.
17. C. Kosmidis, and P. Chandrasekar. Management of Gram-Positive Bacterial Infections In Patients With Cancer. *LeukandLymphoma*, 53:1-9, 2012.
18. I. G. Boneca, and G. Chiosis. Vancomycin Resistance: Occurance, Mechanisms and Strategies To Combat It. *Expert Opinion on Therapeutic Targets*, 7:311-328, 2003.
19. L. M. Napolitano. Emerging Issues in the Diagnosis and Management of Infections Caused by multi-Drug-Resistant, Gram-Positive Cocci. *Surgical Infections*, 6:2-11, 2005.

20. M. Gel, Z. Chen, H. Russel, J. Kohler, L. L. Silver, R. Kerns, S. Fukuzawa, C. Thompson and D. Kahne. Vancomycin Derivatives That Inhibit Peptidoglycan Biosynthesis Without Binding d-Ala-d-Ala. *Science*, 284:507-511, 1999.
21. J. R. E. Betley, and M. A. Cooper. Antibacterial agents comprising conjugates of glycopeptides and peptidic membrane-associated elements. Patent EP1334117 A1, 2003.
22. R. L. Robison. Vancomycin-HCL solutions and the lyophilization thereof. Patent US4885275 A, 1989.
23. A. S. Antipas, D. Vander Velde, S. D. S. Jois, T. Siahaan, and V. Stella. Effect of Conformation on the Rate of Deamidation of Vancomycin in Aqueous Solutions. *Journal of Pharmaceutical Sciences*, 89:6-10, 2000.
24. C. Ponder, and M. Overcash. Cradle-To-Gate Life Cycle Inventory of Vancomycin Hydrochloride. *Science of the Total Environment*, 408:1331–1337, 2010.
25. B. Li, K. V. Brown, J. C. Wenke, and S. A. Guelcher. Sustained Release of Vancomycin From Polyurethane Scaffolds Inhibits Infection of Bone Wounds In A Rat Femoral Segmental Defect Model. *Journal of Controlled Release*, 145:221–230, 2010.
26. S. Huang, Y. Chen, Y. Chuang, S. Chiu, C. Fung, P. Lu, L. Wang, T. Wu and J. Wang. Prevalence of Vancomycin-Intermediate Staphylococcus Aureus (VISA) and Heterogeneous VISA Among Methicillin- Resistant S. Aureus With High Vancomycin Minimal Inhibitory Concentrations In Taiwan: A Multicenter Surveillance Study, 2012-2013. *Journal of Microbiology, Immunology and Infection*, 49:701-707, 2016.
27. P. Courvalin. Vancomycin Resistance in Gram-Positive Cocci. *Clinical Infectious Diseases*, 42:25-34, 2006.
28. Z. Jia, M. O'Mara, J. Zuegg, M. Cooper, and A. Mark. Vancomycin: Ligand Recognition, Dimerization and Super-Complex Formation. *The FEBS Journal*, 280:5-12, 2013.



29. D. Paolino, P. Sinha, M. Fresta, and M. Ferrari. Drug Delivery Systems. *Encyclopedia of Medical Devices and Instrumentation*, John Wiley and Sons, 2006.
30. B. Mukherjee, N. S. Dey, R. Maji, P. Bhowmik, P. J. Das and P. Paul. Current Status and Future Scope for Nanomaterials in Drug Delivery. In A. D. Sezer, editor, *Application of Nanotechnology in Drug Delivery*, Chapter 16, InTech, 2014.
31. S. Srinivasan. Multifunctional Nanoparticles for Therapeutic Applications, PhD Dissertation, Florida International University, 2015.
32. R. S. Dhanikula, T. Hammady, and P. Hildgen. On the Mechanism and Dynamics of Uptake and Permeation of Polyether-Copolyester Dendrimers Across an In Vitro Blood–Brain Barrier Model. *Journal Of Pharmaceutical Sciences*, 98:3748-3760, 2009.
33. A. Montellano, T. Da Ros, A. Biancob and M Prato. Fullerene C60 As A Multifunctional System For Drug And Gene Delivery. *Nanoscale*, 3:4035-4041, 2011.
34. M. S. Digge, R. S. Moon, and S. G. Gattani. Applications of Carbon Nanotubes In Drug Delivery: A Review. *International Journal of PharmTech Research*, 4:839–847, 2012.
35. M. Çağdaş, A. D. Sezer, and S. Bucak. Liposomes as Potential Drug Carrier Systems for Drug Delivery. In A. D. Sezer, editor, *Application of Nanotechnology in Drug Delivery*, Chapter 1, InTech, 2014.
36. X. Xu, and D. J. Burgess. Liposomes as Carriers for Controlled Drug Delivery. In J. E. Wright and D. A. Burgess, editors, *Longacting Injections and Implants*, pages 195-220, Springer, 2011.
37. G. Gregoriadis and A. T. Florence. Liposomes in Drug Delivery. *Drugs*, 45:15-28, 1993.

38. R. Guráň, M. Komínková, P. Kopel, D. Chudobová, O. Zítka, V. Adam, and R. Kizek. Liposomes As Drug Carriers and Their Characterization Using Different Analytical Methods. *MendelNet*, 2013:913-918, 2013.
39. J. Scholtz. Liposomes as drug delivery systems, [http://dspace.nwu.ac.za/bitstream/handle/10394/4878/scholtz\\_jc\\_chapter2.pdf?sequence=4](http://dspace.nwu.ac.za/bitstream/handle/10394/4878/scholtz_jc_chapter2.pdf?sequence=4), [retrieved 24 April 2012].
40. X. Xu, M. Khan, and D. J. Burgess. Predicting Hydrophilic Drug Encapsulation Inside Unilamellar Liposomes. *International Journal of Pharmaceutics*, 423:410-418, 2012.
41. I. I. Salem, D. L. Flasher and N. Düzgüneş. Liposome Encapsulated Antibiotics. *Methods in Enzymology*, 391:261–291, 2005.
42. A. Papagiannaros, and C. Demetzos. Release Advantages of A Liposomal Dendrimer-Doxorubicin Complex, Over Conventional Liposomal Formulation of Doxorubicin. In M. R. Mozafari, editor, *Nanomaterials and Nanosystems for Biomedical Applications*, pages 135-144, Springer, 2007.
43. O. Pillai, and R. Panchagnula. Polymers In Drug Delivery. *Chemical Biology*, 5:447-451, 2001.
44. H. M. Mansour, M. Sohn, A. Al-Ghananeem, and P. P. DeLuca. Materials for Pharmaceutical Dosage Forms: Molecular Pharmaceutics and Controlled Release Drug Delivery Aspects. *International Journal of Molecular Science*, 11:3298-3322, 2010.
45. A. K. Srivastavaa, B. Bhartiab, K. Mukhopadhyaya, and A. Sharma. Long Term Biopotential Recording by Body Conformable Photolithography Fabricated Low Cost Polymeric Microneedle Arrays. *Sensors and Actuators A: Physical*, 236:164–172, 2015.
46. J. R. Joshi, and R. P. Patel. Role Of Biodegradable Polymers In Drug Delivery. *International Journal of Current Pharmaceutical Research*, 4:74-81, 2012.

47. I. Metzmacher. Enzymatic Degradation and Drug Release Behavior of Dense Collagen Implants, PhD Dissertation, Ludwig-Maximilians-University, 2005.
48. U. Gbureck, E. Vorndran and J. E. Barralet. Modeling Vancomycin Release Kinetics From Microporous Calcium Phosphate Ceramics Comparing Static and Dynamic Immersion Conditions. *Acta Biomaterialia*, 4:1480–1486, 2008.
49. H. Gautier, J. Caillon, A. M. LeRay, G. Daculsi, and C. Merle. Influence of Isostatic Compression On The Stability of Vancomycin Loaded With A Calcium Phosphate-Implantable Drug Delivery Device. *Journal of Biomedical Materials Research*, 52:308-322, 2000.
50. M. P. Ginebra, T. Traykova, and J. A. Planell. Calcium Phosphate Cements as Bone Drug Delivery Systems: A Review. *Journal of Controlled Release*, 113:102-110, 2006.
51. A. Khangtragool, S. Ausayakhun, P. Leesawat, C. Laokul, and R. Molloy. Chitosan as an Ocular Drug Delivery Vehicle for Vancomycin. *Journal of Applied Polymer Science*, 122:3160-3167, 2011.
52. E. Gavini, P. Chetoni, M. Cossu, M. G. Alvarez, M. F. Saettone, and P. Giunchedi. PLGA Microspheres For The Ocular Delivery of A Peptide Drug, Vancomycin Using Emulsification/Spray-Drying As The Preparation Method: In Vitro/In Vivo Studies. *European Journal of Pharmaceutics and Biopharmaceutics*, 57: 207-212, 2004.
53. Q. Yang, S. Wang, P. Fan, L. Wang, Y. Di, K. Lin and F. S. Xiao. pH-Responsive Carrier System Based on Carboxylic Acid Modified Mesoporous Silica and Polyelectrolyte for Drug Delivery. *Chemical Materials*, 17:5999-6003, 2005.
54. L. F. Zhang, D. J. Yang, H. C. Chen, R. Sun, L. Xu, Z. C. Xiong, T. Govender, and C. D. Xiong. An Ionically Crosslinked Hydrogel Containing Vancomycin Coating On A Porous Scaffold For Drug Delivery and Cell Culture. *International Journal of Pharmaceutics*, 353:74-87, 2008.

55. Z. Ruszczak, and W. Friess. Collagen As A Carrier For On-Site Delivery of Antibacterial Drugs. *Advanced Drug Delivery Reviews*, 55:1679-1698, 2003.
56. M. H. Xiong, Y. Bao, X. Z. Yang, Y. C. Wang, B. Sun, and J. Wang. Lipase Sensitive Polymeric Triple-Layered Nanogel for On-demand Drug Delivery. *Journal of the American Chemical Society*, 134:4355-4362, 2012.
57. Y. W. Han, and M. A. Watson. Production of Microbial Levan From Sucrose, Sugarcane Juice and Beet Molasses. *Journal of Industrial Microbiology*, 9:257-260, 1992.
58. K. B. Uppuluri. Cost Effective Production and Applications of Levan from *Acetobacter xylinum* NCIM 2526 using Synthetic and Complex Medium. *International Conference and Exhibition on Biopolymers and Bioplastics*, San Francisco, USA, 4:98-104, 2015.
59. F. Küçükaşık, H. Kazak, D. Güney, I. Finore, A. Poli, O. Yenigün, B. Nicolaus, and E. Toksoy Öner. Molasses as Fermentation Substrate for Levan production by *Halomonas* sp. *Applied Microbiology and Biotechnology*, 89:1729-1740, 2011.
60. K. Hann, and L. Lentz. Compositions Containing Aloe Vera Isolate and a Prebiotic and Their Therapeutic Application, WO2006055711 A1, 2006.
61. F. Sima, E. Cansever Mutlu, M. S. Eroğlu, L. E. Sima, N. Serban, C. Ristoscu, S. M. Petrescu, E. Toksoy Öner and I. N. Mihailescu. Levan Nanostructured Thin Films by MAPLE Assembling. *Biomacromolecules*, 12:2251-2257, 2011.
62. S. Gonta. The Levan Synthesising Bacteria Immobilisation and Chemical Modification of Polysaccharide Levan To Obtain Biologically Active Products, PhD Dissertation, Rîgas Tehniskā Universitāte, 2005.
63. A. D. Sezer, H. Kazak, E. Toksoy Öner and J. Akbuğa. Levan Based Nanocarrier System For Peptide and Protein Drug Delivery: Optimization and Influence of Experimental Parameters On The Nanoparticle Characteristics. *Carbohydrate Polymers*, 84:358-363, 2011.

64. A. D. Sezer, H. Kazak Sarılmışer, E. Rayaman, A. Çevikbaş, E. Toksoy Öner and J. Akbuğa. Development and Characterization of Vancomycin-Loaded Levan-Based Microparticulate System For Drug Delivery. *Pharmaceutical Development and Technology*, Early Online, 1:1-8, 2015.
65. A. R. Leach. *Molecular Modeling Principles and Applications*, 2nd Edition, Pearson Education Lmt., Great Britain, 2001.
66. D. W. Borhani, and D. E. Shaw. The Future of Molecular Dynamics Simulations In Drug Discovery. *Journal of Computer-Aided Molecular Design*, 26:15-26, 2012.
67. J. Li. *Handbook of Materials Modeling*, Springer, Netherlands, 2005.
68. J. Meller. Molecular Dynamics, <https://dasher.wustl.edu/chem478/reading/md-intro-1.pdf>, [retrieved 1 May 2001]
69. T. L. Chantawansri, E. F. C. Byrd, B. M. Rice and J. W. Andzelm. Molecular Dynamics Simulations of Hugoniot Relations for Poly[methyl methacrylate]. *Weapons and Materials Research Directorate*, ARL, USA, 2011.
70. Swiss Institute of Bioinformatics. Molecular Dynamics, <http://www.ch.embnet.org/>, [retrieved 14 December 2010]
71. M. P. Allen. *Introduction to Molecular Dynamics Simulation*. NIC Series, 23:1-28, 2004.
72. R. J. Woods, and M. B. Tessier. Computational Glycoscience: Characterizing The Spatial and Temporal Properties of Glycans and Glycan-Protein Complexes. *Current Opinion in Structural Biology*, 20:575-583, 2010.
73. M. A. González. Force fields and molecular dynamics simulations. *Collection SFN*, 12:169-200, 2011.

74. H. Sun, S. J. Mumby, J. R. Maple and A. T. Hagler. An ab Initio CFF93 All-Atom Force Field for Polycarbonates. *Journal of American Chemical Society*, 116:2978-2987, 1994.
75. B. R. Brooks, R. E., Bruccoleri, B. D. Olafson, and D. J. S. States. CHARMM: A Program for Macromolecular Energy, Minimization, and Dynamics Calculations. *Journal of Computational Chemistry*, 4:187-217, 1983.
76. J. Wang, M. W. Romain, W. C. James, A. K. Peter, and A. David. Case Development and Testing of A General Amber Force Field. *Journal of Computational Chemistry*, 25: 1157–1174, 2004.
77. F. Wilfred, D. Xavier, E. M. Alan. GROMOS Force Field. *Encyclopedia of Computational Chemistry*, 2002.
78. M. Tuckerman, Classical microscopic states or microstates and ensembles. [http://www.nyu.edu/classes/tuckerman/stat.mech/lectures/lecture\\_1/node6.html](http://www.nyu.edu/classes/tuckerman/stat.mech/lectures/lecture_1/node6.html), [retrieved 8 January 2003].
79. J. Leszczynski. *Handbook of Computational Chemistry*, Springer, USA, 2012.
80. University of Massachusetts Lowell. Different ensembles in molecular dynamics simulations, <http://faculty.uml.edu/>, [retrieved 8 May 2012]
81. Universitat Rovira I Virgili. Molecular Dynamics - Statistical Ensembles, <http://www.fq.urv.cat/>, [retrieved 3 November 2011]
82. W. Cai. Handout 9. NPT and Grand Canonical Ensembles. Class-Notes, Stanford University, 2011.
83. Rutgers University. Force Field-Based Simulations, [benedick.rutgers.edu/software-manuals/forcefield.pdf](http://benedick.rutgers.edu/software-manuals/forcefield.pdf), [retrieved 6 July 2008]

84. D. Janezic. Implicit Runge-Kutta Method for Molecular Dynamics Integration. *Journal of Chemical Information and Computer Sciences*, 33:252-257, 1993.
85. A. G. Mansoori. *Principles of Nanotechnology: Molecular-Based Study of Condensed Matter in Small Systems*, World Scientific Publishing, Singapore, 2005.
86. M. Elimelech, X. Jia, J. Gregory and R. Williams. *Particle Deposition and Aggregation: Measurement, Modelling and Simulation*, Butterworth-Heinemann Publications, USA, 1998.
87. D. C. Rapaport. *The Art of Molecular Dynamics Simulation*, 2nd Edition, Cambridge University Press, UK, 2004.
88. Central Michigan University. Model Box Periodic Boundary Conditions, <http://isaacs.sourceforge.net/phys/pbc.html>, [retrieved 5 May 2012]
89. J. Blomqvist. Ab Initio And Dft Derived Potential Energy Functions In Simulations Of Selected Polyesters Based On Atomistic Models, Report Series In Physics, University of Helsinki, 2001.
90. S. Shenogin, and R. Ozisik, XenoView: Visualization for atomistic simulations, XenoView, <http://xenoview.mat.rpi.edu>, 3.4:1-5, 2007.
91. S. Plimpton, Fast Parallel Algorithms for Short-Range Molecular Dynamics. *Journal of Computational Physics*, 117:1-19, 1995.
92. W. Humphrey, D. Andrew, S. Klaus. VMD: Visual molecular dynamics. *Journal of Molecular Graphics*, 14:33-38, 1996.
93. Gromacs. Radius of Gyration, [http://www.gromacs.org/Documentation/Terminology/Radius\\_of\\_Gyration](http://www.gromacs.org/Documentation/Terminology/Radius_of_Gyration), [retrieved 21 January 2013]

94. Sandia National Laboratories. Radius of Gyration, [http://lammmps.sandia.gov/doc/compute\\_gyration\\_molecule.html](http://lammmps.sandia.gov/doc/compute_gyration_molecule.html), [retrieved 14 March 2013].
95. M. Y. Lobanov, N. S. Bogatyreva, and O. V. Galzitskaya. Radius of Gyration As An Indicator of Protein Structure Compactness. *Molecular Biology*, 42:623–628, 2008.
96. M. L. Eggersdorfer, D. Kadau, H. J. Herrmann, and S. E. Pratsinis. Number and Size of Primary Particles In Agglomerates From Mass and Mobility Measurements. *American Institute of Chemical Engineers Conference Proceedings*, 2011.
97. D. W. Heermann. *Computer Simulation Methods in Theoretical Physics*, 2nd Edition, Springer-Verlag, 1995.
98. M. Feig. *Modeling Solvent Environments*, Wiley-VCH, 2009.
99. C. L. Brooks, M. Karplus, and B. M. Pettitt. *Advances in Chemical Physics, Proteins: A Theoretical Perspective of Dynamics, Structure, and Thermodynamics*, Wiley-Interscience, 1990.
100. E. J. Brandas, and E. Kryacho. *Advances in Quantum Chemistry, Volume 47: A Tribute Volume in Honour of Professor Osvaldo Goscinski*, Elsevier Academic Press, 2004.
101. P. Bultinck, H. De Winter, W. Langenaeker, and J. P. Tollenare. *Computational Medicinal Chemistry for Drug Discovery*, CRC Press, 2003.
102. O. M. Becker, A. D. MacKerell Jr., B. Roux, and M. Watanabe. *Computational Biochemistry and Biophysics*, CRC Press, 2001.
103. H. D. Höltje, W. Sippl, D. Rognan, and G. Folkers. *Molecular Modeling: Basic Principles and Applications*, 2nd Edition, Wiley-VCH, 2003.



104. C. G. Malmberg, and A. A. Maryott. Dielectric Constant of Water from 0° to 100° C. *Journal of Research of the National Bureau of Standards*, 56:1-8, 1956.
105. Minitab Inc, <http://www.minitab.com/en-us/>, [retrieved 19 January 2016].
106. D. Pavel, J. Lagowski and C. J. Lepage. Computationally Designed Monomers For Molecular Imprinting of Chemical Warfare Agents - Part V. *Polymer*, 47:8389-8399, 2006.
107. S. Herlambang, and R. Saleh. The Comparison of Substrate Stability in Neuraminidase Type 2 (N2) Active Site between A/Tokyo/3/67 and A/Pennsylvania/10218/84 with Heating Dynamics Simulation. *World Journal of Condensed Matter Physics*, 1:77-87, 2011.
108. P. K. Srivastava, Structure, molecular dynamics, and stress in a linear polymer under dynamic strain, Department of Aerospace Engineering Indian Institute of Science, 2010.
109. M. Sargolzaei, M. R. Housaindokht, S. F. Tayyari and M. R. Bozorgmehr. Temperature Effects On Spinach Plastocyanin:Molecular Dynamics Simulation Study. *Romanian Journal of Biochemistry*, 48:101-118, 2011.
110. A. C. Fogarty, and D. Laage. Water Dynamics in Protein Hydration Shells: The Molecular Origins of the Dynamical Perturbation. *The Journal of Physical Chemistry*, 118:7715-7729, 2014.
111. R. M. Espinosa-Marzal, G. Fontani, F. B. Reusch, M. Roba, N. D. Spencer and R. Crockett. Sugars Communicate Through Water: Oriented Glycans Induce Water Structuring. *Biophysical Journal*, 104:2686-2694, 2013.
112. V. Manzoni, M. L. Lyra, R. M. Gester, K. Coutinho, and S. Canuto. Study of The Optical and Magnetic Properties of Pyrimidine In Water Combining PCM And QM/MM Methodologies. *Physical Chemistry Chemical Physics*, 12:2-15, 2010.

113. E. J. Yoon, S. H. Yoo, J. Chac and H. G. Lee. Effect of Levan's Branching Structure On Antitumor Activity. *International Journal of Biological Macromolecules*, 34:191–194, 2004.
114. G. M. T. Calazans, C. E. Lopes, R. M. O. C. Lima and F. P. Franca. Antitumour Activity of Levans Produced by *Zymomonas Mobilis* Strains. *Biotechnology Letters*, 19:19-21, 1997.
115. I. Cumpstey. Chemical Modification of Polysaccharides. *International Scholarly Research Notices Organic Chemistry*, 2013:1-27, 2013.
116. M. Yalpani. Survey Of Recent Advances In Selective Chemical And Enzymic Polysaccharide Modifications. *Tetrahedron*, 41:2957-3020, 1985.
117. S. Nakaponga, R. Pichyangkura, K. Ito, M. Iizuka and P. Pongsawasdi. High Expression Level of Levansucrase From *Bacillus Licheniformis* RN-01 and Synthesis of Levan Nanoparticles. *International Journal of Biological Macromolecules*, 54:30–36, 2013.
118. A. M. Abdel-Fattah, A. M. Gamal-Eldeen, W. A. Helmy, and M. A. Esawy. Antitumor and Antioxidant Activities of Levan and Its Derivative From The Isolate *Bacillus Subtilis* NRC1aza. *Carbohydrate Polymers*, 89:314–322, 2012.
119. E. J. Yoon, S. H. Yoo, J. Cha, and H. G. Lee. Effect of Levan's Branching Structure On Antitumor Activity. *International Journal of Biological Macromolecules*, 34:191–194, 2004.
120. M. Erginer, A. Akcay, B. Coskuncan, T. Morova, D. Rende, S. Bucak, N. Baysal, R. Ozisik, M. S. Eroglu, M. Agirbasli, and E. Toksoy Oner. Sulfated Levan From *Halomonas Smyrnensis* As A Bioactive, Heparin-Mimetic Glycan For Cardiac Tissue Engineering Applications. *Carbohydrate Polymers*, 149:289–296, 2016.